Design Feasibility of an Active Ankle-Foot Stabilizer

by

Taresh D. Mistry

A thesis
presented to the University of Waterloo
in fulfillment of the
thesis requirement for the degree of
Master of Applied Science
in
Systems Design Engineering

Waterloo, Ontario, Canada, 2010

© Taresh D. Mistry 2010

I hereby declare that I am the sole author of this thesis. This is a true copy of the thesis, including any required final revisions, as accepted by my examiners.

I understand that my thesis may be made electronically available to the public.

Abstract

Walking is the most common form of mobility in humans. For lower limb mobility impairments, a common treatment is to prescribe an ankle-foot orthosis (AFO) or brace, which is a passive device designed to resist undesired ankle-foot motion. Recent advances in actuator technology have led to the development of active AFOs (AAFOs). However, these devices are generally too bulky for everyday use and are limited to applications such as gait training for rehabilitation. The aim of this research was to investigate the feasibility of developing a novel Active Ankle-Foot Stabilizer (AAFS). The design criteria were mainly based on the strengths and limitations of existing AFOs. The sagittal plane functional requirements were determined using simulated gait data for elderly individuals and drop foot patients; however, it is intended that the device would be suitable for a wider range of disabilities including ankle sprains. A model of the foot was introduced to modify the moment of a deficient ankle where young healthy adult kinematics and kinetics were assumed. A moment deficit analysis was performed for different gait periods resulting in an AAFS model with two components: a linear rotational spring to modify the ankle joint rotational stiffness, and a torque source. The frontal plane functional requirements for the AAFS were modeled as a linear rotational spring which responded to particular gait events. A novel Variable Rotational Stiffness Actuator (VSRA) AFO was also investigated. It consisted of an actuated spring medial and lateral to the ankle to control sagittal plane ankle stiffness and a passive leafspring posterior to the ankle to control frontal plane ankle stiffness. Due to high forces and profile limitations, a spring and rotation actuator that satisfied the design criteria could not be developed, resulting in an infeasible design. Considering the high forces and moments required by the AAFS, a pneumatic approach was adopted. A novel Airbeam AFO, which consisted of a shank cuff and a foot plate to which airbeams were attached proximally and distally to the ankle, was examined. The joint rotational stiffness of the ankle would be controlled by the inflation of these individual cylindrical airbeams. To satisfy the functional requirements, the airbeam diameters and pressures were too large to meet the design criteria and were unrealistic for a portable device. Finally, a Pneumatic Sock AFO, which proved to best satisfy the functional requirements within the design criteria, was examined. The design consisted of an inner sock worn on the ankle, surrounded by anterior, posterior, medial, and lateral bladders which inflate against outer fabric shells. Although promising, the Pneumatic Sock AFO requires further investigation in regards to manufacturing and behaviour characterization before a functional prototype can be developed. Mechanical test methods to characterize the behaviour of the Pneumatic Sock AFO in the sagittal and frontal planes were developed including the control components required, the configuration of a test rig, and test procedures.

Acknowledgements

I am heartfully thankful to all of those who have made this thesis possible. I would especially like to thank my supervisors, Dr. Jonathan Kofman from the University of Waterloo and Dr. Edward Lemaire from The Ottawa Hospital Rehabilitation Centre for giving me the opportunity to pursue this thesis, supporting me throughout the project, and challenging me to my limits.

I would like to show my gratitude to the staff at The Ottawa Hospital Rehabilitation Centre for their feedback and assistance during my stay in Ottawa. I am also thankful to my colleagues Sean Sullivan and Alex Spring for their technical and moral support throughout this project. I would also like to thank my thesis readers, Dr. John Medley and Dr. Eihab Abdel-Rahman, for their support and time in the completion of this thesis.

I am especially grateful to my friend, Nada, who taught me that no matter how cloudy the day is, the sun is still shining.

Lastly, financial assistance through the University of Waterloo, Ontario Graduate Scholarships in Science and Technology (OGSST), The Ottawa Hospital Rehabilitation Centre, the Natural Sciences and Engineering Research Council (NSERC), and MITACS is appreciated.

Dedication

To Mom and Dad, *for their never-ending unconditional love and support,*

To Mala, *for her love and for always believing in me.*

Contents

List of Tables

List of Figures

Acronyms

AAFO	Active Ankle-Foot Orthosis	**HAT**	Head (and neck), Arms, and Trunk
AAFS	Active Ankle-Foot Stabilizer	**HC**	Heel Contact
AFO	Ankle-Foot Orthosis	**HO**	Heel Off
BOS	Base of Support	**MIT**	Massachusetts Institute of Technology
CD	Controlled Dorsiflexion	**MRF**	Magnetorheological Fluid
CMT	Charcot-Marie-Tooth	**MTJ**	Midtarsal Joint
COG	Center of Gravity	**NT**	Neutral
COM	Center of Mass	**PLS**	Posterior Leaf Spring
COP	Center of Pressure	**PMA**	Pneumatic Muscle Actuator
CP	Controlled Plantarflexion	**PP**	Powered Plantarflexion
DAQ	Data Acquisition	**SEA**	Series-Elastic Actuator
EMG	Electromyography	**STJ**	Subtalar Joint
ERF	Electrorheological Fluid	**TCJ**	Talocrural Joint
FF	Foot Flat	**TO**	Toe Off
FSR	Force Sensing Resistor	**VSRA**	Variable Stiffness Rotational Actuator
GC	Gait Cycle	**YHA**	Young Healthy Adult
GRF	Ground Reaction Force		

Chapter 1

Introduction

1.1 Background

Walking, or gait, is the most common form of mobility in humans. However in 2000-2001, approximately 540,000 Canadians who were living in private households required a mobility support device other than a wheelchair [2]. The use of these devices increased with age from 1.7% of persons aged 45-64 to 14.6% of persons aged 65-84 and nearly doubles, 32%, in persons aged 85 and older. Nearly one quarter of the causes of mobility impairment were due to natural aging, nearly half due to illness or disease, and almost one fifth due to injury.

Ankle-foot orthoses (AFOs) are a common prescription for ankle injuries and pathological conditions affecting the lower leg and foot. They restrict the degrees of freedom of the ankle and foot to maximize stabilization, but can hinder natural locomotion [3, 4]. Recent advances in AFO technology have led to active AFOs (AAFOs) which use actuators to control ankle-foot motions. These are limited to specific pathological conditions such as drop-foot and are mostly for rehabilitative training purposes [5, 6, 7]. The biomechanical principles of AFOs may be applied to create a stabilization device for populations with ankle and foot gait deficiencies. These principles can include applying mechanical forces and moments at the ankle joint, shank, or foot to correct the gait deficiencies. The populations studied in this thesis include elderly individuals, drop-foot patients, and individuals with sustained ankle-sprain injuries, however it is intended that the device would be suitable for a wider range of ankle disabilities. In the elderly, mobility impairments are attributable to muscular degeneration and loss of balance mechanisms [1, 8] resulting in decreased velocity, increased stride time, decreased range of ankle motion, and decreased push-off force and power. Gait disorders due to neurological conditions from stroke or disease further deterio-

rate the ability to walk and can lead to higher falls risks [9]. Drop-foot patients are unable to lift their foot causing unnatural gait patterns with slower speeds [10]. In ankle-sprain injured individuals, functional instability is caused by ligament or muscle weakness with a high risk of injury reoccurrence [3, 11]. Devices currently available for drop foot patients and sprain-injured individuals are inadequate because they are passive devices which limit natural gait movements and are unable to adapt to changes in gait such as velocity.

This thesis examines the feasibility of developing an Active Ankle-Foot Stabilizer (AAFS) to control the motion of the ankle and foot during gait by actuating the device when deviations from healthy gait occur. The goal of this research is to restore the function of the ankle and foot of the populations mentioned above through external forces and moments to achieve more normal kinematic and kinetic gait patterns. This would allow them to walk more comfortably and confidently, and ultimately improve mobility and lifestyle.

1.2 Thesis Overview

An overview of this thesis is as follows. In Chapter 2, an extensive literature review is conducted. First, a review of the ankle and foot and their role in gait is examined. Second, a review of target populations with ankle-foot gait deficiencies is reviewed including the elderly, drop foot patients, and ankle sprain-injured individuals. Thirdly, a review of orthotic management at the ankle and foot is outlined, followed by an investigation of passive and active AFO technology and its inadequacy for an AAFS. Finally, a brief overview of actuator technologies is discussed for possible use in an AAFS design.

In Chapter 3, a statement of rationale is established for the design of an AAFS followed by the thesis objectives. The design criteria are also established.

In Chapter 4, the functional requirements of the AAFS are determined. For the sagittal plane, a work-energy simulation of clinical data is performed to determine the required device characteristics. In the frontal plane, the requirements are based on response to specific gait events outlined in the literature review.

In Chapter 5, several design concepts are explored and selected designs are investigated for their feasibility in satisfying the design criteria and functional requirements of an AAFS.

In Chapter 6, testing methods are developed for the AAFS based on the functional requirements determined in Chapter 4. The control scheme and control components of a favoured design are also included.

Chapter 2

Literature Review

The design of an AAFS device requires a firm understanding of the ankle and foot biomechanical functions along with orthotic management techniques to correct lack of these functions by applying external forces and moments. The following literature review provides the fundamental knowledge of the functional limitations of passive commercial AFOs and active laboratory-researched AFOs with an emphasis on their inadequacy as an AAFS. This chapter examines the role of the ankle and foot in gait, the characteristics of populations with ankle-foot gait deficiencies, the design and function of AFOs, and finally a review of potential actuator technologies which may be useful in developing a novel AAFS.

2.1 Role of the Ankle and Foot in Gait

Walking, also referred to as gait, transports the body safely and efficiently across the ground, on the level, uphill and downhill [1]. It is one of the most complex and totally integrated movements humans perform [1]. Functionally, successful gait and stability require the ankle and foot to perform effectively. Ankle and foot function are reviewed next.

2.1.1 Ankle and Foot

The body has two functional divisions with regards to gait: the passenger unit and the locomotor unit [10]. The passenger unit consists of the head (and neck), arms and trunk, also referred to as HAT, which represents two thirds of the body mass [1]. The locomotor unit consists of the two lower limbs and pelvis which are responsible for propulsion, stance stability, shock absorption and energy conservation of which the ankle and foot actively

participate in [10]. The bone structure, joint articulation, and musculature of the ankle and foot which are essential in understanding AFO design are reviewed.

2.1.1.1 Bones

The bones of the foot can be divided into three sections: the rearfoot, midfoot, and forefoot as shown in Figure 2.1 [4]. The rearfoot consists of the calcaneus and talus. The midfoot consists of the cuboid; medial, intermediate, and lateral cuniforms; and the navicular. The forefoot consists of the metatarsals and phalanges. The first largest toe is the hallux and consists of two phalanges, unlike the lesser toes which consist of three phalanges each.

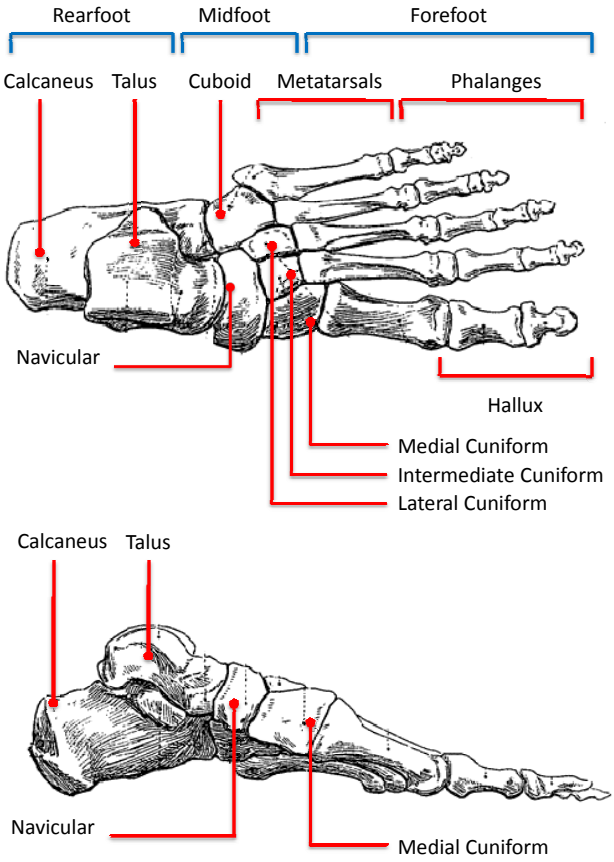

Figure 2.1: Dorsal and medial view of the bones of the left ankle and foot (adapted from [4, 12]). The foot is divided into rearfoot, midfoot, and forefoot sections.

2.1.1.2 Joint Articulation

The body can be divided in three planes: the sagittal plane, the frontal (or coronal) plane, and the transverse plane (Figure 2.2). In the sagittal plane, dorsiflexion describes pointing the foot towards the head and plantarflexion describes pointing the foot away from the head (see Figure 2.3a); in the coronal plane, inversion describes rotating the sole of the foot medially and eversion describes rotating the sole of the foot laterally; and in the transverse plane, adduction describes rotating the foot medially and abduction describes rotating the foot laterally [4]. If the foot is placed on level ground and the shank is vertical, this joint orientation corresponds to neutral (NT) position.

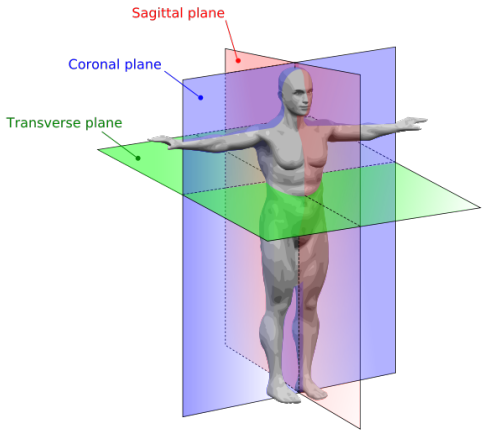

Figure 2.2: Image of body planes [13]. The three body planes are the sagittal, coronal and transverse plane.

Additionally, supination describes tilting of the sole of the foot medially and pronation describes tilting the sole of the foot laterally (see Figure 2.3b). These are composite motions involving triplanar movement in all three of the body planes [14]. Supination involves inversion, adduction, and plantarflexion. Pronation involves eversion, abduction, and dorsiflexion. These two terms are used more commonly [4].

The major joint axes of the of ankle and foot complex including the talocrural (ankle) joint (TCJ), subtalar joint (STJ), and midtarsal joint (MTJ) shown in Figure 2.4. The TCJ is a synovial hinge joint with distal ends of the tibia and fibula articulating with the talus. The range of motion for the TCJ is 20 deg dorsiflexion and 30 to 50 deg plantarflexion [14].

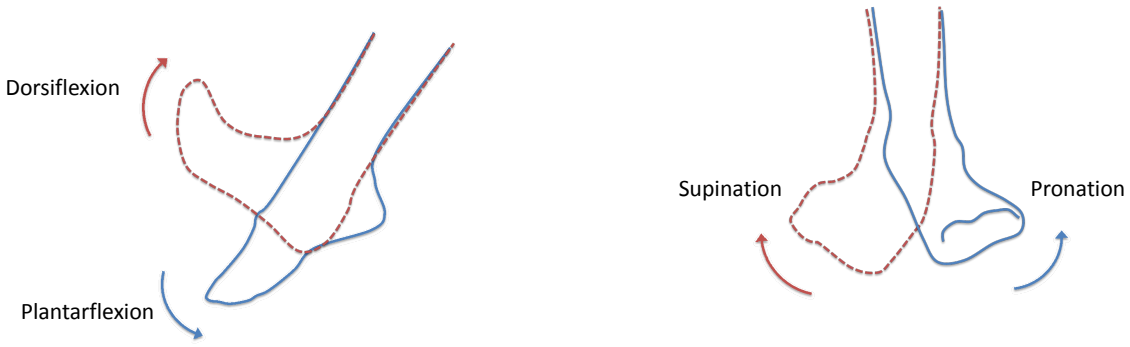

(a) Dorsiflexion/Plantarflexion (b) Supination/Pronation

Figure 2.3: Motions of ankle and foot (adapted from [4]). a) shows a medial view of the right foot in dorsiflexion and plantarflexion, and b) shows a front view of the right foot in supination and pronation.

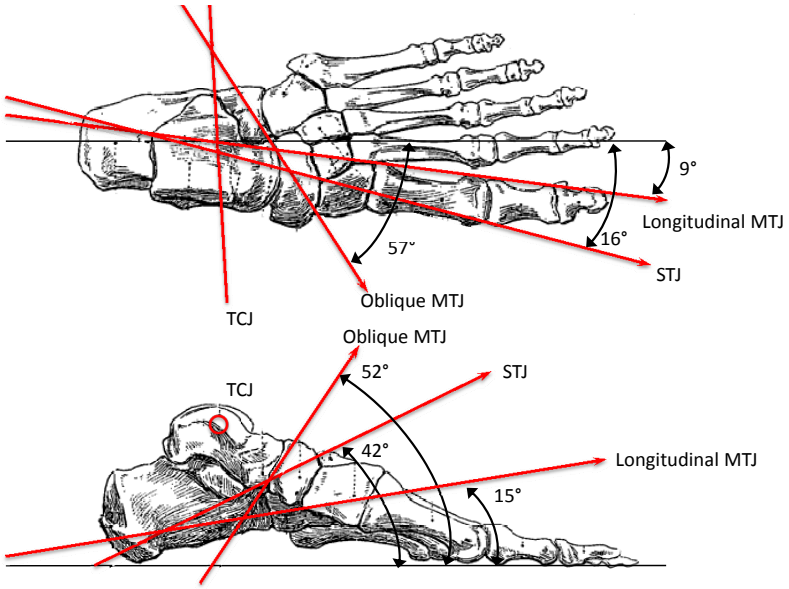

Figure 2.4: Dorsal and medial view of the left ankle and foot joint axes (adapted from [4, 14, 12]). The orientation of the talocrural joint (TCJ), subtalar joint (STJ), and longitudinal and oblique midtarsal joints are shown.

The STJ consists of three articulations with two aspects: the posterior talocalcaneal joint and the anterior talocalcaneonavicular joint. The STJ is a single axis joint which behaves like a mitered oblique hinge [15] where its motions depend on whether the foot is free to move unrestricted (e.g., swing phase) or restricted by the ground (e.g., stance phase).

Unrestricted motion is described as "open kinetic chain" movement and restricted motion is described as "closed kinetic chain" movement [15]. However since these movements are related to joint articulation, a more accurate description would be an open or closed "kinematic chain". Table 2.1 summarizes the differences using the terminology in [15]. These motions do not occur about the TCJ or MTJ [15].

Table 2.1: Kinetic chains of subtalar joint [15]

	Open Kinetic Chain	Closed Kinetic Chain
Supination	Calcaneal Inversion	Calcaneal Inversion
	Calcaneal Adduction	Talar Abduction
	Calcaneal Plantarflexion	Talar Dorsiflexion
Pronation	Calcaneal Eversion	Calcaneal Eversion
	Calcaneal Abduction	Talar Adduction
	Calcaneal Dorsiflexion	Talar Plantarflexion

During open kinetic chain movement, the location of the subtalar axis remains predominantly fixed. During closed kinetic chain movement, internal and external rotations occur which cause the subtalar axis to translate medially and laterally. The degree of translation is more pronounced on the dorsal surface of the foot [16]. Since the triplanar motions of the subtalar joint complicate its motion assessment, inversion and eversion are typically reported. The ranges of motion are 20 deg for inversion and 10 deg for eversion [3]. In a study by Ball et al. [17], the values were up to 30 deg inversion and 20 deg eversion.

The MTJ, also known as Chopart's joint consists of two joints: the calcaneocuboid joint laterally and the talonavicular joint medially, which contribute to the midtarsal axes (longitudinal and oblique). The midtarsal joint axes in Figure 2.4 are shown in the neutral foot position. The orientation of these axes depends on the STJ rotation [15]. When the STJ is pronated, the planes of midtarsal axes become parallel which results in an unlocking of the MTJ changing the foot into a mobile structure reducing stability. This results in the "softening" of the foot enabling it to accommodate varying terrain. As the STJ moves from a pronated through the neutral position to a supinated position, the planes of the axes converge. The convergence locks the bones in the MTJ creating a rigid foot structure necessary for maximum stability.

The range of motion of the talonavicular joint can be up to 15 deg from dorsiflexion to plantarflexion, and up to 34 deg from supination to pronation. The range of motion of the calcaneocuboid can be up to 9 deg from dorsiflexion to plantarflexion, and up to 15 deg from supination to pronation [18].

Understanding joint articulation of the ankle and foot is useful for the design of an AFO as it defines the axes of motion and ranges of motion of each joint of which the AFO would control. As subsequently discussed, currently available AFOs highly restrict joint articulation, and thus one of the goals of the AAFS is to enable as much natural joint motion as possible.

2.1.1.3 Muscles

Soft tissues of the ankle and foot such as ligaments and fascia aid in shock absorption and passive stabilization [10], but active actuation is controlled by the musculature surrounding the joints. Muscle activation is necessary for propulsion and dynamic stability [10]. This is achieved by the contraction of muscles surrounding the ankle and foot to provide an active force across a joint axis. The result is a net moment about the joint axis which changes the motion of the joint. Figures 2.5 to 2.7 present the musculature of the ankle and foot with the joint axes crossed by each muscle and their functional role. Understanding how muscles control the ankle and foot about each joint axis can aid in the placing of actuators of an AAFS to provide corrective moments.

The ankle and foot bones, joints, and musculature are important to control ankle and foot motion. The bones and joint axes provide the foundation by which the musculature can apply forces and moments to achieve desired kinematics. However, when these forces are not adequate, changes in walking or gait patterns can occur and a device such as an AAFS to provide the force or moment deficit becomes necessary. Understanding healthy gait kinematic and kinetic patterns is thus reviewed next.

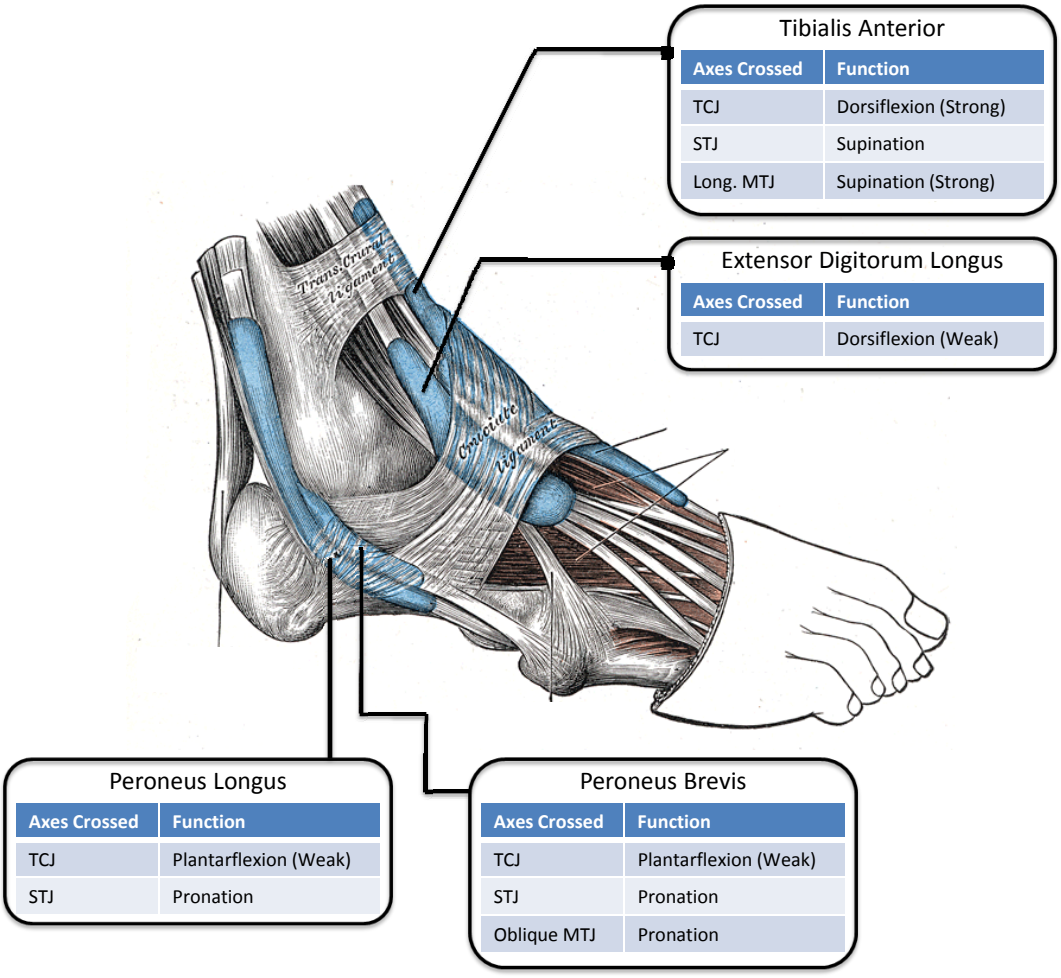

Figure 2.5: Lateral view of ankle and foot showing tibialis anterior, extensor digitorum longus, peroneus longus and peroneus brevis muscles (adapted from [10, 4, 19]).

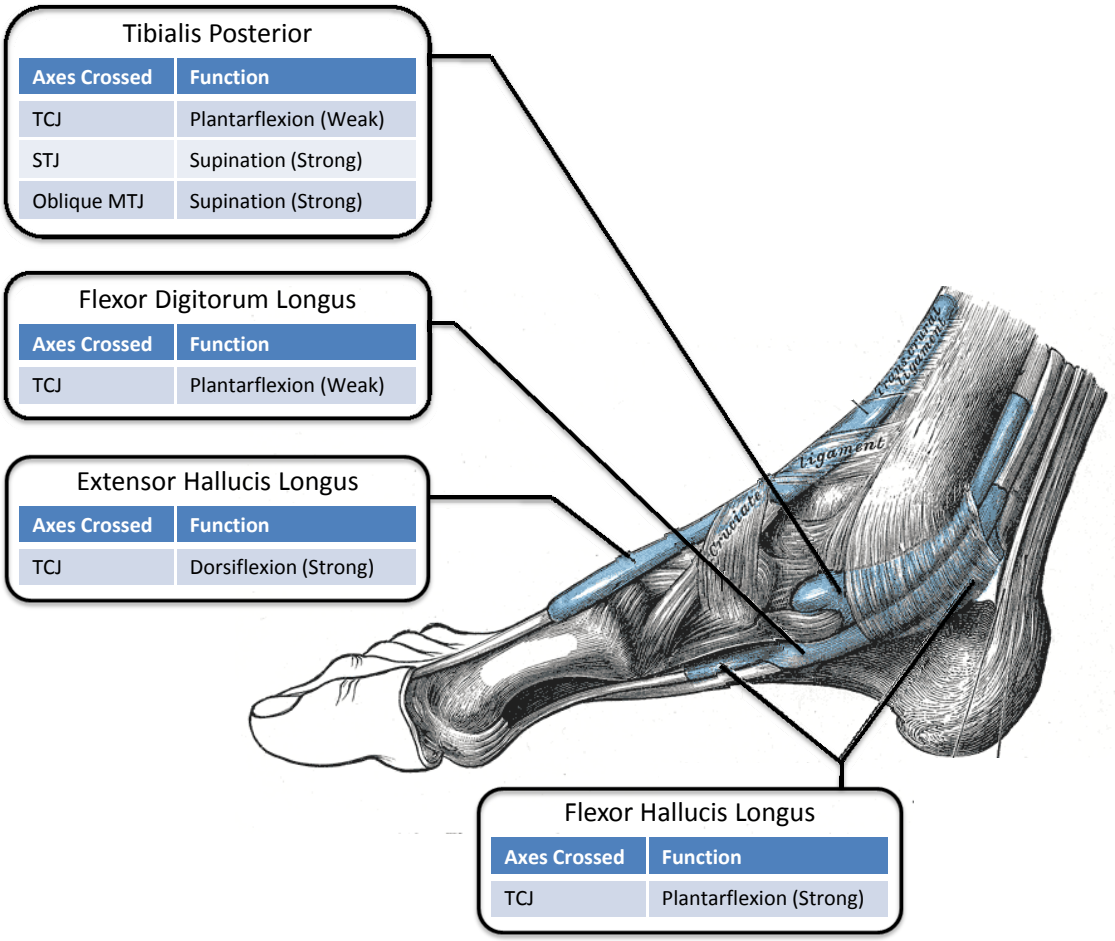

Figure 2.6: Medial view of ankle and foot showing tibialis posterior, flexor digitorum longus, extensor hallucis longus and flexor hallucis longus muscles (adapted from [10, 4, 20]).

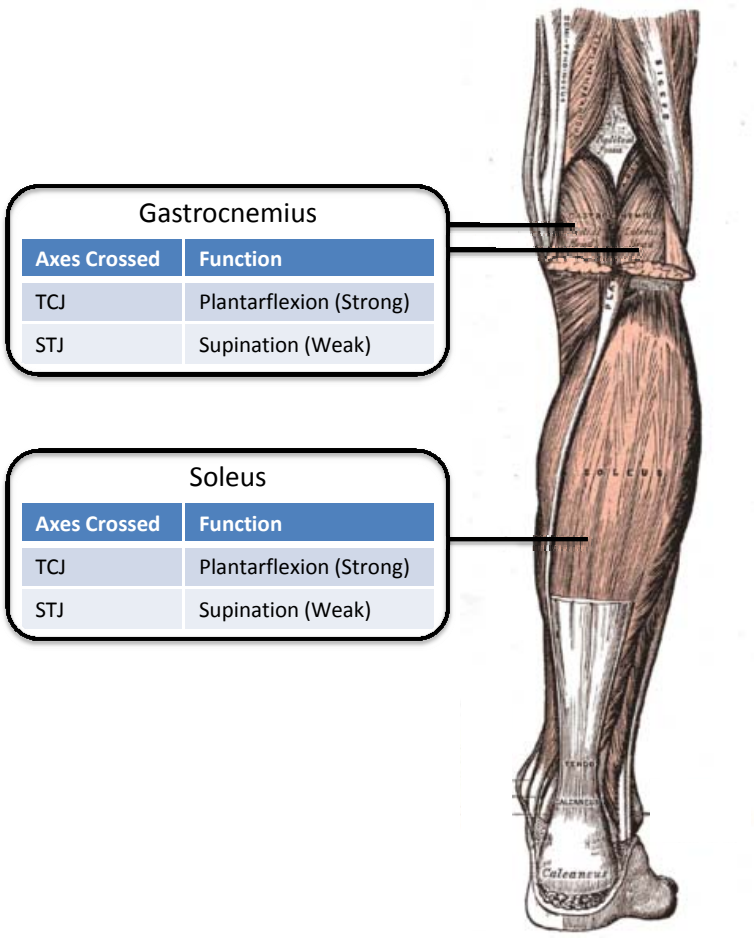

Figure 2.7: Posterior view of foot, ankle, and shank showing the triceps surae consisting of gastrocnemius (medial and lateral heads shown as cut muscles) and soleus muscles (adapted from [10, 4, 21]).

2.1.2 Gait

The following is a review of the aspects of gait which are controlled directly by the ankle and foot.

2.1.2.1 Gait Cycle

Walking is described by the gait cycle (GC) which is divided into two phases: the stance and swing phases [10]. Stance is the duration of the foot on the ground and swing is the duration of the foot in the air for limb advancement [10]. The typical duration (see Figure 2.8) of the floor contact periods are 60% for stance and 40% for swing, the total of which is one stride. The main single events are heel contact (HC), foot flat (FF), heel off (HO), and toe off (TO) as illustrated. Furthermore, stance can be divided into three intervals: initial double support (10% of GC duration), single limb support (40% of GC duration), and terminal double support (10% of GC duration). For young healthy adults (YHA) at natural cadence, the average stride length is 1.56 m with a velocity of 1.44 m/s [1]. Consequently, the duration of a single stride is 1.08 s.

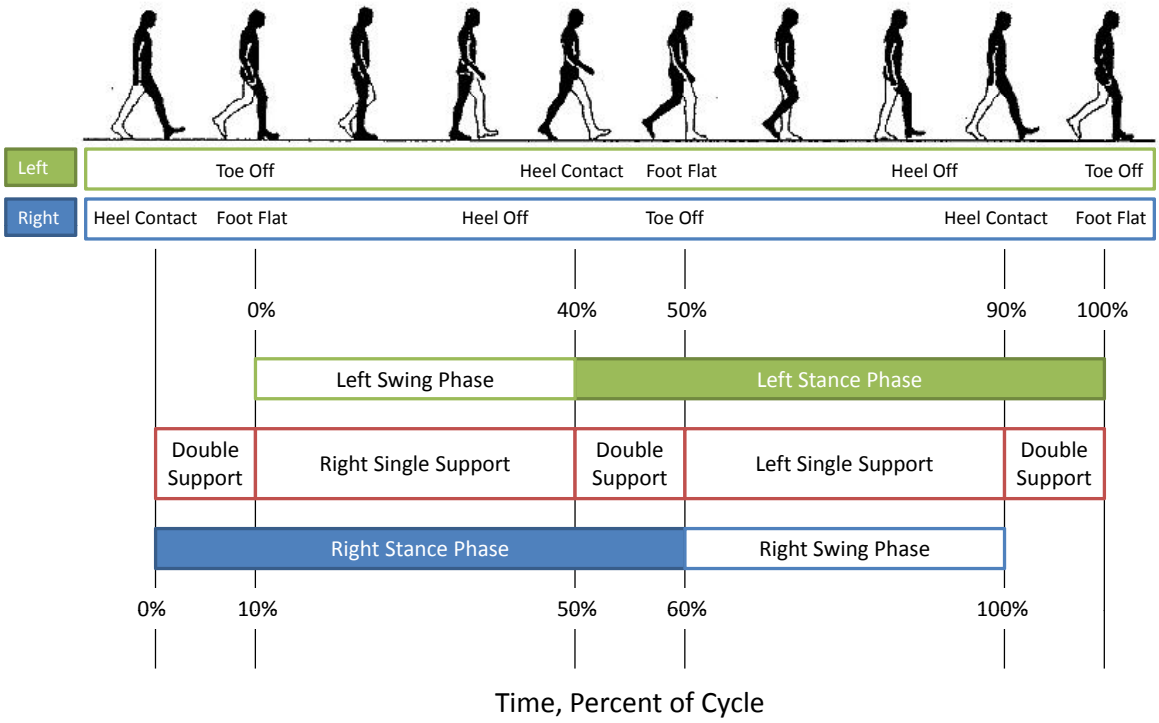

Figure 2.8: Gait cycle (adapted from [10, 4]).

From a functional level, the gait cycle can be divided into three main tasks: weight

acceptance, single limb support, and limb advancement. Table 2.2 decomposes each of these tasks into the individual sub-tasks that form the gait cycle.

Table 2.2: Functional division of gait cycle (adapted from [10]).

Task	Sub-task	% GC	Objective
Weight Acceptance	Initial Contact	0-2%	Start stance
	Loading Response	0-10%	Shock absorption Weight-bearing stability Preservation of body progression
Single Limb Support	Mid Stance	10-30%	Progression of the body over the stationary foot Limb and trunk stability
	Terminal Stance	30-50%	Progression of the body beyond the supporting foot
Limb Advancement	Pre-Swing	50-60%	Position the limb for swing Weight transfer
	Initial Swing	60-73%	Foot clearance from the floor Advancement of the limb from its trailing position
	Mid Swing	73-87%	Limb advancement Foot clearance from the floor
	Terminal Swing	87-100%	Complete limb advancement Prepare the limb for stance

Thus far the gait cycle has been described by the positioning of the lower limbs. Since the design of an AAFS considers only the shank, ankle, and foot, the gait cycle can be defined specifically at the ankle joint as four main periods as shown in Figure 2.9. The periods consists of three stance periods which are controlled plantarflexion (CP), controlled dorsiflexion (CD) and powered plantarflexion (PP), and a single swing phase. Each is described in more detail in the next section as it relates to joint kinematics and kinetics. For a young healthy adult [1], foot flat occurs at approximately 10% of the gait cycle and heel off occurs at approximately 45% of the gait cycle. This definition of the gait cycle

is later utilized to determine the sagittal plane functional requirements of the AAFS in Chapter 4.

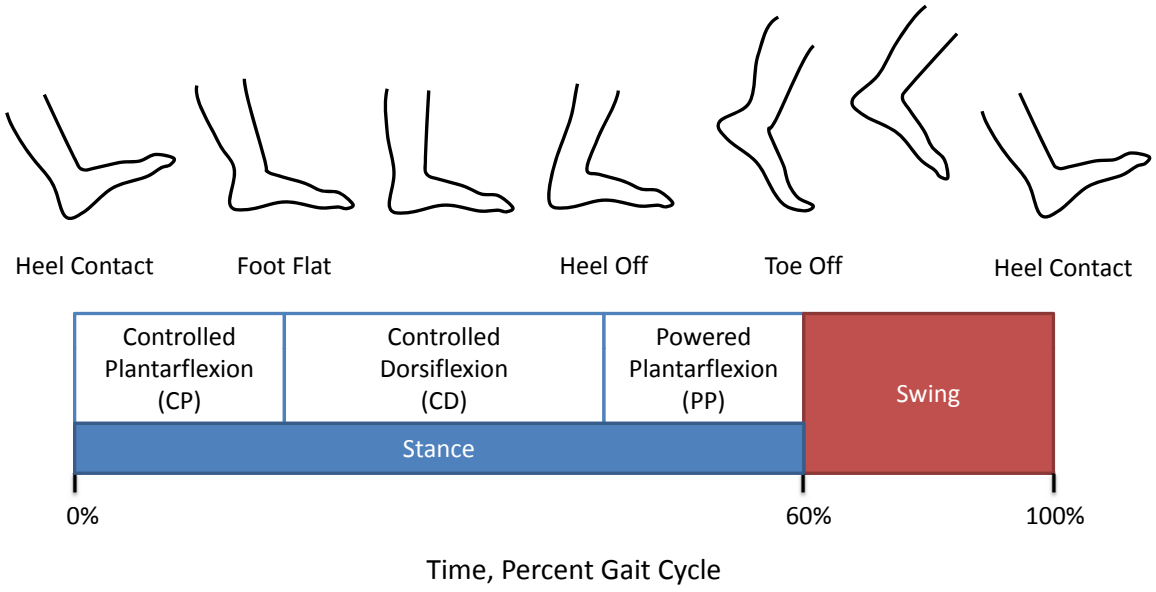

Figure 2.9: Functional breakdown of gait cycle at ankle (adapted from [10, 22]. There are four periods which are controlled plantarflexion (heel contact to foot flat), controlled dorsiflexion (foot flat to heel off), powered plantarflexion (heel off to toe off), and swing (toe off to heel contact).

2.1.2.2 Joint Kinematics and Kinetics

The external forces affecting the kinematics of the ankle and foot are known as ground reaction forces (GRFs). These are the forces of the ground acting on the plantar surface of the foot. A force plate is often used to measure these forces along three orthogonal axes (vertical, fore-aft, and mediolateral) [4] as shown in Figure 2.10. From these measured forces, joint forces and moments can be calculated using the link segment model developed in [23].

The ankle and foot segments move about the joint axes in particular patterns during the gait cycle. These constitute the interaction between the GRFs, resistance from passive tissues, and active muscle activation. Figure 2.11 illustrates the typical TCJ, STJ and MTJ motions for one complete stride.

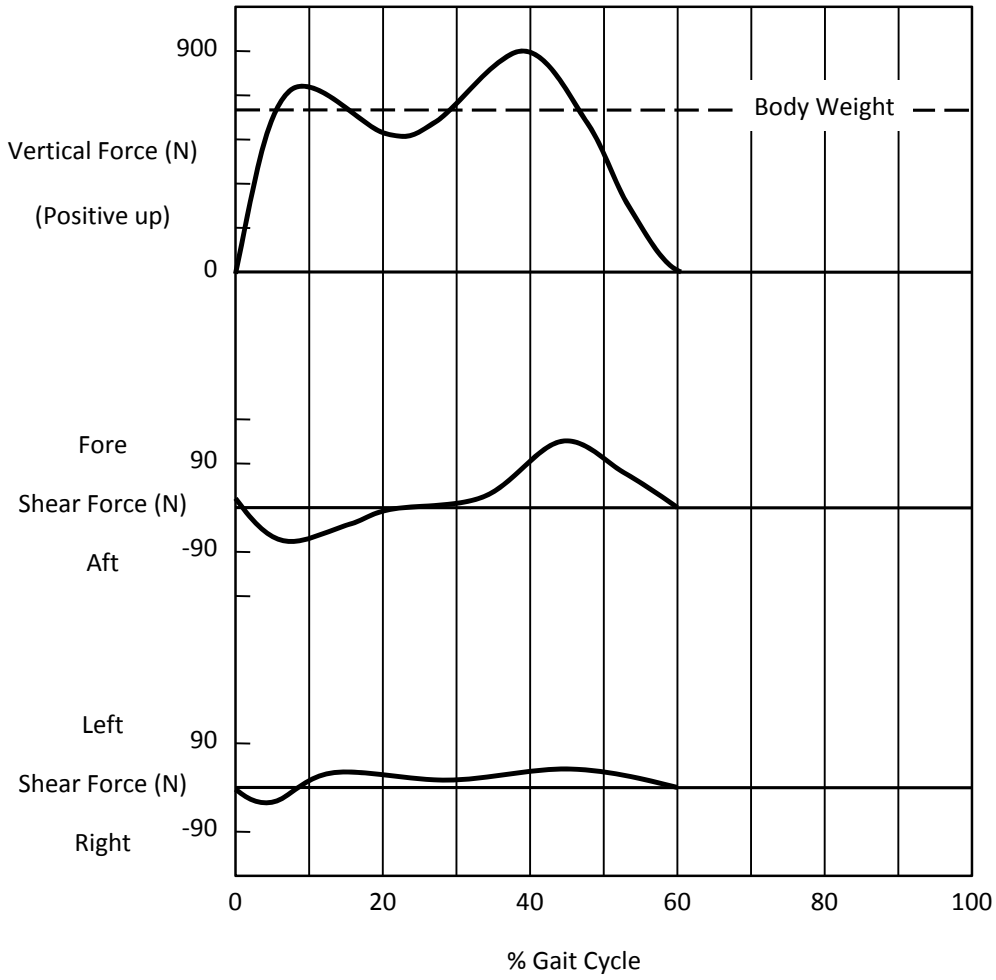

Figure 2.10: Typical ground reaction force profiles for right foot (adapted from [10, 4]). The dashed line indicates the vertical force corresponding to body weight.

During CP, the ankle undergoes plantarflexion from the neutral position to approximately 10 deg of plantarflexion due to the plantarflexion moment created by the GRF acting on the heel passing posterior to the ankle [4]. The rate of plantarflexion is controlled by the action of the anterior tibial muscles to decelerate the foot drop and in turn, drawing the tibia forward [10]. The tibialis posterior also decelerates the pronation of the STJ during early stance [4]. As mentioned previously, shock absorption occurs during the initial load bearing phase of CP [10].

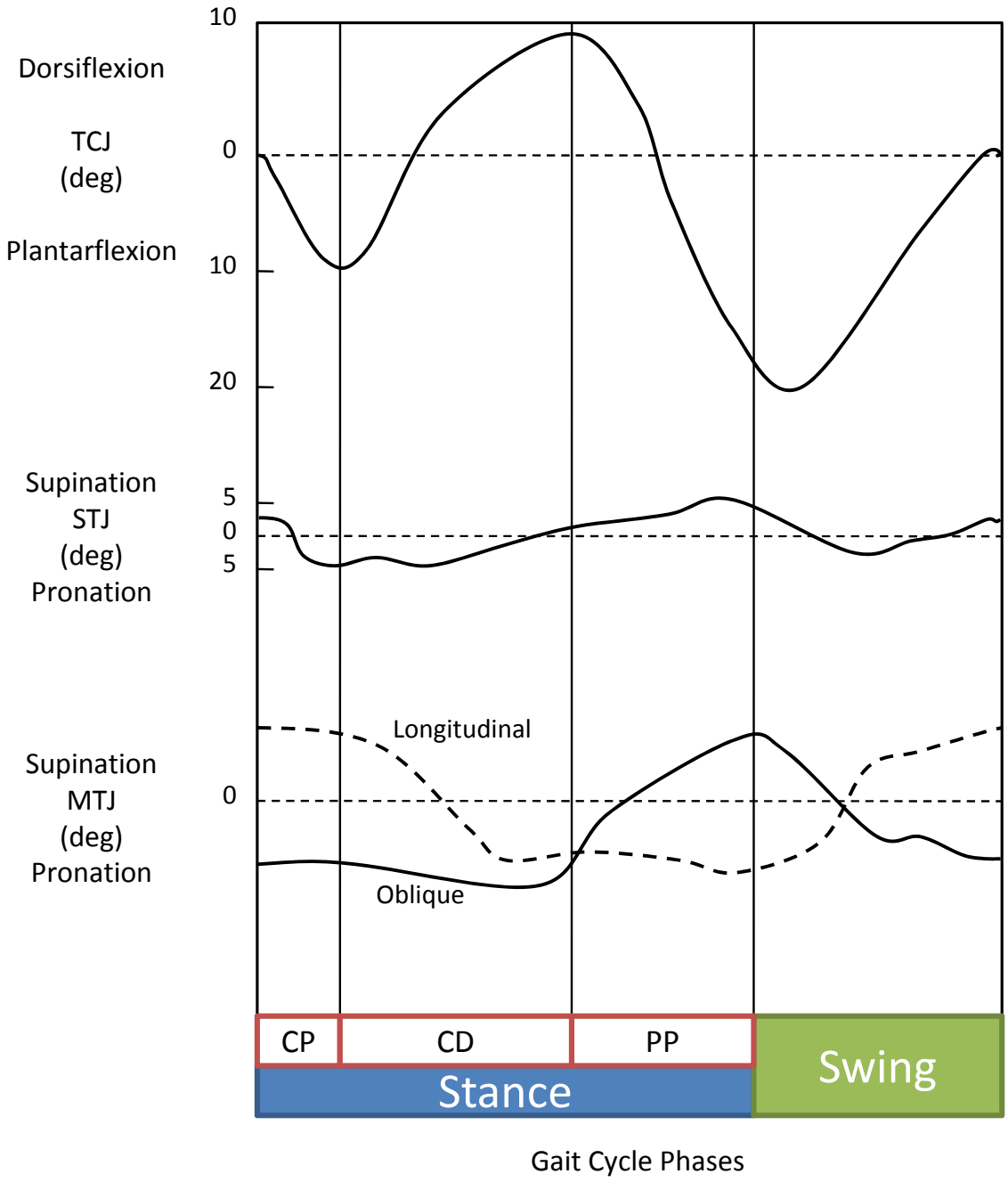

Figure 2.11: Graph of typical joint angles of the ankle joint (talocrural joint), subtalar joint, and midtarsal joints for a single stride of a young healthy adult (adapted from [10, 4, 22]). The stance phase is divided into three periods: controlled plantarflexion (CP), controlled dorsiflexion (CD), and powered plantarflexion (PP).

During CD, the ankle acts as a fulcrum to allow the lower leg to roll forward due to the forward body momentum ([4, 22, 10]). The foot is firmly located on the ground and as the

lower leg moves forward the ankle joint attitude changes from 10 deg of plantarflexion to about 10 deg dorsiflexion [4, 10]. Dorsiflexion occurs and the GRF moves anterior to the ankle joint [4]. The GRF is controlled by the plantarflexors, in particular the soleus, to decrease the rate of rotation of the shank about the TCJ [10]. The tibialis posterior also supinates the STJ with the assistance of the gastrocnemius muscle [4].

The characteristic feature of the PP phase is the rapid plantarflexion of the ankle from 10 deg of dorsiflexion to 20 deg of plantarflexion [4, 10] decelerating the rate of tibial progression [10]. This occurs, due to the plantarflexor (gastrocnemius and soleus) activity, in spite of the large dorsiflexion moment induced by the GRF. During this phase extension of the toes occurs [4]. The soleus is used to stabilize the lateral forefoot in the frontal plane and the peroneal muscles pronate the STJ [4].

During the swing phase, the anterior tibial muscles maintain the foot in a neutral attitude to aid toe clearance [4]. Prior to heel-contact, the tibialis anterior supinates the foot.

In general, the side to side movement of the body and axial rotation of the leg during midstance phase are possible because of the mobility of the joints within the foot, particularly the STJ [4]. Also, throughout stride, the tibialis anterior prevents excessive pronation and the tibialis posterior stabilizes the MTJ.

The TCJ is the dominant joint in the ankle and foot complex. Since its axis is virtually perpendicular to the sagittal plane (see Figure 2.4), the kinematics and kinetics for the TCJ are more readily determined. Typical graphs of the mean ankle angle, angular velocity, moment and power for one stride for young healthy adults (YHA) are shown in Figure 2.12. In particular, the plantarflexion power developed by the ankle is the single most important energy generation phase and results in 80-85% of that generated during the entire gait cycle [1]. This occurs at approximately 50% of the gait cycle. For perspective, if a person has a body mass of 90 kg, the peak moment is 146 Nm and the peak power is 300 W.

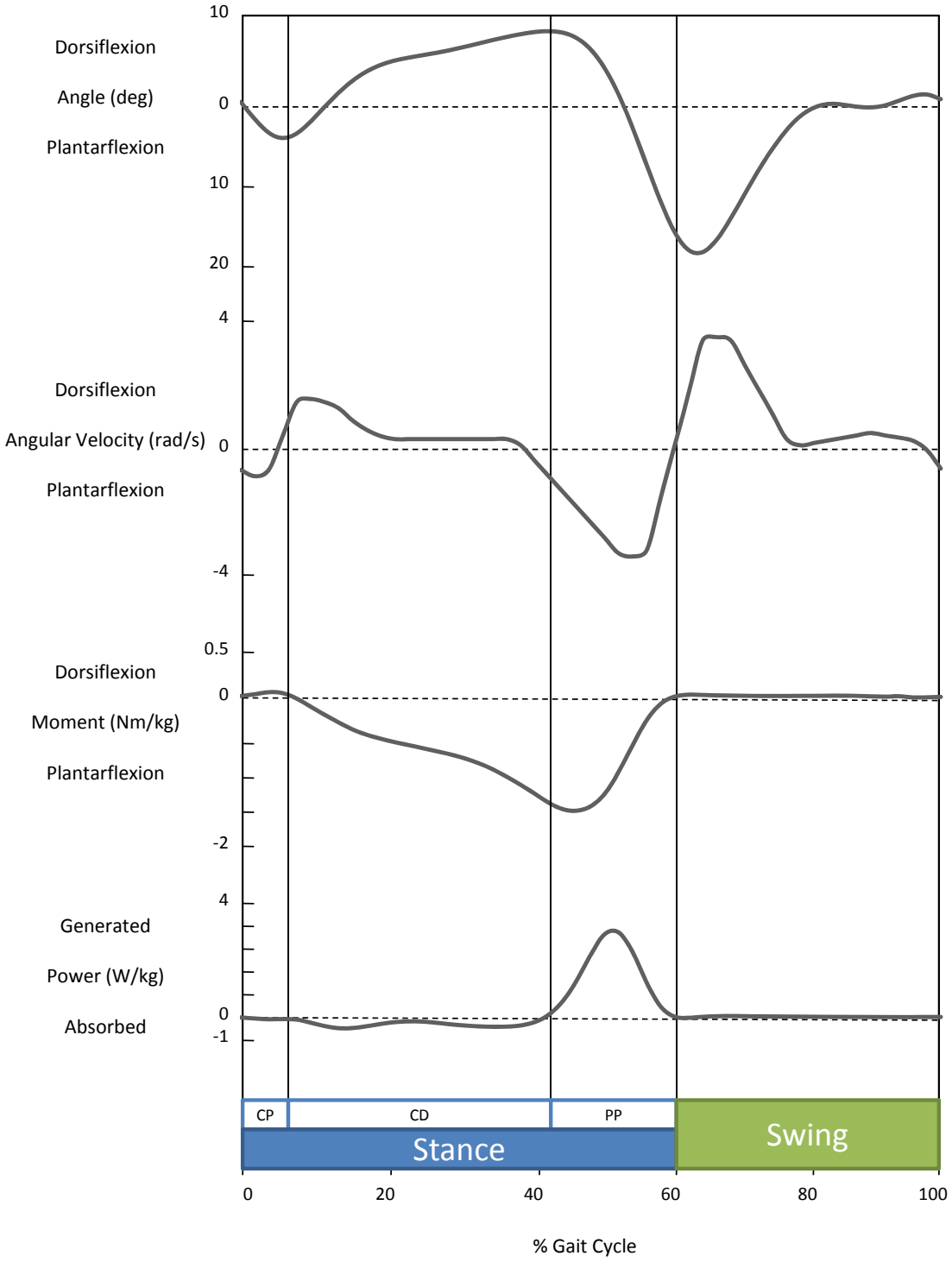

Figure 2.12: Graph of mean ankle angle, angular velocity, moment, and power versus percentage gait cycle for a young healthy adult (adapted from [1]).

2.1.3 Balance and Stability

Stance stability is affected by the center of pressure (COP) and center of mass (COM) which can be controlled by the ankle and foot. The COP is the point location of the vertical GRF vector where the weighted average of the pressures over the surface of the area in contact with the ground do not produce a net moment. If one foot is on the ground, the net COP lies within the contact area of the foot and ground. If both feet are in contact with the ground the net COP lies somewhere between the lateral boundaries of the two feet, depending on the relative weight taken by each foot. Furthermore, when both feet are in contact, there are separate COPs of each foot [24]. The outermost bounding region defined by the boundaries of the foot defines where the COP can be located and is known as the Base of Support (BOS) [25].

The center of mass (COM), or center of gravity (COG), is a point where the total body mass in the global reference system is located and is defined by the distance-weighted average of the COM of each body segment in three-dimensional space. It is a passive variable controlled by the balance control system which is independent of the COP [24]. In standing, the balance task is to keep the body's COM safely within the BOS [24]. Figure 2.13 illustrates this phenomenon in various standing trials [25]. As the BOS decreases, the COM location spans broader to maintain stability as indicated by the floating dot within the span area (dark area). In balance during quiet or slight perturbed standing the ankle muscles (plantarflexors/ dorsiflexors) dominate in the anterior/posterior direction, whereas in the tandem (heel-to-toe) position the ankle muscles (supinators/pronators) dominate in the medial/laterial direction [24].

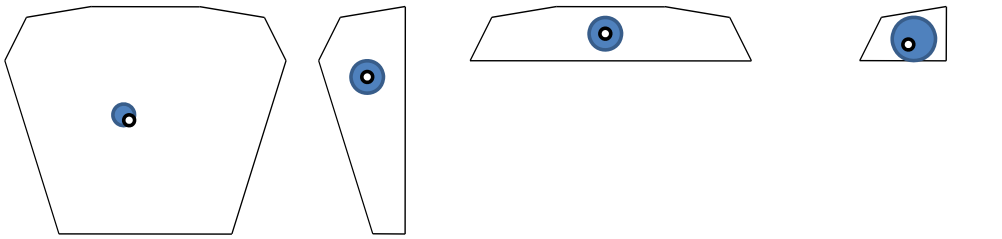

(a) Two feet (b) One foot (c) Two feet on toes (d) One foot on toes

Figure 2.13: Standing trial plots of the center of mass within the base of support (adapted from [25]). In each trial, the center of mass is indicated by the white dot which varies within the dark span area. As the base of support decreases, the span area increases.

At the start of locomotion, the goal is to move the body outside the BOS and yet prevent

falling [24]. This is referred to as gait initiation which involves the hip and ankle joints. Figure 2.14 illustrates the relationship between the COM and COP during this motion where the right leg steps forward [24]. During the release phase the COP moves posteriorly towards the swing limb, thus accelerating the COM forward and towards the stance limb. Posterior COP displacement results from a deactivation of the plantarflexors and, in some cases, an activation of the dorsiflexors (tibialis anterior). The lateral displacement of the COP results from a momentary loading of the swing limb (right) by body weight due to the action of the hip abductors. Unloading is achieved by a rapid activation of the stance limb (left) hip abductors and deactivation of the right hip abductors. After unloading of the right limb the COP under the stance limb moves forward under the control of the plantarflexors to achieve a forceful push-off. During this single support time, the COM accelerates forward and away from the stance limb. Gait termination is a virtual mirror image of gait initiation [24]. After heel contact of the stance foot, the COP moves rapidly forward due to increased plantarflexor activity [24].

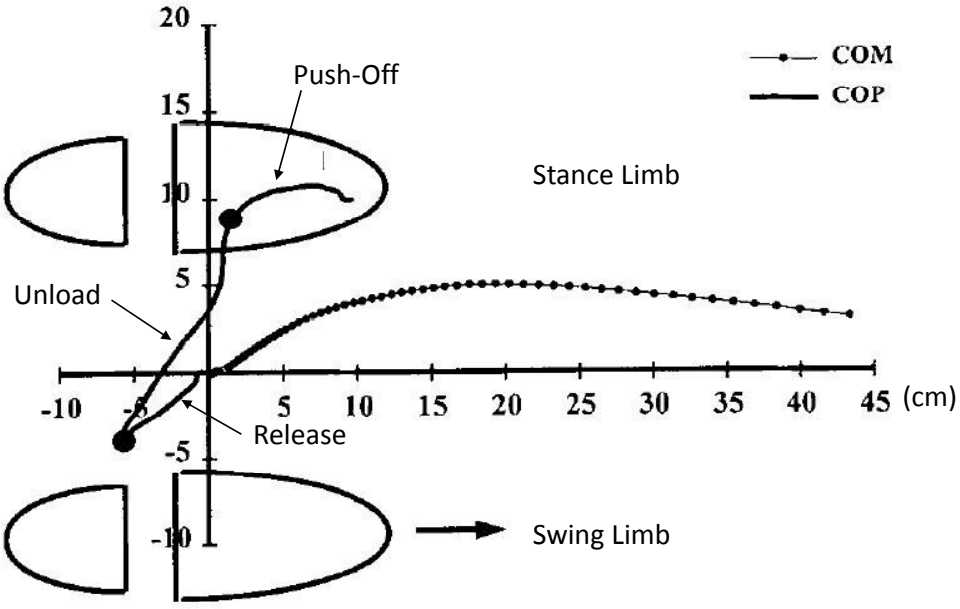

Figure 2.14: Center of mass projection and center of pressure trajectories during gait initiation with motion beginning at the origin (0,0) (adapted from [24]).

In steady-state walking or running, the COM is always outside the BOS (except during the short double support period in walking). This is described as dynamic balance where the swing limb has a trajectory which will achieve balance conditions during the next stance phase [24]. During steady-state gait, the projection of the COG follows a smooth sinusoidal motion as illustrated in Figure 2.15. The COP under each foot during stance

progression is also shown in Figure 2.15. Gait time markers for each foot on the COG projection curve correspond to the gait time markers on the COP curve for each foot.

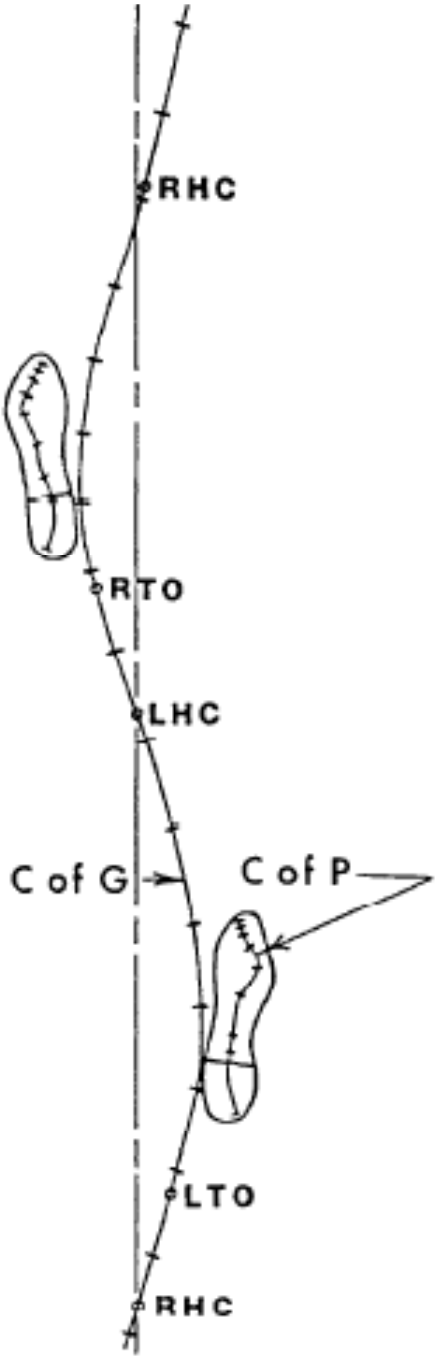

Figure 2.15: Center of gravity and center of pressure path during gait (adapted from [1]. R = right, L = left, HC = heel contact, TO = toe off.

The ankle and foot fine tune gait patterns particularly during stance in both the ante-

rioposterior and mediolateral directions. The ankle muscles of the stance foot themselves cannot always avert a fall, and thus safe placement of the swing foot is necessary once every step. Restabilization can take place during the two short double-support periods, but during this time the support base is not very firm (one foot is accepting weight on the small area of the heel while the other is pushing off on the forepart of the foot).

The supinators and pronators of the ankle and foot are also plantarflexors and dorsiflexors, and thus anterioposterior control of balance in particular, requires collaboration between right and left plantarflexors and dorsiflexors. Also, because of the small width of the foot, the maximum moment that could be generated by either supinators or pronators would only be about 10 Nm for quiet standing. Anything above 10 Nm of muscle moment would cause the foot to roll over on its medial or lateral borders [24].

The ankle and foot bones, joint axes, and musculature are critical to successful gait. The ankle joint is the single most power generator during propulsion and is important in balance and stability. The deterioration or diminished capacity of the ankle and foot joint complex can result in difficult locomotion causing activity avoidance and limited independence. In particular, there are three populations of interest with ankle and foot gait deficiencies which are reviewed next.

2.2 Populations with Ankle-Foot Gait Deficiencies

There are at least three populations with ankle and foot gait deficiencies that would benefit from an AAFS. These are the elderly, drop foot patients, and individuals who have sprain-injured ankles. The characteristics of each population and benefits of using an AAFS are discussed next.

2.2.1 Elderly People

The ability to walk becomes increasingly difficult with age. Natural muscular and neurological deterioration occur, and abrupt decreases in mobility due to conditions such as a stroke or neurological disorder can arise [9, 8]. To maintain mobility, many elderly people use assistive devices. In fact, more than 23% of non-institutionalized adults aged 75 and older use a mobility technology device, with 49% using a cane, 24% using a walker, and 12% a wheelchair [9]. An understanding of elderly gait and identification of the corrective measures required to achieve normal gait can lead to the development of an AAFS for elderly people.

Elderly individuals may be considered as either non-fallers or fallers. Non-fallers are healthy and fit with no previous history of falls. Fallers are elderly individuals who have previously fallen or who have high risk factors of falling and also have characteristics of non-fallers. Both groups are discussed in detail.

2.2.1.1 Non-fallers

The differences in non-faller gait patterns compared with young, healthy adults are based on biomechanical, plantar pressure, and spatio-temporal characteristics.

Biomechanical Characteristics Age contributes to the deterioration of balance mechanisms and loss of muscle mass resulting in greater instability [8]. Elderly non-fallers exhibit decreased stride-to-stride variation in muscle activation compared with younger adults [1]. Elderly people also tend to exhibit flat-footed landings attributable to muscle weakness and increased base of support [26] and a slower reaction time [27, 28, 29]. In a study by Tucker et al. [28], static and dynamic reaction times were investigated based on postural sway testing. Elderly subject reactions were at least 100 ms slower than young subjects for both conditions.

A decrease in joint range of motion is also observed in the elderly although there is a small increase in range of motion until 45% gait cycle. At the STJ, the average overall range of motion decreased from 53.2 deg in 20-year-olds to 44.3 deg in 60-year-olds [17]. At the TCJ during gait, push-off begins at 12.35 deg dorsiflexion and ends at 12.53 deg plantarflexion, resulting in a total of 24.9 deg range of motion versus 29.3 deg in younger adults [1]. Peak plantarflexion is reduced from 17 deg to 13 deg [8]. Lower muscle mass contributes to lower strength and power and results in a decreased range of motion. At the TCJ, the plantarflexion moment is reduced from 1.63 Nm/kg to 1.44 Nm/kg and the peak ankle power reduces from 3.27 W/kg to 2.75 W/kg during push-off [1]. This is significant since push-off is the single most important energy generating phase required for gait. The typical angle and moment profile of a non-faller is shown in Figure 2.16. As shown, the overall dorsiflexion to plantarflexion angle range of motion and peak plantarflexion moment are less than those of young healthy adults.

Additionally, changes at ankle and foot result in compensatory strategies at the knee and hip joints. For example, at maximum pace, elderly people increase hip power to maintain speed whereas young adults increase power at all joints [30]. The elderly used their hip extensors more and knee extensors less when walking at the same speed compared with young adults [31].

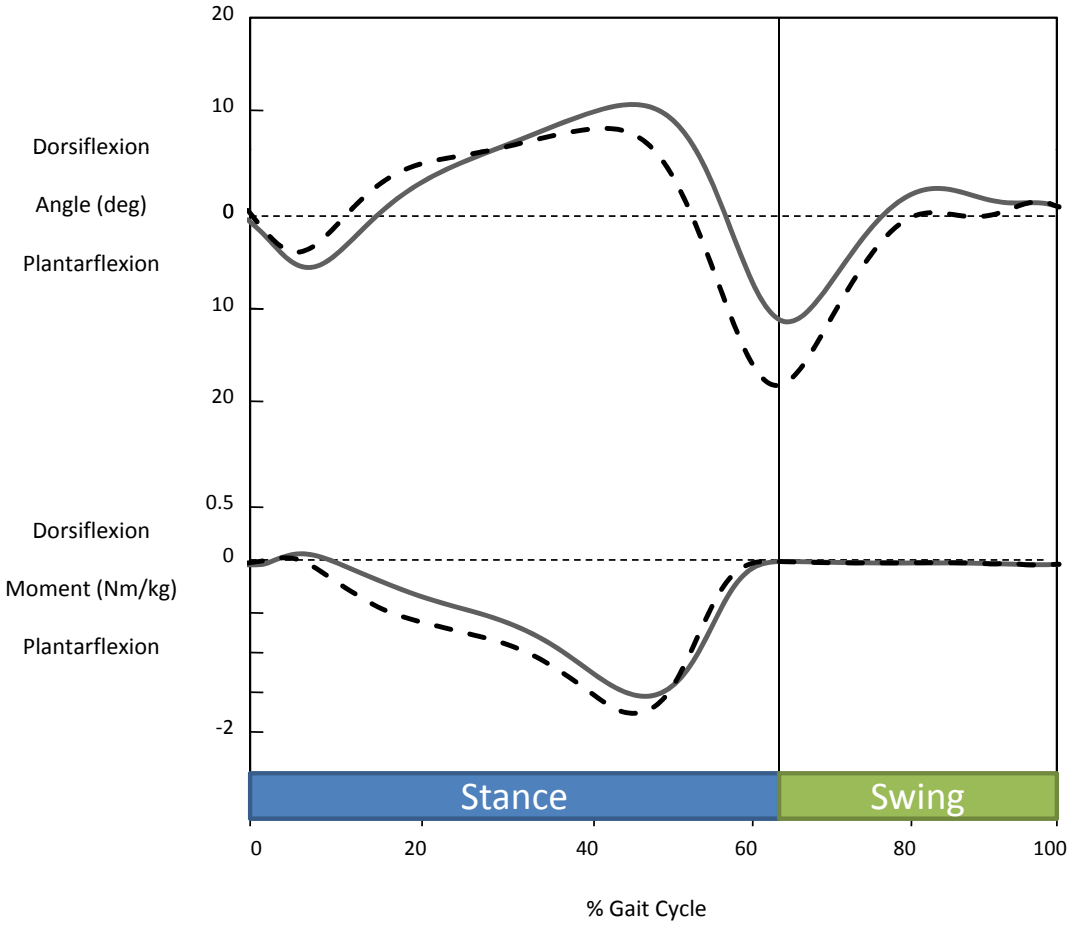

Figure 2.16: Graph of mean ankle angle and moment versus percentage gait cycle for elderly individuals (solid line) [1] compared with young healthy adults (dashed line) [1].

Plantar Pressure Characteristics During gait, plantar pressures follow a particular pattern, with individual intrastride variation. In elderly people, the plantar pressures differ in magnitude for particular regions. For example, decreased pressure is observed in the rear and midfoot regions as a result of aging [32]. Plantar pressure is also decreased at the hallux qualified by a decreased push-off force [33, 34].

Plantar pressures are also an indicator of stability. Weak dorsiflexors of elderly people have shown to decrease mediolateral stability [35]. As heel-contact occurs, medial and lateral shifts in the COP under the foot occur since the foot cannot be supinated correctly. The result is greater instability due to the unlocking effect of the foot bones.

Spatio-temporal Characteristics The biomechanical changes in the elderly result in spatio-temporal characteristics. First, a shorter stride length of 1.38 m is observed ver-

sus 1.56 m in young adults [1]. Walking velocity in healthy elderly people is also lower [1, 9], 1.29 m/s compared with 1.44 m/s in young healthy adults [1]. Other factors such as head stability and anterioposterior body accelerations contribute to lower velocity. Consequently, the elderly have a higher stance time of 65.5% versus 62.3% in young adults. In conjunction, their double support time is also increased to 31.0% from 24.6% for young adults. Finally, their mediolateral stride spacing increases to aid in stabilization particularly during obstacle crossing [36, 37] to increase their BOS.

By reducing velocity, increasing stance and double support time, and increasing stride spacing, elderly people are maximizing their stabilization time while maintaining balance. It was concluded by Winter [24] that the ankle has an insignificant role in mediolateral control during steady-state gait in young, healthy individuals. However, the characteristics exhibited by elderly individuals, particularly increased stance time and decreased reaction time, infer that mediolateral control at the ankle is significant. Perturbations to gait such as crossing and avoiding obstacles require considerable mediolateral control. Since dorsiflexors and plantarflexors are, in essence, supinators and pronators, the loss of anterioposterior control is associated with a loss of mediolateral control, the finer adjustments of which are controlled by the ankle and not the hips.

2.2.1.2 Fallers

One-third of those over 65 years of age fall at least once per year in the world. Approximately 50% of these individuals will suffer recurrent falls [38]. Direct care costs of injuries resulting from falls for people age 65 and older is expected to reach $32.4 billion by the year 2020 (Englander et al., 1996, as cited in [39]). Falls in the elderly are a major source of morbidity and mortality [40]. In 2003, a total of 13,700 persons aged 65 years and older died from falls, and 1.8 million were treated in emergency departments for nonfatal injuries from falls [41]. Falling causes the majority of hip fractures, which often result in long-term functional impairments that might require admission to a nursing home for a year or more [41]. Gait disorders are a common risk factor for falls [9] and can be attributed to many diagnoses particularly neurological disorders leading to diminished locomotion. Table 2.3 reviews primary diagnoses contributing to gait disorders and the percentage presented [9].

The typical profile of a faller includes many of the abnormal stride parameters of non-fallers (e.g., broad BOS, slower speed, decreased stride symmetry, etc.) along with further deterioration of balance mechanisms. Additionally, there are many other factors that can contribute to falls including: impaired range of motion [34]; greater lateral sway [42]; loss of sensation [34]; delayed or prolonged muscle activation disrupting normal gait sequencing [43]; greater variability in step length and wider stride width [44]; longer gait termination

time [45]; decreased toe plantarflexor strength [34]; hallux Valgus deformity [34]; disabling foot pain [34]; weak dorsiflexors resulting in mediolateral COP shifts [35]; increased gait asymmetry [46]; and joint kinetic changes [47] such as higher peak hip extension moment in stance, lower peak hip extension moment in pre-swing, lower knee flexion moment in pre-swing, and lower knee power absorption in pre-swing.

Table 2.3: Diagnoses in older adults presenting with gait disorders (adapted from [9]).

Diagnosis	% Presenting
Frontal gait disorder (gait apraxia)	20-28
Normal-pressure hydrocephalus	4
Multiple strokes/Binswanger's disease	16-28
Sensory imbalance	4-18
Neuropathy	4
Multiple sensory deficits	4-18
Myelophathy	16-24
Cervical Spondylosis	22
Vitamin B12 deficiency	16-24
Parkinsonism	10-12
Idiopathic Parkinson's disease	8
Drug-induced parkinsonism	10-12
Progressive supranuclear palsy	2
Cerebellar atrophy	8
Other	14-16
Essential ("senile") gait disorder	6-14

Any of the above conditions can be considered a risk factor of falling in the elderly and are directly or indirectly related to stabilization. There are two important events to be considered as well: slipping and tripping. As a result of reduced or delayed hamstring activation, high horizontal velocities occur during heel contact, 1.15 m/s versus 0.872 m/s in young adults [1]. Normally, the heel velocity decreases significantly and enough friction is present to allow safe planting of the swing foot. However, when walking over slippery surfaces such as ice or fine gravel, induced slipping can occur.

Toe clearance is an important factor during obstacle avoidance in elderly people. During the mid swing phase, the toe clearance can be as low as 0.87 cm in the elderly [1]. Furthermore, decreased cognitive function and muscular performance in elderly fallers predisposes them to a high risk of falling when crossing obstacles [48]. Once a fall begins, recovery is critical to avoid injury. Due to their inadequate biomechanical capacities, elderly fall-

ers have difficultly recovering from the onset of falling. For example, weak plantarflexor strength resulting in lower maximum push-off force is an identifier of high-risk fallers during trip recovery [49]. For stepping reactions to avert a fall, the main problems pertain to control of lateral stability [50]. This involves arresting the lateral body motion that occurs during forward and backward steps and controlling lateral foot movement so as to avoid collision with the stance limb during lateral steps. Older adults appear to be more reliant on arm reactions than young adults but are less able to execute reach-to-grasp reactions rapidly.

Tripping can also occur in stroke patients, where a common symptom is drop-foot gait [51]. Drop foot is caused by weak dorsiflexors which are unable to provide a dorsiflexor moment to lift the foot during the swing phase of gait [4]. During swing, the foot drops and the toe drags, increasing the risk of falling. In fact, drop foot has been linked to hip fractures [52, 53]. Therefore, drop foot patients who may also benefit from an AAFS to correct gait are studied next.

2.2.2 Drop Foot Patients

One of the most common ankle and foot gait deficiencies is excessive plantarflexion. This same gait error could also be classified as inadequate dorsiflexion [10]. During stance, the primary functional penalty of excessive ankle plantarflexion is loss of body progression leading to a shortened stride length and reduced gait velocity [10]. There is also decreased stability. During swing, excessive plantarflexion obstructs limb advancement leading to a shortened step [10]. There are several causes of excessive plantarflexion which include pretibial muscle weakness, plantarflexion contracture, soleus and gastrocnemius spasticity, and voluntary excessive ankle plantarflexion [10]. Pretibial muscle weakness, or drop foot, is of particular interest since it is a commonly corrected pathology using an AFO.

Drop foot affects the early stance phase and swing phase of gait. Between HC and FF, weak dorsiflexors are no longer able to control the plantarflexion of the foot resulting in an audible foot slap [4]. During the swing phase, weak dorsiflexors can no longer support the weight of the foot, leading to toe contact with the ground (drop foot, toe drag) at mid-swing [4]. Consequently there is a danger of tripping. During late stance, the gait mechanics depend on the patient's ability to roll onto the forefoot [10]. If heel rise is not attained, the advancement of the body is limited to the extent that knee hyperextension or trunk lean and pelvic rotation improve the forward reach of the opposite limb [10]. An example of a drop foot patient's ankle angle and moment profile throughout the gait cycle is shown in Figure 2.17. Significant differences between the ankle angle and moment of the

drop foot patient compared with young healthy adults are seen throughout the gait cycle, except for the ankle moment during swing.

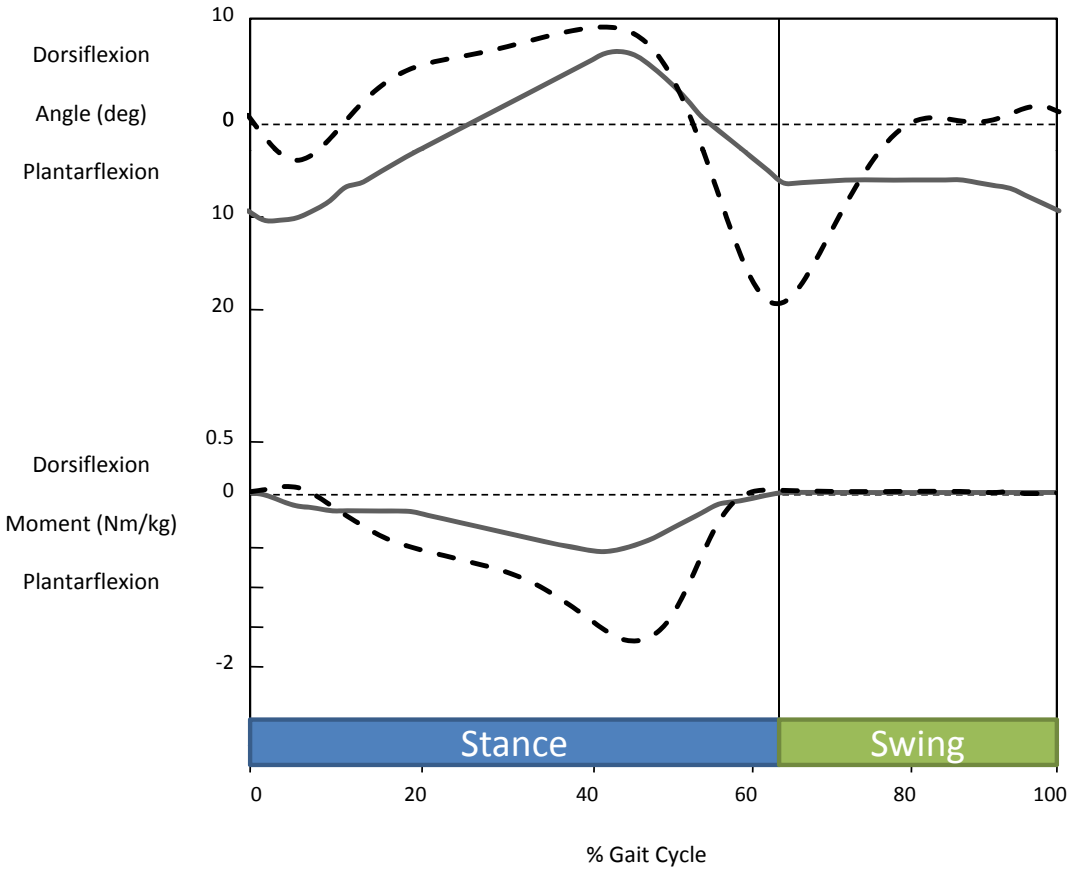

Figure 2.17: Graph of ankle angle and moment versus percentage gait cycle for a drop foot patient (solid line) [54] compared with mean ankle angle and moment for young healthy adults (dashed line) [1].

Drop foot is characterized by steppage gait with increased knee and hip flexion during the swing phase [4]. Toe clearance is also achieved through circumduction (swing phase abduction of the non-supporting hip), hip hiking (elevation of the pelvis and non-supporting leg during midstance) (see Figure 2.18), or vaulting (midstance plantarflexion of the supporting foot) [4]. In more severe cases, heel contact is replaced by flat footed landings (foot nearly parallel with the ground and knee fully extended) or toe contact (a mixture of ankle equinus and knee flexion) [10].

Drop foot is a motor deficiency caused by total or partial central paralysis of the muscles innervated by the common peroneal nerve, or the anterior tibial muscle and the peroneal group [6]. The most common causes of drop foot are stroke, spinal cord injuries, cerebral

palsy, multiple sclerosis, and trauma [55]. In rare instances, ankle sprains have been known to cause peroneal nerve palsy resulting in drop foot gait [56]. In a study by Sidney et al. [57], it is suggested that the ankle weakness which frequently follows sprains and other forced inversion injuries may often be due to entrapment of the common peroneal nerve. Paresis may occur and in some cases, is severe enough to cause drop foot. Individuals with sprain-injured ankles, who may also benefit from an AAFS, are studied next.

Figure 2.18: Image of hip hiking of drop foot patient [58].

2.2.3 Ankle-Sprain Injured Patients

Ankle sprains are the most commonly sustained injuries in physically active individuals [3]. They can be recurrent and also have been known to disrupt proprioception [3]. One of the most common injuries is an ankle inversion sprain [11]. In the United Kingdom, 5000 ankle inversion injuries are treated daily [11]. Sports such as basketball, volleyball, and soccer have a high incidence of ankle injuries where it is common for an athlete to land in a supinated position from a jump, perform a cutting manoeuvre, or encounter uneven terrain [11]. Since ligamentous support of the lateral ankle is much weaker than its medial counterpart, the typical mechanism of injury are either falling away to the opposite side with the foot firmly planted, or supinating the plantarflexed foot while weight bearing [11]. As a result, 40% of individuals who have had inversion sprains are left with functional ankle instability (FAI) [11]. Functional ankle instability results from a loss of neuromuscular control [59]. The main impairments contributing to functional ankle instability are proprioceptive deficits, mechanical insufficiency of ligaments, and muscle weakness, specifically of the ankle evertors [60, 59]. Chronic ankle instability (CAI) is a condition characterized by a tendency of the ankle to 'give way' during normal activity and can be caused by FAI [61]. Once an ankle has been sprained, there is high susceptibility of re-spraining the ankle due to several reasons including reduced muscle strength, slower

reaction times, and kinematic changes, as explained in the following subsections.

2.2.3.1 Reduced Muscle Strength

The muscles involved in ankle sprains are the invertors and evertors. To understand muscle activation during ankle sprain simulations, past studies have investigated the tibialis anterior [62], peroneus longus [62, 63], and peroneus brevis [62]. Other studies have examined the evertors in general [64, 65]. Reduced muscle strength is associated with sprained ankles. Weakened eccentric invertor strength was found to limit the control of inversion during sudden inversion tests [60]. In comparison to stable ankles, evertor muscle strength in unstable ankles due to ankle sprains is significantly reduced by 0.1 Nm/kg [65]. For average body mass of 72 kg, there was a 7.2 Nm reduction in evertor strength [65], which is consistent with another study where the difference was up to 10 Nm [64].

2.2.3.2 Slower Reaction Times

Reaction times are reduced in a sprain-injured ankle. In the study by Hopkins et al. [62], healthy subjects had reaction times of 60 ms while walking and 75 ms while standing during sudden inversions. This is consistent with a study by Karlsson et al. [66], who reported reaction times of 70 ms in a stable ankle. However, in the unstable ankle the reaction time was significantly increased to 80 ms. The unstable group in a study by Iwamoto [63] showed a significantly slower peroneus longus reaction time (59 ms) compared with the control group (46 ms).

2.2.3.3 Kinematic Changes

In ankle-sprained individuals, upon heel contact, the foot is commonly oversupinated which can predispose the ankle to rolling over its lateral edge and cause another ankle sprain. For CAI patients, an over inversion of 2.5 deg was reported in a study by Drewes et al. [67] and up to 7 deg in a study by Monaghan et al. [61]. For FAI patients, an over inversion of up to 4 deg was reported in a study by Delahunt et al. [68]. In fact, throughout the entire gait cycle, there was a significant mean difference of 2.07 deg between CAI and control subjects.

Higher inversion angular velocity is also observed upon heel contact in ankle-sprain individuals. For example, CAI subjects were inverting at a rate of approximately 29 deg/s during the immediate 5 ms period prior to and post-HC while control subjects were slowly everting at a rate of approximately 6 deg/s during the same period [61].

Furthermore, during ankle inversion sprain simulations, the angular speed of inversion is much higher. For example, to measure muscle strength, speeds of 30 deg/s to 120 deg/s are typically used. To define muscle power, speeds of 120 deg/s to 300 deg/s are used [65]. Anything above is considered a risk to the subject. Examples of high speed ankle inversion tests are 261 deg/s by [62] and 403 deg/s by [69]. For an unstable ankle, the inversion angular velocity is significantly faster (153 deg/s) than a control ankle (83 deg/s) [63] which indicates higher susceptibility for re-spraining.

There is reduced toe clearance of 13 mm in ankle-sprained individuals versus 23 mm in normals [68] which can result in tripping during obstacle crossing and higher susceptibility of rolling over the lateral edge while walking.

2.3 Ankle-Foot Orthoses(AFOs)

An orthosis is defined as a device applied external to the body used to modify the structural or functional characteristics of the neuromusculoskeletal system [4]. The application of an orthosis, or orthotic management, has several objectives including the prevention or correction of deformity, the support or immobilization of a body segment, and the assistance or restoration of mobility and function [3]. Fundamentally, an orthosis modifies the systems of external forces and moments acting across a joint [4]. This is achieved in four different ways: the first three direct and the fourth indirect.

a) Control of moments across a joint. This is known as three-point fixation by applying three controlling forces to the limb: one placed through the joint center, the other two, acting in opposite direction to the first, placed proximal and distal to the joint, as shown in Figure 2.19a.

b) Control of normal forces across a joint. For joints that have lost structures to restrain translation, instability occurs where significant shear forces act. Applying forces on the limbs to alter the moments across the joint restores the translational equilibrium, as shown in See Figure 2.19b.

c) Control of axial forces across a joint. In healthy joints, axial loading is carried across joints through bony structures and layers of cartilage. Loss of the structural integrity of these features leads to excessive compressive deformation of the joint. Orthotic management is applied to reduce the contact force in the joint by redistributing loads across the joint, as shown in Figure 2.19c.

d) Control of line of action of ground reaction. The ground reaction force applies moments about each joint. By changing the line of action of this force, effectively the moments about each joint can be controlled. This is achieved by altering the angular relationship either between the plantar surface of the foot and the floor, between the articulating segments at a more distal anatomical joint, or by changing the point of contact of the foot with the floor as seen in Figure 2.19d.

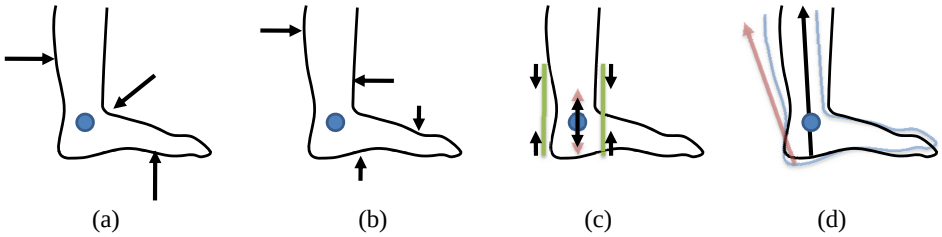

Figure 2.19: External force application techniques in orthotic management (adapted from [4]) illustrating the control of: a) moments across a joint, b) normal forces across a joint, c) axial forces across a joint, and d) the line of action of the ground reaction force.

Applying these forces and moments poses design concerns pertaining to the human-orthotic interface. Conditions such as abrasions, blisters [11], contact dermatitis [11], edema [11] and pressure sores [4] are directly related to loading characteristics of the orthosis on the limbs and mechanics of the tissues contacting the orthosis [11, 4]. Some patients may be more susceptible to these conditions than others and must be considered in orthotic management. Therefore, careful choice in materials and shape design is necessary in the development of an orthosis.

Ankle-foot orthoses are amongst the most commonly prescribed categories of lower limb orthoses [4]. They are simple and small yet have been proven to be highly effective [4]. AFOs are commonly passive devices ranging from simple canvas-like socks to customized molded plastics incorporating advanced fabric interfaces such as Otto-Bock's Sensa line. Passive AFOs are designed to support by restricting ankle dorsiflexion, plantarflexion, supination and/or pronation. For the case of distal deformities of the foot, the AFO may be used to restrict motions of the midfoot, forefoot or toes. Major manufacturers of passive AFOs include Ossur, Otto Bock, Donjoy, Breg, Bledsoe, McDavid, and Townsend Bracing.

Some passive AFOs can restore motion and function by storing energy in a flat spring; however, recent advances in robotic technology have inspired a new breed of AAFOs which use actuators to control ankle motion in real-time. These are typically used in rehabilitative applications for patients with neurologic involvement.

The following sections detail passive AFOs and AAFOs with examples available commercially and currently under research.

2.3.1 Passive AFOs

Passive AFOs are AFOs which rely on their material properties and configurations to control ankle-foot motion. Although there are many types of passive AFOs, the focus will be on those used in gait mobility.

2.3.1.1 AFOs for Ankle Sprains

The typical solution to prevent further ankle sprains is orthotic management using a passive ankle stabilizer [3]. The simplest type is taping, where adhesive tape surrounds the ankle and restricts motion. This approach is less effective than orthoses and less cost effective since the repeated application of tape must be performed [3]. Orthotic management has been shown to be the best alternative to taping [3] and falls into several categories.

Stirrup Stirrup AFOs (Figure 2.20a) control the medial and lateral movement of the subtalar joint but still allow dorsiflexion and plantarflexion [11]. They are typically rigid or semi-rigid plastic uprights which span across the subtalar joint on either side of the ankle. Recent advances in commercial AFOs include air inflatable stirrups to adjust pneumatic compression and gel stirrups for thermal therapeutic use such as those offered from Ossur. Five commonly used stirrup AFOs are: Aircast Air-Stirrup, Multi-Phase Ankle System, Sure Step Ankle Support System, Active Ankle System, and Richie Brace.

Lace-up Lace-up AFOs (Figure 2.20b) are similar to taping and are used as a preventative device [11]. The midfoot, subtalar and talocrural joints are encapsulated in a vinyl or nylon shell with a front lacing system. To add additional torque resistance, most lace-up orthoses have Velcro straps that help limit inversion and may create a figure-8 cradle. Examples include: Ankle Stabilizing Orthosis and SwedeO Lightning Lok.

Prophylactic A prophylactic AFO (Figure 2.20c) decreases the incidence of ankle injury [11] by providing support in a figure-8 configuration similar to taping, without rapid loss of effectiveness. Examples include: Spatz and Arizona Ankle Orthosis.

(a) (b) (c)

Figure 2.20: Examples of AFOs for ankle sprains: a) Stirrup AFO [70], b) Lace-up AFO [71], and c) Prophylactic AFO [72].

Limitations The effectiveness of passive AFOs for ankle sprains is still under controversy. Some studies have shown a detrimental impact on performance whereas others have no difference or even no improvement [73]. Comfort is a critical factor in athletic performance that influences perception of the orthotic intervention. Soft AFOs were found to be most comfortable but the semi-rigid offer better stability [73]. Since these passive AFOs cannot be deactivated, the mobility of the ankle is constantly restricted. A new device, such as an AAFS, should incorporate both the comfort of a soft AFO with the protection of a semi-rigid AFO to prevent injury when needed and otherwise permit natural motion.

2.3.1.2 AFOs for Stress Fractures and Severe Sprains

Controlled Ankle Motion (CAM) Walkers CAM walkers (Figure 2.21a) are similar to a removable cast but have an adjustable range of motion and a rocker bottom to allow a more natural gait pattern [11]. They are available in tall or short versions. The taller version is for fractures of midtibia or fibula to the midfoot or for cases of third-degree ankle sprains. The shorter is for midfoot sprains, metatarsal fractures, post-surgical incision protection and immobilization for inflammatory conditions. The benefit of the CAM walker is its high patient compliance because it is removable for bathing or sleeping [11].

Leg Braces Leg braces (Figure 2.21b) are also used for stress fractures but rely on compression to relieve stress and promote healing [3]. The tibia and fibula are unloaded by the stabilization of the surrounding musculature. They may also incorporate a heel rocker to aid in gait. Examples include: Aircast Air-Stirrup Leg Brace and Aircast Brace.

(a) (b)

Figure 2.21: Examples of AFOs for stress fractures and severe sprains: a) CAM Walker [74] and b) Leg Brace [75].

Limitations The AFOs for stress fractures and severe ankle sprains are designed to immobilize the ankle and foot while donned by providing compression of the shank, ankle, and foot. The ability of these AFOs to completely restrict motion in the ankle and foot may be a useful feature and consequently, some of their design aspects could be incorporated in the design of a new AAFS.

2.3.1.3 AFOs for Neurologic Involvement

An AFO is commonly worn by individuals with neurologic disorders [11]. In general, the indications for AFO use include flexible deformity of the foot and/or ankle, weakness or loss of the foot and ankle musculature, and a need to stabilize the foot for the use of musculature above the foot [11]. The following describes the various types and their efficacy. Typical examples of AFOs for neurologic involvement are shown in Figure 2.22.

(a) (b) (c) (d)

Figure 2.22: Examples of AFOs for neurologic involvement: a) Solid AFO [76], b) Hinged AFO [76], c) PLS AFO [76], and d) Ossur's Foot-Up AFO [77].

Solid AFO or Fixed AFO Solid AFOs (Figure 2.22a), typically made of rigid polypropylene, are usually prescribed to patients with partial, total paralysis, or spasticity [3]. These AFOs provide maximal tibial restraint to prevent either excessive ankle dorsiflexion or plantarflexion from occurring during stance [3] and are usually set at a fixed angle of 2 to 3 deg dorsiflexion [11]. The shape also controls STJ movement for greater stability during stance [3].

Hinged (Articulated) AFO Hinged AFOs (Figure 2.22b) are similar to solid AFOs; however, they incorporate a hinge corresponding to the anatomical ankle joint [4]. The material near the hinge is cut away in a wedge shape to allow free but limited dorsiflexion and/or plantarflexion by use of a stop [11, 4]. In a study by Radtka [78], hinged AFOs increased plantarflexion moments and power generation during pre-swing compared with solid AFOs in children with spastic diplegic cerebral palsy, indicating greater plantarflexor muscle concentric contraction for push-off.

Dorsiflexion-Assist AFO There are two types of dorsiflexion-assist AFOs: posterior leaf spring (PLS) and spiral [11]. PLS AFOs (Figure 2.22c) consist of a spring-like band which runs along the posterior of the tibia down to the heel [4]. They are typically made of plastic and resist plantarflexion beyond the ankle neutral position and provide assisted dorsiflexion from a plantarflexed foot position to neutral [4, 11].

The spiral AFO is made of plastic, and coils around the shank and supports the foot [11]. The spiral AFO uses a four-force system and not the standard three-point fixation [3]. Unfortunately, this type of orthosis is time consuming and difficult to fit and prone to breakage [3].

Improvements in dorsiflexion-assist AFOs have led to restoration of some plantarflexion muscle strength through the use of carbon fiber springs by absorbing energy during terminal stance as the shank is rotating over the ankle and returning this energy upon push-off [79, 80, 81].

Floor Reaction Orthosis or Ground-Reaction AFO Floor reaction AFOs are rigid [4] and are molded to fit around the front of the leg [11]. The heel and leg are held in place [11] in slight dorsiflexion and this completely prevents plantarflexion [4]. It also alters the line of action of the ground reaction force resulting in a stabilizing knee extension moment or hip moment depending on the dorsiflexion angle [4, 11].

Other AFOs for Neurologic Involvement The Foot-Up by Ossur (Figure 2.22d) consists of two main parts: an ergonomic ankle wrap and a plastic inlay. The plastic inlay fits discretely between the tongue and laces of the shoe and attaches to the ankle wrap via an elastic strap with a quick-release clip. During push-off, the foot plantarflexes extending the elastic strap which returns to its original length upon toe off. As a result, a dorsiflexor moment is provided during swing which prevents drop foot or similar conditions.

Limitations Passive AFOs for neurologic involvement are limited in their effectiveness and adaptability. For example, Carlson et al. [82] found that AFOs did not improve gait velocity or stride length in children with cerebral palsy. For drop-foot patients, Lehmann et al. [83] discovered that although a constant stiffness AFO was able to provide safe toe clearance, the device did not reduce the occurrence of slap foot. A constant stiffness AFO is not able to adapt to the different stages of gait where during CP a patient may require one stiffness, and during swing may require another. Therefore, a variable stiffness AFO would be required to successfully meet the individual's moment deficit. Many current AFO designs used for foot-drop treatment are effective at controlling the undesirable plantarflexion during swing, but do not permit free ankle motion during the stance phase of gait [84]. Also, these AFOs do not address the needs of Charcot-Marie-Tooth (CMT) patients who present weak dorsiflexors and associated foot-drop. As the plantarflexors are frequently not affected, the ideal AFO for CMT should permit free ankle plantarflexion (with low resistance) and dorsiflexion during stance phase and block plantarflexion during swing, (i.e., prevent foot-drop) [84]. PLS AFOs do not have articulated ankle joints and instead are dependent upon the material properties and geometry which determine the bending stiffness and thus the motion control characteristics. Because the thermoplastics (i.e. polypropylene) used in these AFO strut designs provide resistive moments when deformed, they cannot permit free movement [84]. It is also difficult to select the proper trimline or plastic thickness to achieve a desired stiffness [85]. Stability is also effected by the use of these AFOs. For example, in a study of Multiple Sclerosis patients by Cattaneo et al. [86], solid AFOs and hinged AFOs were determined to improve static stability but negatively impact dynamic stability. This resulted in greater walking difficulty and slower gait speeds.

The adaptability of these devices is highly limited. Passive AFOs do not adapt to the gait of the user, to step-to-step changes in gait pattern due to changing speed or terrain, or to long-term gait changes due to changes in muscle function [6]. They are not capable of replicating all dynamic characteristics of the natural ankle complex including free ankle motion, natural supination and pronation, and unhindered push-off [87]. In an attempt to improve adaptability, hinged AFOs, which have a better anatomical/mechanical joint

alignment and provide more diverse motion control options, such as stops and assists [84], are used. However, the drawback of these AFO designs is that the motion control elements cannot be timed to and operated during different periods of the gait cycle [84]. Lack of adaptability can also adversely affect other joints. For example, Lehmann et al [83] reported that the greater the plantarflexion resistance, the greater the bending moment at the knee, and that plantarflexion resistance should be easily adjustable according to the gait ability of patients with hemiplegia.

2.3.1.4 General Limitations

Passive AFOs restrict the ability of the ankle and foot to naturally pronate and supinate. Although this has the benefit of stabilization, the loss of natural motion may cause muscle atrophy and unnatural gait patterns. Patients can become dependent on support originally intended for prophylactic or rehabilitative use.

The use of passive AFOs is prescribed for specific conditions. Although designs vary between conditions, few functional requirements are resolved by a single device. There is also no adaptability to the user's gait which can adversely affect natural movement and performance. In addition, no one device addresses the gait deficiencies of the elderly, drop foot patients, and ankle-sprain injured individuals. An AAFS able to perform multiple functions including allowing free motion, restricting supination and pronation, and varying sagittal plane stiffness is necessary.

2.3.2 Active AFOs

The inadaptability of passive AFOs reduces their ability to correct gait. The ankle joint normally varies its impedance throughout the gait cycle and during other activities [6]. An AFO that can actively mimic this phenomenon is desirable. Active AFOs (AAFOs) are only reported in the literature, and as of yet, none are available in the commercial market. They are limited to specific categories including drop foot AAFOs, plantarfexion assist AAFOs, and combinations of the two. All of these are discussed in the next sections. The application of most of these devices is for rehabilitation training. Images of these devices are shown in Figures 2.23 through 2.26. A complete AAFS has not been developed and is not available on the market.

2.3.2.1 Drop Foot

Oil Damper AFO Yamamoto et al. [85] developed an AFO with an assistive oil damper (Figure 2.23a), known as GaitSolution, for patients with hemiplegia. The oil damper is a small shock absorber that utilizes hydraulic resistance to provide a resistive moment to plantarflexion during initial stance on the paretic side to prevent foot slap. The AFO was adjustable to control the initial dorsiflexion angle and the resistive force to plantarflexion. The range of dorsiflexion permitted was more than 30 deg from the initial ankle joint angle, to accommodate standard gait, ascent and descent of stairs and slopes, and squatting. The plantarflexion resistive moment at the initial stance phase was adjustable for the condition of each patient, in the range of 5 to 20 Nm for every 10 deg of plantarflexion. The AFO with the oil damper permitted sufficient plantarflexion of the ankle and low flexion of the knee by setting a proper plantarflexion resistive moment during initial stance phase. It also provided a more comfortable gait than AFOs with a plantarflexion stop. Drawbacks to this design are the use of an articulated joint that restricted natural supination and pronation and resistance to powered plantarflexion.

Series-Elastic Actuator AFO Blaya and Herr [6] from the Massachusetts Institute of Technology's (MIT) Artificial Intelligence Laboratory developed an AAFO where the impedance of the orthotic joint is modulated throughout the walking cycle to treat drop-foot gait. The device (Figure 2.23b) consists of a series-elastic actuator (SEA) mounted posterior to the ankle on a polypropylene hinged AFO with control sensors and electronics. The mass of the device excluding the off-board power supply is 2.6 kg. During early stance, the torsional spring control is applied where sagittal joint stiffness is actively adjusted to minimize forefoot collisions with the ground. Throughout late stance, joint impedance is minimized to not impede the subject's powered plantarflexion movements, and during the swing phase, a torsional spring-damper control lifts the foot to provide toe clearance. Evaluation yielded a reduced occurrence of slap foot with greater powered plantarflexion and less kinematic difference during swing when compared with normals. A finite-state machine control algorithm was implemented for each phase of the gait cycle.

The SEA, previously developed for legged robots in MIT's Leg Laboratory [88], consists of a DC motor in series with a spring (or spring structure) via a mechanical transmission [6]. The SEA provides precise force control by controlling the extent to which the series spring is compressed. Using a linear potentiometer, the actual force applied to the foot can be obtained by measuring the deflection of the series spring. The SEA is used to control the impedance of the ankle joint.

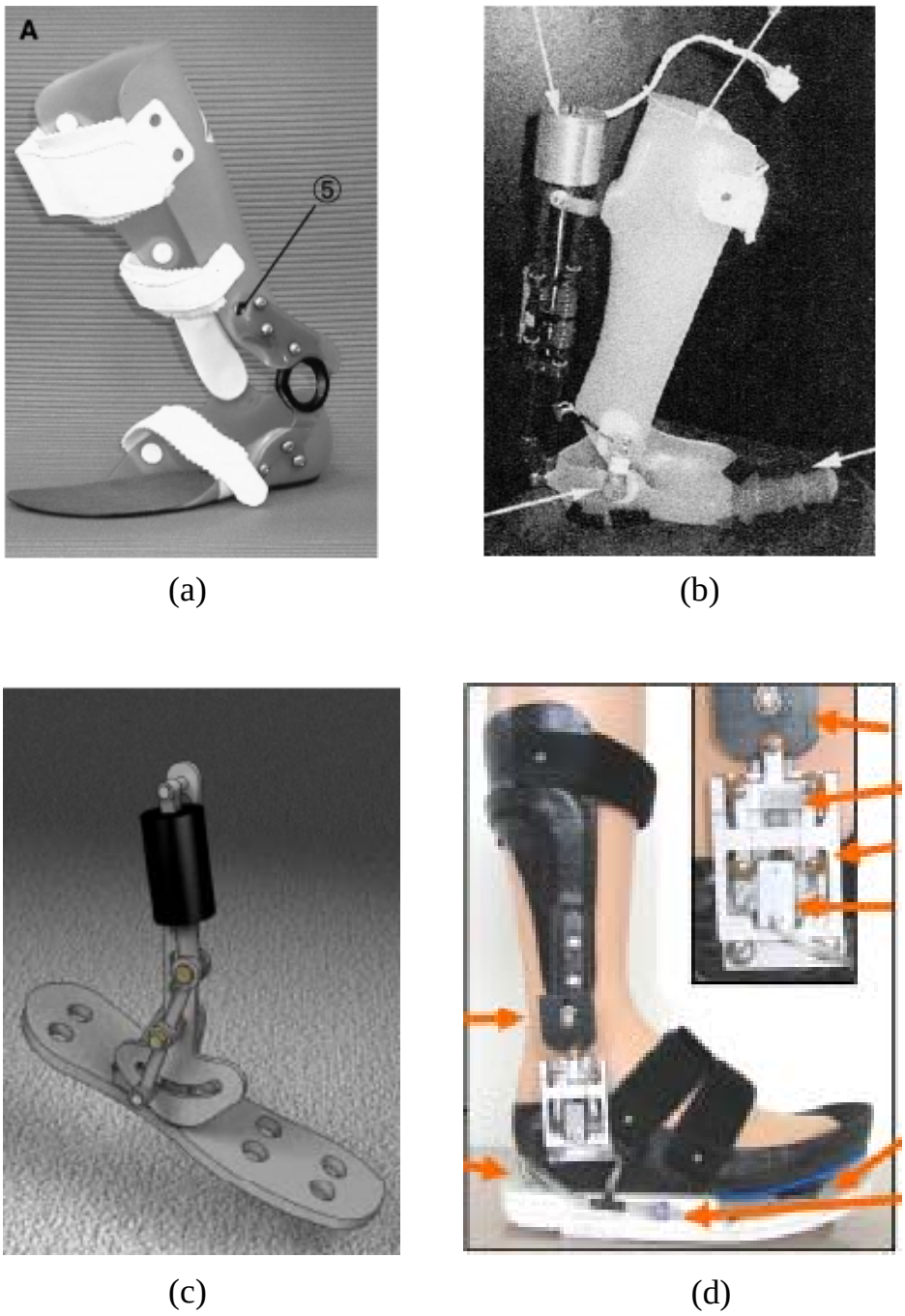

Figure 2.23: Examples of active AFOs for drop foot: a) Oil Damper AFO [85], b) Series-Elastic Actuator AFO [6], c) Semi-Active AFO [87], and d) Pneumatic Power Harvesting AFO [84].

In order to produce a linear torsional stiffness, the linear spring needs to be continually adjusted. As a result, the SEA used in this investigation is too heavy and power intensive to be practical in a commercially available active ankle-foot system, and would, therefore, have to be redesigned. The use of an articulated joint also restricts natural supination and pronation and there is no plantarflexion assist even though this is a powered device.

Semi-Active Ankle-Foot Orthosis A novel design using a Lord magnetorheological fluid (MRF) damper was developed by Manzoor et al. [87] to correct drop foot gait (Figure 2.23c). The SAAFO used body weight, ankle angle, and FSRs to control when the MRF damper held and released the ankle via activation and deactivation, respectively. The force measured by four FSRs, strategically placed on the sole of the footplate, was used to detect the various gait phases during level, uphill and downhill walking. The device required an articulated joint, and since the MRF damper was situated on the side of the ankle, it added to bulk.

Biofeedback AFO A design concept for a biofeedback AFO, that incorporates a modified walking brace with a back-drivable motor and ball-screw assembly posterior to the ankle, was developed by Chang et al. [89]. The proposed closed-loop control scheme is based on EMG sensors placed over the tibialis anterior muscle. Detection of tibialis-anterior activation activate the device to provide a dorsiflexor moment. There is no spring for compliance, rather the device relies on the back-drivability of the ball-screw. The walking brace has an articulated joint that restricts natural supination and pronation.

Pneumatic Power Harvesting AFO A self-contained, self-controlled, pneumatic power harvesting ankle-foot orthosis to correct foot-drop was developed by Chin et al. [84] at University of Illinois at Urbana-Champaign (Figure 2.23d). The objectives for the prototype were to provide toe clearance during swing, permit free ankle motion during stance, and harvest the needed power with an underfoot bellow pump pressurized during the stance phase of walking.

The pneumatic power harvesting AFO was constructed from a two-part (tibia and foot) carbon composite structure with an articulating ankle joint for a US men's size 11. Ankle motion control was accomplished through a cam-follower locking mechanism actuated via a pneumatic circuit connected to the bellow pump and embedded in the foam sole. The device and attachments have a total mass of 1 kg.

Toe clearance during swing was successfully achieved during all trials which were performed on a treadmill. The average clearance was 44 mm. Free ankle motion was observed

during stance, and plantarflexion was blocked during swing. In addition, the 4.5 cm diameter bellow component repeatedly generated an average of 169 kPa per step of pressure during ten minutes of walking, which was sufficient to achieve the device function.

The PhAFO uses an articulated joint that restricts natural supination and pronation. The use of a bellow under the sole of the foot can also affect proprioception impacting stability.

2.3.2.2 Plantarflexion Assist

Dynamically Controlled Ankle-Foot Orthosis A dynamically controlled AFO (Figure 2.24a) with regenerative kinetics that harnesses elastic energy from a robotic tendon actuator similar to human muscle was developed by Sugar and colleagues at Arizona State University [7]. The actuator is attached from the posterior of the tibia to a lever arm at the heel, and is designed to assist plantarflexion upon push-off. The robotic tendon actuator consists of a DC motor, lead-screw, and spring. The DC motor effectively controls the location of the spring and thus the deflection of the spring. This reduces the energy/power density problem resulting in greater portability. The result of an example problem reveals a feasible lead screw design that has a power-to-device-weight ratio of 277 W/kg, approaching that of the DC motor (312 W/kg), as well as a mechanical efficiency of 0.74 and a maximum strength-to-weight ratio of 11.3 kN/kg. The actuator mass was 0.95 kg. The device is bulky, employing a longer moment arm to maximize torque. Although successful, this device only provides 50% plantarflexion power assistance and it does not modify any of the other gait phases.

Pneumatically-Controlled AFOs Gait rehabilitation devices consisting of pneumatic muscle actuators (PMA) have been developed by Ferris et al. from the University of Michigan [5, 90]. A single and double PMA was positioned posterior to the lower leg to produce active plantarflexion torque [5, 90] (Figure 2.24b). The subjects underwent walking trials and the results indicated a reduction in muscle forces generated with the single PMA and further reduction with the double PMA. EMG was used to control the activation of the PMAs during gait assist trials. Each orthosis configuration generated nearly 57% of the peak ankle plantarflexor torque during stance and performed nearly 70% of the positive plantarflexor work done during normal walking. Excluding the mass of the air source, the single PMA orthosis was 1.3 kg and the double PMA orthosis was 1.7 kg.

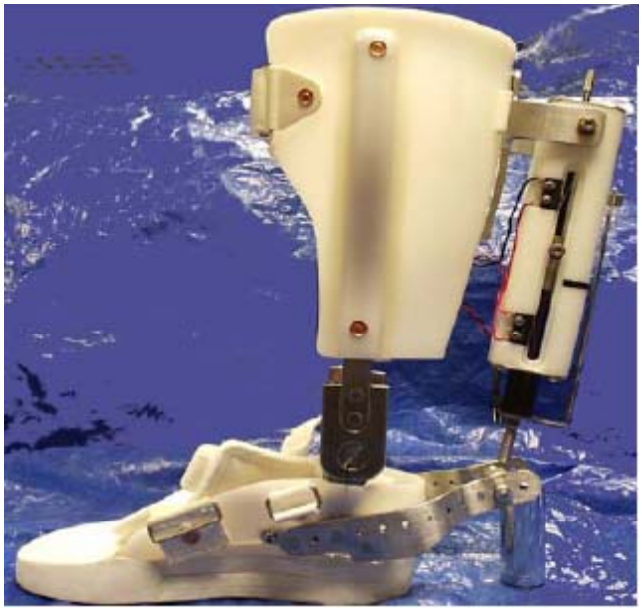

(a)

(b)

Figure 2.24: Examples of active AFOs for plantarflexion assist: a) Dynamically Controlled AFO [7] and b) Pneumatically Controlled AFO [5].

Although the PMA orthoses were effective for rehabilitation, the devices are bulky, noisy and require a separate air supply. The PMAs require activation to generate force

since the passive PMA configuration provides little resistance force. The dependence of ankle joint angle on the length of the PMA adversely affected the kinematics of the ankle from FF to HO [5]. The foot was accelerated into a more plantarflexed position resulting in abnormal kinematics. The PMAs were attached to an articulated passive AFO that restricted supination and pronation.

2.3.2.3 Combination

Yonsei University SEA AFO A SEA AFO designed for the prevention of foot drop and toe drag similar to MIT's efforts (Figure 2.25a) was developed by Hwang and group from Yonsei University of South Korea [91]. The AAFO controlled the dorsiflexion and plantarflexion of the ankle joint during walking. Three different gait conditions were compared: normal gait without AFO, solid AFO gait with the conventional plastic AFO, and AAFO gait with the developed AFO. The results showed that the AAFO provided sufficient dorsiflexion moment to prevent foot drop and toe drag, and sufficient plantarflexion moment to aid push-off. The maximum torque generated by the AAFO was 97 Nm. The device was controlled by detecting FSR signals on the plantar surface of the foot plate and implementing a gait phase detection algorithm. In normal gait, the maximum power was about 1.7 W/kg during pre-swing whereas the maximum power of AAFO gait was about 1 W/kg. MIT's SEA AFO did not address powered plantarflexion assist; however, the Yonsei device is even bulkier and heavier, with a larger motor to achieve 100% plantarflexion assist. Also similar to MIT's SEA AFO, the SEA has to be continually adjusted, resulting in increased power requirements. Again, the device is based on a single-axis articulated joint that restricts natural supination and pronation.

Ferris Antagonistic An improved device was developed with antagonistic PMAs: one anterior and one posterior to the tibia [92] (Figure 2.25b). EMG was used to control the device with activation of the soleus muscle actuating the posterior PMA and inhibiting the anterior PMA. Activation of the tibialis anterior actuated the contrary conditions. Peak plantarflexion torque was 50.7 Nm and peak dorsiflexion torque was 20.7 Nm. The total mass of the device was 1.7 kg. Initially, manual pushbutton control by patients required too much cognitive awareness [93] so a control loop was required to increase effectiveness. Myoelectric control was later implemented [92]. For the antagonistic PMA configuration, abnormal kinematics were observed from HC to FF; however, there was improvement in push-off kinematics from HO to TO. Since PMAs were both anterior and posterior of the ankle, the size of the device also increased. As with the plantarflexion assist PMA AFOs, the antagonistic AFO is based on an articulated joint that restricts natural supination and

pronation.

(a)

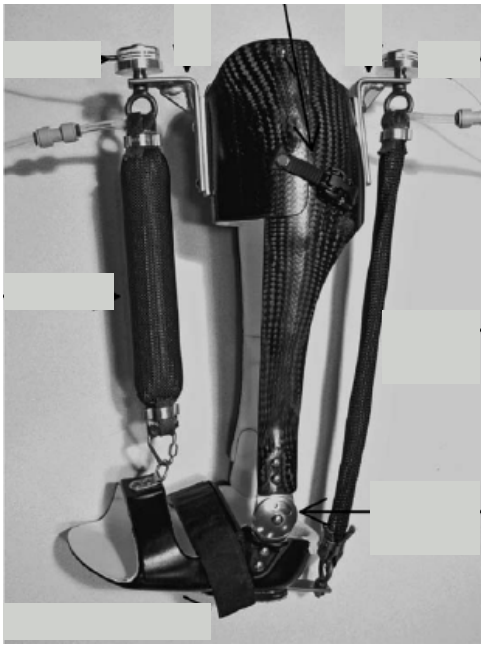

(b)

Figure 2.25: Examples of active AFOs for combined dorsiflexion and plantarflexion assist: a) Yonsei University AFO [91] and b) Ferris Antagonistic AFO [92].

2.3.2.4 Other Active AFOs

Two-Degree of Freedom AFO A two-degree of freedom AFO (Figure 2.26a) that can articulate at both the TCJ and the STJ joint was designed by Agrawal et al. [94] from the University of Delaware. This is a novel device that can be used to measure forces and moments applied by the human at both joints. The intent is to correct drop-foot by assisting dorsiflexion and training a patient to restore normal gait. Actuators have yet to be implemented; however, this device, which is still under development, has shown that rotational joints can be successfully implemented for the TCJ and STJ on the human body. The device, unfortunately, consists of bulky and heavy adjustable metal brackets to determine the joint axes and therefore, further development is required to make the device more wearable.

Robotic Gait Trainer A robotic gait trainer (Figure 2.26b), an ankle rehabilitation device for assisting stroke patients during gait by use of repetitive task training, was developed by Bharadwaj and Sugar [95] of Arizona State University's Human/Machine Integration Laboratory. Structurally based on a tripod mechanism, the device is a parallel robot that incorporates two pneumatically powered, double-acting, compliant, spring-over-muscle actuators as actuation links that move the ankle in dorsiflexion/plantarflexion and inversion/eversion. A spring-over-muscle actuator consists of a pneumatic muscle attached in parallel with a standard compression spring. In this arrangement, the spring resists compressive forces while a pressurized pneumatic muscle resists tensile forces. A unique feature in the tripod design is that the human anatomy is part of the robot, the first fixed link being the patient's leg. The device does not have an articulated ankle joint, but rather assumes that the subject's ankle behaves as a ball joint. The device protrudes anteriorly from the shank and foot and is very bulky extending just distal to the knee. The total device mass was not reported. Some design aspects of the Robotic Gait Trainer may be useful for developing an AAFS including the use of ball joint to model the ankle and the spring-over-muscle actuator.

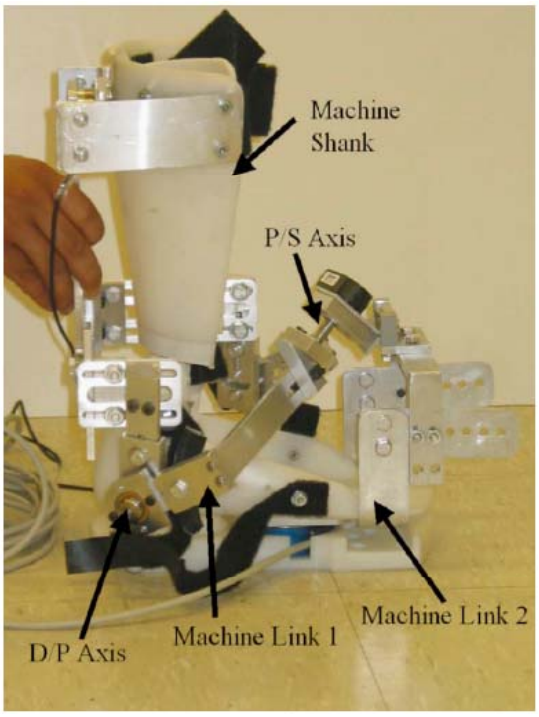

(a)

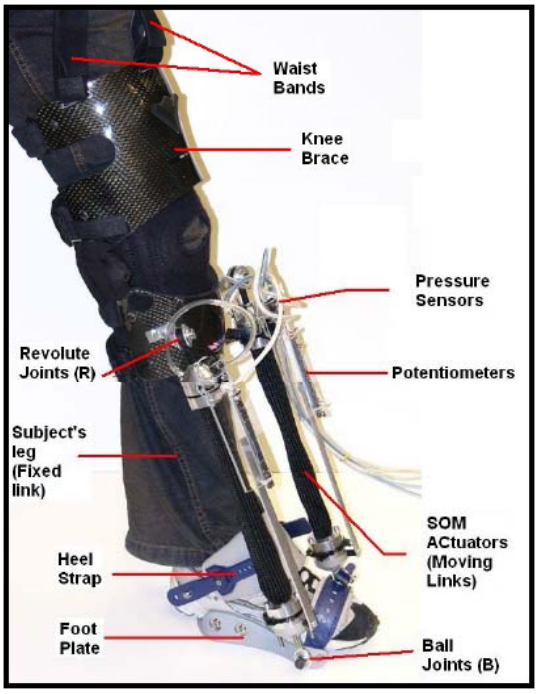

(b)

Figure 2.26: Examples of other active AFOs: a) Two Degree of Freedom AFO [94] and b) Robotic Gait Trainer [95].

2.3.2.5 General Limitations

AAFOs are similar to passive AFOs in that their functionality and actuation are specific to a particular pathology. With the exception of the two-degree of freedom AFO and robotic gait trainer, each AAFO consists of an articulated passive AFO with implemented actuators which inherently restrict natural pronation and supination. Active mediolateral stabilization does not occur since an emphasis is placed on restoring sagittal gait patterns only. The devices are bulky and heavy and thus lack the portability for everyday use which is consistent with their rehabilitative purpose. For motorized AAFOs, the power requirements are greater since a large motor is required to generate the necessary moments about the TCJ and a potentially large battery pack would be required to make the devices portable. AAFOs also have greater mass than their passive AFO counterparts, at nearly 1 kg or more not including the power source. Similar masses are observed with PMA AFOs that do not include the air supply source. The device mass alone may be acceptable since improvement in gait is observed; however, the ultimate goal of the AAFS is to achieve a portable and self-contained device.

The development of AAFOs has been limited to specific applications but have yet to be viable commercial options for patients. The limitations of existing actuator technologies has inspired hybrid actuators such as the SEA, spring-over-muscle, and antagonistic PMA. A device that can satisfy the ankle functional needs of the elderly, drop foot patients, and sprain-injured individuals does not exist. The development of an AAFS is necessary as a solution.

2.3.3 Actuator Technologies

The previous section has reviewed the various actuator technologies currently in use for AAFOs. These include the SEA, spring over muscle, PMA, lead screw and motor, oil damper, and MRF damper. Since the AAFS in this thesis is a new device, an investigation of existing actuator technologies was necessary in determining the feasibility of a new design. Therefore, a brief overview of available actuator technologies follows.

2.3.3.1 Electromagnetic Actuators

Electromagnetic actuators use the Lorentz interaction between a flowing electrical charge and magnetic field to supply either translational energy or rotational mechanical energy to a coil [96]. The magnetic field can be established either by means of permanent magnets or by a second coil [96]. Common examples include a DC motor, a loudspeaker, and a solenoid

actuator. When combined with other components such as a leadscrew, a rotary motor can become a linear actuator [97]. Combining an electromagnetic actuator with other components could result in a hybrid actuator. These components could be compliant, such as a spring, and encourage a more natural human-orthosis interface. Maxxon is a common manufacturer of motors for prostheses and orthoses. MicroMo Electronics Inc. is a manufacturer of miniature actuators including motors, linear actuators, and rotary actuators and may be useful for minimizing the size of an AAFS.

2.3.3.2 Shape Memory Alloys

Shape memory alloys typically consist of a wire made of nitinol (nickel and titanium) [96]. By supplying input thermal energy, a martensitic phase transition in the alloy is triggered, which results in shape recovery of a previously deformed state. The process is a reversible and diffusionless transformation. Shape memory alloy actuation is a slow process for the purpose of active AFO actuation. The process is limited by the heat transport mechanisms during cooling. In fact, the process could take up to one second in actuation and recovery time. The actuation is also dependent on temperature so ambient temperature should be monitored. Although slow, shape memory alloy actuators exhibit high forces and have excellent static performance. An example of a shape memory alloy commercial manufacturer is Dynalloy Inc. which make Flexinol.

As mentioned previously, a single stride during the gait cycle is approximately 1 s. Since the recovery time of shape memory alloys is around the same, shape memory alloys would not be suitable for an AAFS unless improvements in the cooling mechanism of the wires can be greatly improved.

2.3.3.3 Magnetorheological Fluid Actuators

Magnetorheological fluid (MRF) actuators exhibit changes in their rheological properties when subjected to external magnetic fields [96]. They consist of suspensions of noncolloidal, multidomain and magnetically soft particles in base organic or aqueous liquids. The apparent viscosity of these materials is modified according to an applied magnetic field. MRF actuators are semiactive actuators in that they only dissipate energy. MRF actuators can activate and deactivate within milliseconds and they can accurately resist a high yield strength. They operate in three modes: shear, flow or squeeze [96]. In shear mode, the MRF is confined between two plates where one is fixed and the other is translating parallel to fixed plate due to an applied force. The activation of the MRF resists this translation. In flow mode, the MRF flows between two fixed plates and upon activation, decreases its

flow as the applied magnetic field increases. In squeeze mode, the MRF fluid is compressed between two plates as an applied force draws the two plates together. The result is radial flow of the MRF away from the plates which decreases as the applied magnetic field increases. Lord Corporation is a commercial manufacturer of MRF and MRF actuators with custom applications in prosthetics and automobile suspensions. MRF actuators are expensive and potentially bulky which is a drawback in using them for an AAFS.

2.3.3.4 Electrorheological Fluid Actuators

Electrorheological fluid (ERF) actuators are similar to MRF actuators, however they change their rheological properties when an electric field is applied and not a magnetic field [96]. ERF actuators consist of suspensions of electrically active particles in an electrically insulating liquid. They also operate similarly to the MRF actuators with similar actuation times in the milliseconds. The major drawback of electrorheological actuators is that they require a high activation voltage in kV magnitude and thus may not be suitable for an AAFS. Smart Technologies in the United Kingdom has worked with Mavroidis et al. [98] to develop a knee orthosis using ERFs; however, the devices were quite bulky.

2.3.3.5 Shear Thickening Fluids

A shear thickening fluid, also known as a dilatant, is one in which viscosity increases with the rate of shear [99]. It is an example of a non-Newtonian fluid. Examples of uses include traction control during viscous coupling and body armour providing rigidity during weapon strikes. They are actuated by shear or vibration and act in damping mode. They also exhibit almost instantaneous actuation and recovery time. D3O is an example of a manufacturer of sports protection equipment using a patented shear thickening fluid formula. Shear thickening fluids could potentially be used to dampen the rotation of the ankle in an AAFS, similar to a stirrup AFO. The rotation of the ankle itself could activate the fluid, or the fluid could be activated by external sources such as vibration.

2.3.3.6 Pneumatic Muscle Actuators

An artificial pneumatic muscle actuator consists of an expandable internal bladder surrounded by a braided shell [5]. Pneumatic muscle actuators have biological characteristics and desirable engineering characteristics [88]. Like muscle, a pneumatic actuator typically increases its stiffness as the applied axial force is increased. By regulating the pressure across a pneumatic actuator, the output force may be tuned. Pneumatic muscle actuators

are typically nonlinear, which gives them a mechanical advantage. They are typically used as linear actuators by pressurization of the PMA resulting in contraction with a corresponding force. Manufacturers of PMAs include Festo Inc and Shadow Robot Company. PMAs are available in diameters as low as 6 mm. PMAs require an external air supply. PMAs applied around the shank, ankle, and foot can control the motion of the ankle similar to the existing musculature. For an AAFS, overcoming the challenges of bulk is crucial for successful application.

2.3.3.7 Hydraulic Actuators

Hydraulic actuators utilize hydraulic fluid, typically oil, which is pushed against a surface to produce either a linear or rotary motion. They are typically slow but are able to produce high forces. A reservoir of fluid along with a pump is usually required for active activation. In a passive state, hydraulic actuators act as dampers to reduce high velocity motion. For the purposes of an AAFS, hydraulic cylinders may be too slow.

2.3.3.8 Pneumatic Actuators

Pneumatic actuators are similar to hydraulic actuators, however they utilize air (or a gas) to actuate. They are high speed, high force actuators that require a high pressure. A pressurized air source is required for active activation; however, in a passive state, the actuator would be similar to an airspring.

2.3.3.9 Springs

Mechanical springs are common actuators in mechanical design. When deformed, a spring stores energy. During its return to the rest configuration, the spring's stored energy is released. Types of springs include helical, torsional, leaf, and constant force. As mentioned previously, PLS AFOs, including thermoplastic and carbon fiber leafspring types, are already commonly used by drop-foot patients.

2.4 Concluding Remarks

In this chapter, the role of the ankle and foot during gait and stability was demonstrated. Upon review of populations including the elderly, drop foot patients, and ankle-sprain injured individuals, it was shown that deficiencies in kinematic and kinetic gait patterns

exist. A review of passive AFO and active AFO technologies revealed several limitations for satisfying the needs of each population above. Passive AFOs are unable to deactivate and thus limit natural motion of the ankle. They are also unable to adjust to variations in gait, which limit their efficacy. In order to address some of these limitations, active AFOs have been developed. These are designed for specific applications; including, drop foot prevention, plantarflexion assist, and combinations of the two. Unlike passive AFOs, active AFOs are not available on the commercial market and are only found in the literature. Active AFOs are generally bulky and heavy, which is acceptable only for their rehabilitative purpose. A single device to address the needs of the elderly, drop foot patients, and ankle-sprain injured individuals currently does not exist. Therefore, the design of an AAFS is desirable. Next, Chapter 3 discusses the design overview for developing an AAFS.

Chapter 3

Design Overview

The following provides an overview of the design approach for the AAFS. First, a rationale for the need to to develop an AAFS is discussed, followed by a list of thesis objectives. Lastly, a description of the desired design criteria for the AAFS is established.

3.1 Rationale

The ankle and foot form the most important complex in the human body for gait and gait stability, as demonstrated in Chapter 2. The ankle and foot are responsible for propulsion, ankle and foot joint control, fine-tuning of gait patterns, and stance stabilization.

Unfortunately, deterioration of the ankle and foot can occur, for example, as a result of age and neurological conditions. Older people suffer from slower walking speeds, increased reaction times, and decreased plantar pressures, resulting in abnormal gait. These characteristics are due to loss of muscle, decreased range of motion, and decayed balance mechanisms. Gait disorders and other factors such as greater lateral sway and increased gait asymmetry are associated with a higher risk of falling. Consequently, the need arises for a device to restore lost muscle function and assist stabilization in the elderly to achieve normal locomotion and reduce fall risk.

For drop foot patients, steppage gait, which is caused by weakened dorsiflexors, occurs. Drop foot patients exhibit decreased stride length, gait velocity, and stability. Compensatory strategies improve locomotion but do not resolve the deficiencies at the ankle and foot. A device to provide assistance only during the early stance and swing phases without hindering the other gait phases is desirable.

The ankle and foot complex is also deteriorated with injury, particularly ankle sprains. Individuals who have sustained sprains often suffer from functional instability and reduced

proprioception. Reduced muscle strength increases susceptibility to future sprains since the muscles cannot restrict ankle motion effectively. Increased muscle reaction times are also observed during controlled inversions and reduced foot clearance is evident. In rare cases, drop-foot gait has even been found as a result of ankle sprains. A device to improve stability and prevent further injury without impacting performance is desirable.

A review of current AFO technologies revealed a lack of adaptive devices that can improve both gait kinematics and stability. Passive AFOs for sprains restrict ankle inversion and eversion and provide support. However, better support yields greater discomfort and thus negatively affects perception of performance. Passive AFOs for neurological conditions are typically rigid and their use can lead to unnatural gait patterns. In general, passive AFOs lack the ability to deactivate functionality which reduces the body's full capacity for propulsion and stability. Passive AFOs also address only one or two functional roles; such as, immobilization through compression, inversion/eversion restriction, or fixed dorsiflexion, and therefore do not completely satisfy the needs of older people, drop foot patients, or ankle-injured populations.

Active AFOs were found to be pathology-specific where functional motion was restricted to the sagittal plane. Although variable impedance was achieved in some devices, natural gait patterns were unattainable due to restricted pronation and supination. The majority of devices were bulky, non-portable, and were designed for rehabilitative training, not daily use. Therefore, a device that meets the shortcomings of passive and active AFOs is desirable. The proposed device is referred to as an Active Ankle-Foot Stabilizer (AAFS), the development of which would benefit the populations previously mentioned in Chapter 2. For the elderly, an AAFS could assist in locomotion and lower fall occurrence through stabilization. For drop foot patients, an AAFS could prevent foot slap and drop foot to restore natural gait kinematics. For the ankle-injured, an AAFS could assist restoring gait kinematics and prevent further ankle sprains from occurring in addition to improving proprioception.

3.2 Objectives

The goals of this research are to explore the design feasibility of a novel AAFS that addresses the diminished ankle and foot capacities of elderly individuals, drop foot patients, and active individuals who have sustained destabilizing ankle injuries. Ideally, the AAFS will be both an assistive and preventative device designed for daily use. The research objectives are to:

1. Determine the design criteria for an AAFS.

2. Determine the functional requirements of an AAFS.
3. Explore the design feasibility of an AAFS that best meets design criteria and functional requirements.
4. Develop testing methods to characterize an AAFS based on the functional requirements.

3.3 Design Criteria

An Active Ankle-Foot Stabilizer does not exist yet and therefore careful selection of design criteria is required. The design criteria should focus on critical constraints and provide the desired functionality. The following is a detailed outline of design criteria which will be utilized in the AAFS design. The functional requirements are detailed in Chapter 4.

3.3.1 Engineering Parameters

3.3.1.1 Patient body weight

The selection of patient body weight is important for biomechanical function and failure analysis. The AAFS should be robust and able to withstand the forces that would be applied for an above-average weight of a patient. As a reasonable estimate, specifications on commercial AFO prostheses can be used. For example, Ossur's Proprio Foot assumes a patient weight range of 45 to 116 kg (100 to 250 lb). In the US, the National Health and Nutrition Examination Survey 1999-2002 [100] determined the average male weight between 20-74 years of age was 86.8 kg (191 lb) and average male weight 75 years and over was 78.5 kg (172.7 lb). These are higher than female average weights. Therefore, a reasonable design goal for the AAFS is 90 kg (200 lb).

3.3.1.2 Reaction time

The reaction time of the AAFS will partly determine the actuators required for the device. As previously reviewed, in healthy young adults, muscle reaction times were as fast as 60 ms during ankle inversion simulations. Furthermore, during the gait cycle, the initial contact phase lasts approximately 2% of the gait cycle. Since the gait cycle duration at natural cadence is approximately 1 s, this initial contact phase is 20 ms. The next shortest gait phase is the loading phase of 10%. Assuming that the initial contact can be corrected

during the swing phase, the loading phase corrections should be made within at least half of the swing phase duration. Thus, the reaction time should be less than 50 ms or 5% of the gait cycle. Therefore, taking into account muscle response previously reviewed in sudden ankle inversion studies and gait cycle times, a reasonable reaction time for this device is less than 20 ms.

3.3.1.3 Noise

For a wearable device, noise should be minimized to avoid interfering with conversations and enable the AAFS to be inconspicuous. An example of a discreet device is a mobile phone vibrating in a hand, where the noise output is less than 50 dB [101]. Therefore, the ideal device should output no more than 50 dB of noise.

3.3.1.4 Device weight

The AAFS should be as lightweight as possible. Added weight to the shank or foot changes the inertia of the lower leg and thus modifies the dynamics of the gait cycle. In a study by Browning et al. [102], adding weight to the foot of healthy male subjects significantly increased energy expenditure, increased muscle activation, and altered gait spatial parameters. Significant gait changes were observed with a 4 kg weight on the foot. Hip extension torque was also increased. The active AFOs for which weight specifications were available in the literature ranged from 0.95 kg to 2.6 kg. Therefore, the ideal device should weigh less than 2.5 kg (5.5 lb), since the device is for elderly people, drop foot patients, and ankle-injured patients where muscle or ligament weakness is present and energy conservation is important. The weight of existing active AFOs may have been acceptable, however the power sources were not included and they were still generally bulky.

3.3.1.5 Device Profile and Size

The AAFS should conform to the shape of the ankle and foot to be unnoticeable below a pant leg in a similar manner as a passive AFO. Since shoes are an important accessory, offering a device that can be worn with as many shoes as possible is desirable. An ideal device would be within one to two additional US shoe sizes (1/6 in or 0.42 cm) thickness above the dorsal surface of the foot. The shank portion however, should not protrude past the calf posteriorly and distally. The device should also be able to fit as many foot sizes as possible with a minimum number of device sizes. On the surface of the ankle and shank, the device should be limited to a thickness of 1 cm above their anterior, medial, and lateral

surfaces. For the posterior surface, a limit of 1.5 cm is applied to not protrude past the calf.

3.3.1.6 Charging

The AAFS is a daily use device and therefore, if an electric power source is employed, the device should be able to operate for at least 24 hours before its next charge. The intention is to charge the device overnight similar to a cellular phone.

3.3.1.7 Summary

Table 3.1 summarizes the engineering parameters discussed above.

Table 3.1: Summary of engineering parameters for AAFS.

Engineering Parameter	Value
Patient Body Weight	$\leq$ 90 kg (200 lbs)
Reaction Time	$\leq$ 20 ms
Weight	$\leq$ 2.5 kg (5.5 lb)
Noise Output	$\leq$ 50 dB
Thickness	$\leq$ 0.42 cm above dorsal surface of foot
	$\leq$ 1 cm anterior, medial, and lateral to the surface of the ankle and shank
	$\leq$ 1.5 cm posterior to the surface of the ankle and shank
Battery life (if applicable)	$\geq$ 24 hours

3.3.2 Human Factors

An ideal AAFS should accommodate for many human factors. In terms of wear, the device should be discreet, attractive, comfortable, hypoallergenic, washable/cleanable, and easy to don/doff. The AAFS should also have natural and intuitive activation with ease of calibration for the user. A manual override should be present for activities such as driving as well as a notification when the power supply is low or a malfunction occurs. Lastly, the AAFS should be portable, whether worn or stored in a compact form.

3.3.3 Servicing

There should be reasonable time between servicing, ideally every six months for regular maintenance unless damage or malfunction occurs. The device should also be easy to service and replace parts.

3.3.4 Other Design Criteria

The device should be self contained with no assembly necessary. The price should also be competitive (within CDN $500).

3.4 Concluding Remarks

In this chapter, the need to develop an AAFS was established, the thesis objectives were listed, and the desired design criteria excluding functional requirements for the AAFS were outlined. As mentioned, the next objective is to determine the functional requirements of the device. Chapter 4 investigates these functional requirements in both the sagittal and frontal planes.

Chapter 4

Functional Requirements of an AAFS

The design criteria outlined in Chapter 3 provide a guideline for aspects of the AAFS design such as weight, noise, and reaction time. Before developing design concepts, the most important design criteria, the functional requirements of the AAFS, have to be determined. The AAFS device would not react to only a single event, but rather to changes throughout the entire gait cycle where both kinematic and kinetic changes occur. In this chapter, the functional requirements are established in two main planes of interest, sagittal and frontal, or anterior-posterior and medial-lateral, respectively.

4.1 Sagittal Plane (Anterior-Posterior) Functional Requirements

As previously reviewed, the sagittal plane or anterior-posterior direction is the dominant plane of interest in gait studies. The following sections establish a model to simulate the effects of an AAFS and analyze its required functions.

4.1.1 Background

4.1.1.1 Link Segment Model

In the sagittal plane, forces and moments are typically determined with a link segment model of the foot, as shown in Figure 4.1. The foot is a single segment with a center of mass, COM, and ankle joint axis, A. The external forces acting on the foot are the ground reaction force (if in stance phase), F_G, and the force due to gravity, $m_F g$. The reaction forces at the ankle joint are R_{A_x} and R_{A_y}. The model is dynamic and thus the linear

acceleration of the center of mass is represented by a_F. The force and moment reactions at the talocrural (ankle) joint, A, are represented by R_A and M_A, respectively. The angular velocity and angular acceleration of the foot are represented by ω_F and α_F, respectively. The dashed lines, r, represent the moment arms of each force with respect to the center of mass.

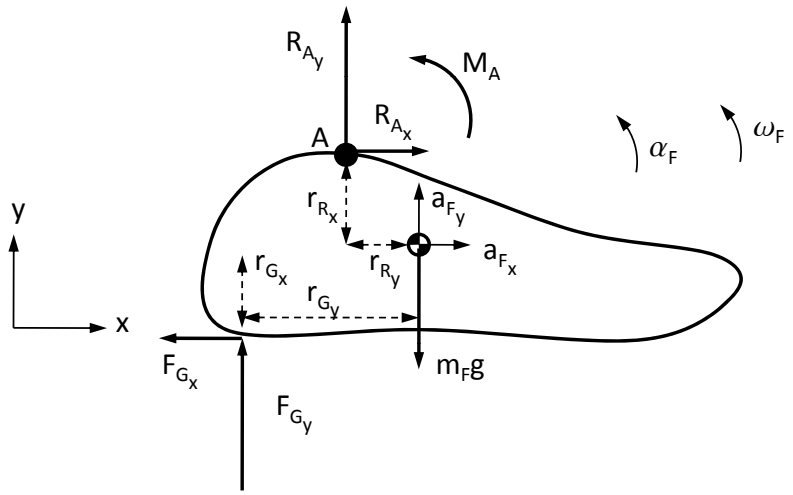

Figure 4.1: Link segment model of foot showing x and y coordinates of forces.

During gait studies [1], the linear accelerations are commonly determined from joint and segment position data obtained by cameras, and external forces are commonly measured. Therefore, performing a force balance in the x and y directions reveals the reaction forces at the ankle joint, A.

$$\begin{aligned} \sum F_x &= m_F a_{F_x} \\ R_{A_x} - F_{G_x} &= m_F a_{F_x} \\ R_{A_x} &= m_F a_{F_x} + F_{G_x} \end{aligned} \tag{4.1}$$

$$\begin{aligned} \sum F_y &= m_F a_{F_y} \\ R_{A_y} + F_{G_y} - m_F g &= m_F a_{F_y} \\ R_{A_y} &= m_F a_{F_y} - F_{G_y} + m_F g \end{aligned} \tag{4.2}$$

Angular velocity, ω, and angular acceleration, α, are also determined from the position data acquired by cameras in this model. I_{F_0} is the moment of inertia of the foot segment

at the center of mass. Performing a moment balance about the COM, reveals the moment reaction, M_A.

$$\begin{aligned} \sum M_{F_0} &= I_{F_0}\alpha_F \\ M_A - R_{A_x}r_{R_x} - R_{A_y}r_{R_y} - F_{G_x}r_{G_x} - F_{G_y}r_{G_y} &= I_{F_0}\alpha_F \\ M_A &= I_{F_0}\alpha_F + R_{A_x}r_{R_x} + R_{A_y}r_{R_y} + F_{G_x}r_{G_x} \\ &\quad + F_{G_y}r_{G_y} \end{aligned} \tag{4.3}$$

In fact, M_A, is the moment due to muscle forces [1] and therefore is the variable of greatest interest when determining the functional requirements of the AAFS in the sagittal plane (anterior-posterior direction). Using the model above, the stance and swing phases are analyzed next.

4.1.1.2 Stance Characteristics

The stance-phase sagittal-plane requirements of the ankle may be determined utilizing two work (or energy) approaches. In both approaches, a 0 deg angle represents the neutral position, a positive angle represents dorsiflexion, and a negative angle represents plantarflexion. For illustration, the data from young healthy adults (YHA) walking at natural cadence is considered [1]. The first approach is studying a power versus time graph [1] where:

$$P = M_A \cdot \omega \tag{4.4}$$

and

$$W = \int P(t)\,\mathrm{d}t \tag{4.5}$$

Power at the ankle (in W) is defined as the product of the sagittal-plane ankle moment, M_A (in Nm) due to muscle force, and the sagittal-plane ankle angular velocity, ω (in rad/s). Work done, W, is defined as the integral of power over time. Winter (1991) [1] has done extensive studies using this approach and has presented normalized data. Specifically, power normalized by body mass and time normalized to 100 percent gait cycle. The area under the normalized power curve corresponds to the normalized work done, and therefore the same analysis performed with the patient's mass and stride time would correspond to the actual work done. Figure 4.2 demonstrates the approach. The area below the horizontal

axis is considered negative work done at the ankle and the area above the horizontal axis is considered positive work done.

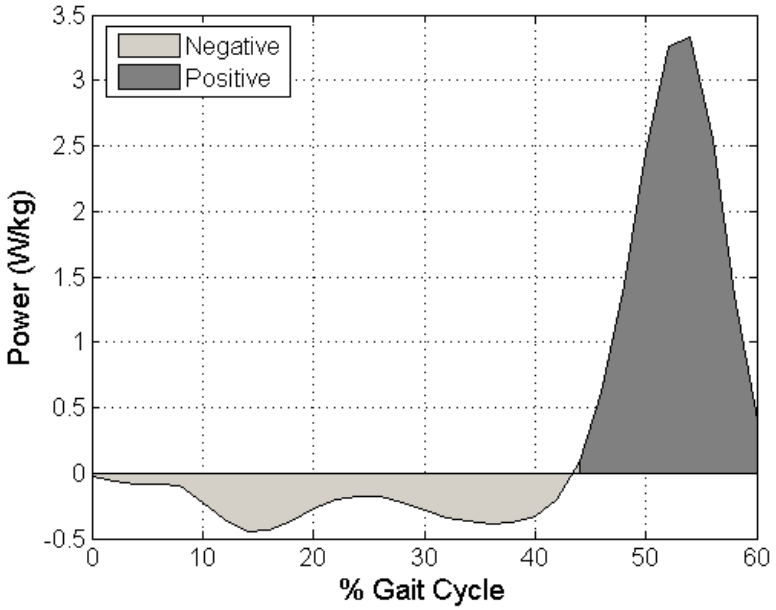

Figure 4.2: Average normalized ankle power versus percentage gait cycle for young healthy adults at natural cadence [1]. Negative work is done during controlled plantarflexion and dorsiflexion, and positive work is done during powered plantarflexion.

The second approach is studying a moment versus angle graph [22, 103] where:

$$W = \int M_A(\theta)\,\mathrm{d}\theta \tag{4.6}$$

Work done at the ankle is defined as the sagittal ankle moment due to muscle force, M_A (in Nm), integrated over ankle angle, θ (in rad). Calculation of power in the first approach requires the differentiation of angle to obtain angular velocity and it is sensitive to noise. Analyzing work done with the second approach is more accurate [103]. Figures 4.3 through 4.5 illustrate the breakdown of a typical M_A versus θ graph where the moment is normalized by body mass for the stance phase. The angle is shown in deg for convenient interpretation. All data in Figures 4.3 to 4.5 are from Winter [1]. The stance phase consists of the Controlled Plantarflexion (HC to FF), Controlled Dorsiflexion (FF to HO), and Powered Plantarflexion (HO to TO) curves as indicated. Arrows show the gait cycle progression. Several areas corresponding to normalized work throughout the gait cycle are highlighted. The actual work would require the individual's body mass and the conversion of ankle angle to radians. Since the data is discrete, the ankle angle in one time step can

cross the Dorsiflexor moment axis (0 deg) in the subsequent time step, resulting in areas that overlap the Dorsiflexor Moment axis. In fact, the highlighted areas should border along the Dorsiflexor Moment axis. Unlike a P versus t graph, the direction of foot rotation, or ω_F, is required to determine whether work done from the M_A versus θ graph is positive or negative. A summary is provided in Table 4.1 with listed areas corresponding to Figures 4.3 through 4.5. Areas 4 and 6 show the overlapping areas mentioned previously.

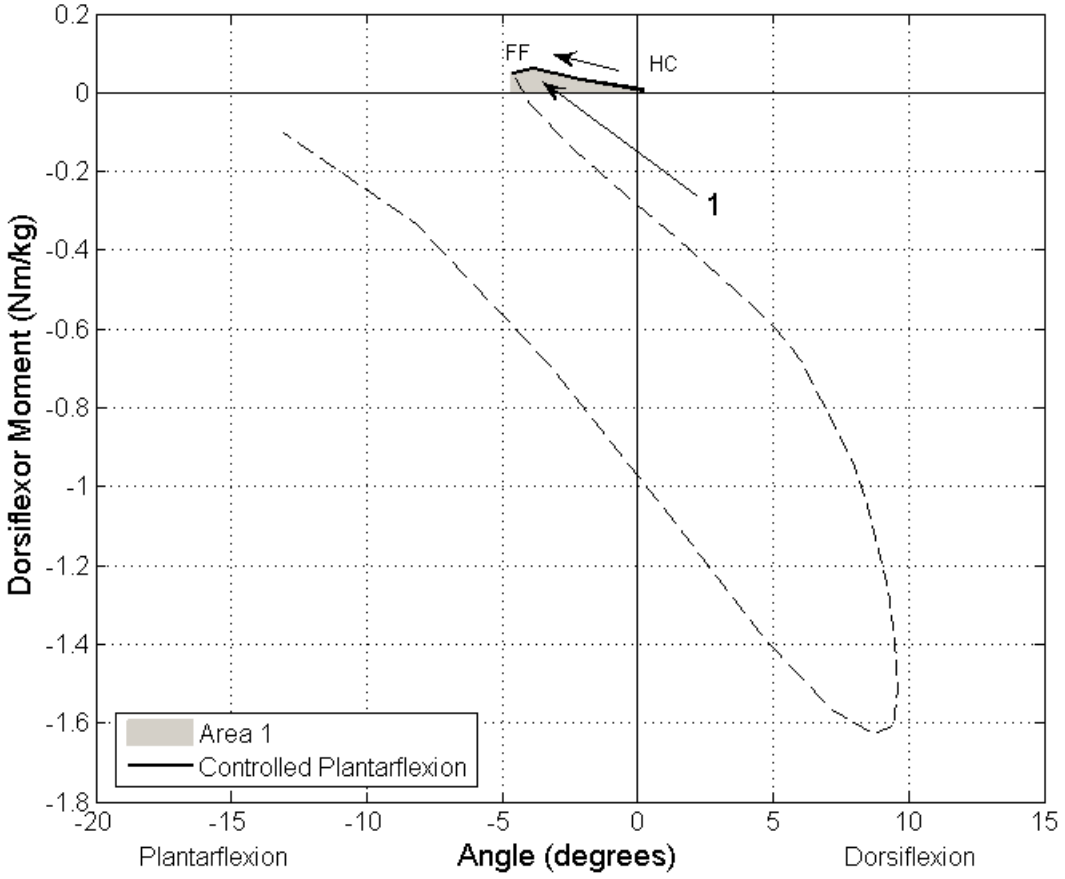

Figure 4.3: Graph of mean normalized dorsiflexor moment versus dorsiflexor angle for young healthy adults at natural cadence during controlled plantarflexion (adapted from [1]). Area 1 represents the negative work done per unit body mass from heel contact (HC) to foot flat (FF). The controlled plantarflexion period is shown as a solid line and the remainder of the stance phase is shown as a dashed line.

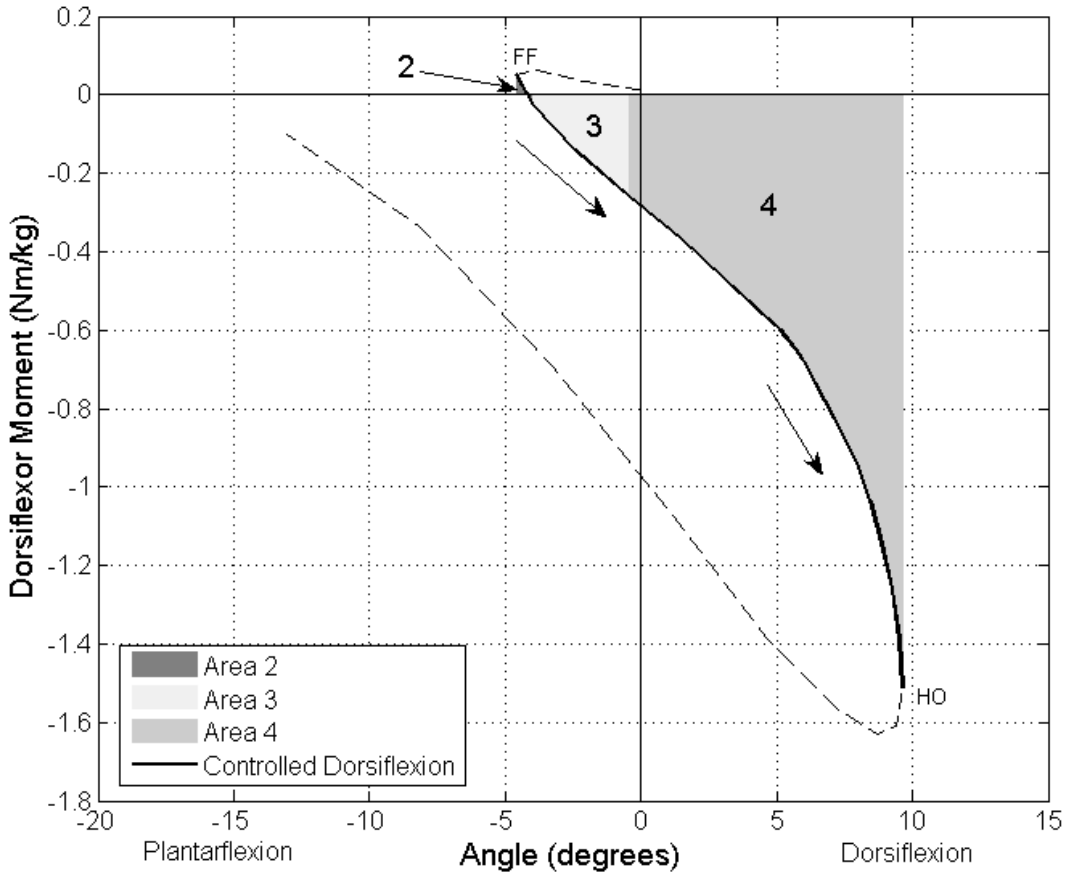

Figure 4.4: Graph of mean normalized dorsiflexor moment versus dorsiflexor angle for young healthy adults at natural cadence during controlled dorsiflexion (adapted from [1]. Areas 2, 3 and 4 represent the work per unit body mass from foot flat (FF) to heel off (HO). Area 2 is a brief period of positive work done since the area is positive whereas areas 3 and 4 are negative work done. The controlled dorsiflexion period is shown as a solid line and the remainder of the stance phase is shown as a dashed line.

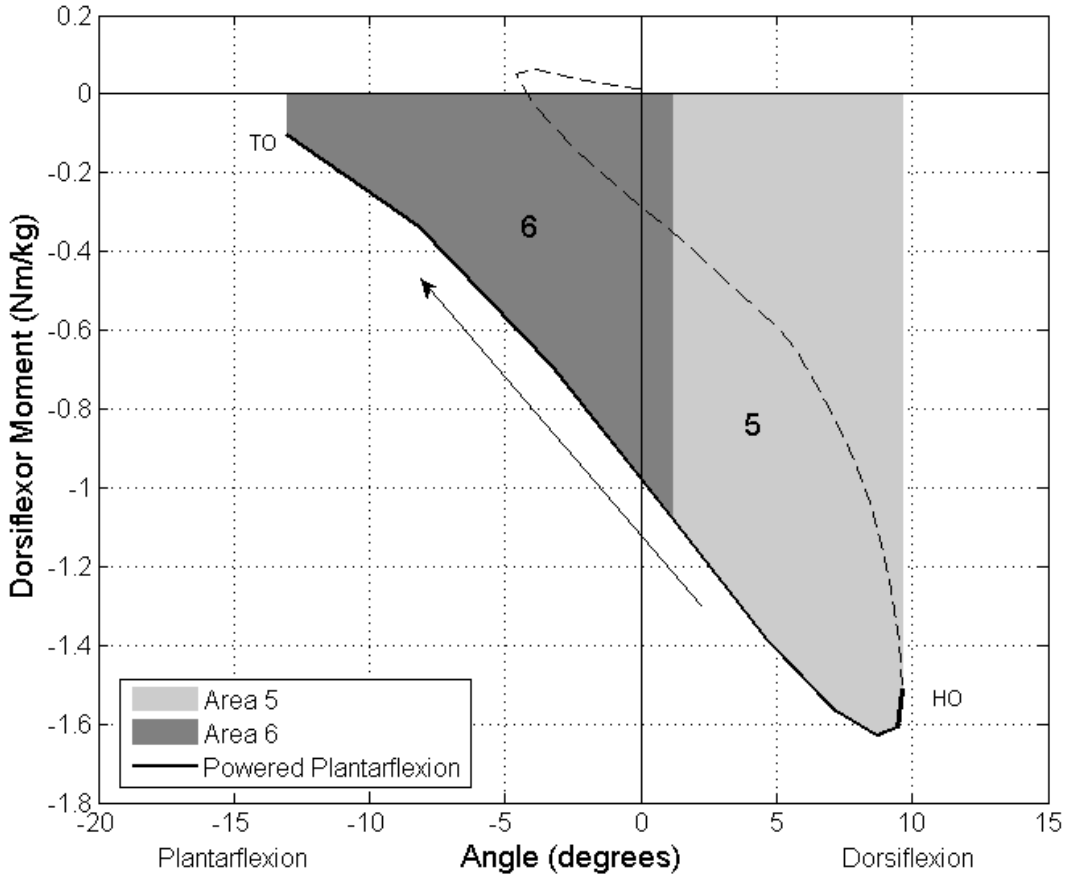

Figure 4.5: Graph of mean normalized dorsiflexor moment versus dorsiflexor angle for young healthy adults at natural cadence during powered plantarflexion (adapted from [1]. Areas 5 and 6 represent the positive work done per unit body mass from heel off (HO) to toe off (TO). The powered plantarflexion period is shown as a solid line and the remainder of the stance phase is shown as a dashed line.

Table 4.1: Summary of graph area definitions.

Direction of Foot Rotation	Moment	Angle	Sign of Net Work Done	Graph Area	Net Work Done (J/kg)
Dorsiflexing	Dorsiflexion	Dorsiflexion	Positive		
		Plantarflexion	Positive	2	1.24×10^{-4}
	Plantarflexion	Dorsiflexion	Negative	4	-0.112
		Plantarflexion	Negative	3	-0.009
Plantarflexing	Dorsiflexion	Dorsiflexion	Negative		
		Plantarflexion	Negative	1	-0.003
	Plantarflexion	Dorsiflexion	Positive	5	0.208
		Plantarflexion	Positive	6	0.130

The overall normalized net work done during stance for a young healthy adult is shown in Figure 4.6. Calculating the net area results in 0.214 J/kg of net positive work done.

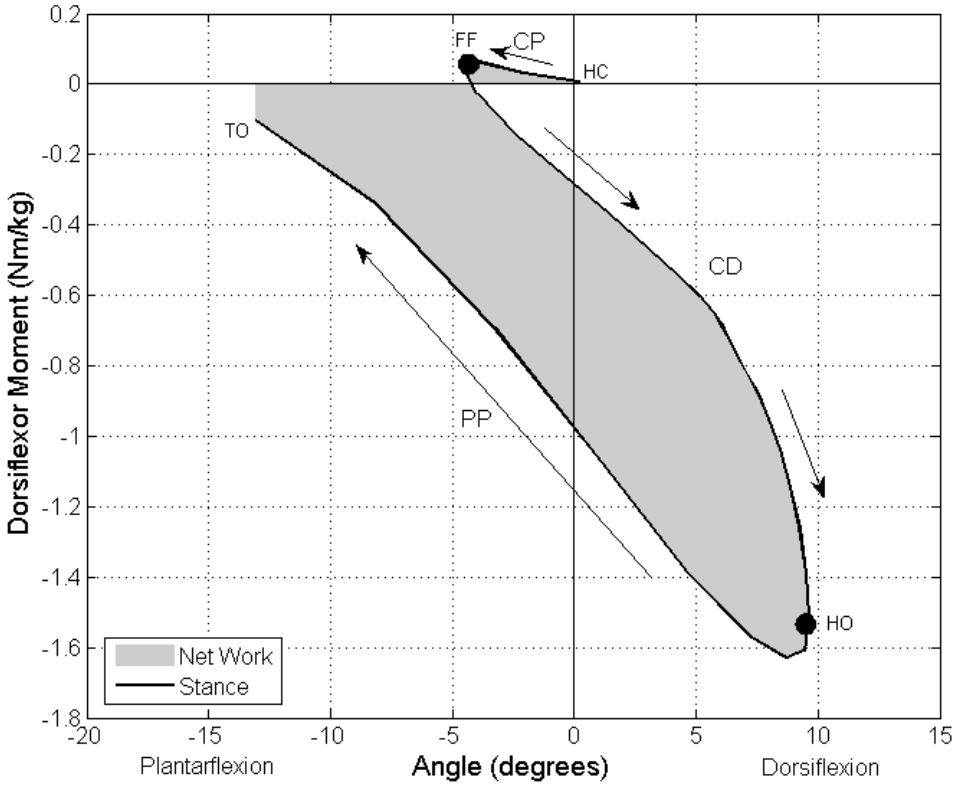

Figure 4.6: Normalized net work during stance for young healthy adults at natural cadence (adapted from [1]).

In addition to determining the net work from these graphs, examining their curves reveal the dynamic joint rotational stiffness [22, 103]. For young healthy adults, the graph characteristics are summarized in Table 4.2. The following analysis and stance characterization based on spring stiffness and work done is taken from [22]. This stance characterization has been used in a powered biomimetic prosthesis developed by MIT [104].

Table 4.2: Graph characteristics of a young healthy adults.

Phase Name	Model [22]	Work Done
Controlled Plantarflexion (CP) (HC to FF)	Linear spring	Negative (Area 1)
Controlled Dorsiflexion (CD) (FF to HO)	Non-linear spring	Briefly positive (Area 2), then negative (Areas 3 & 4)
Powered Plantarflexion (PP) (HO to TO)	Release of non-linear spring work plus torque source	Positive (Areas 5 & 6)

The graph characteristics can be reaffirmed by visual inspection of Figure 4.6. During CP, the curve of the M_A versus θ graph is mostly linear and thus can be modeled as a linear spring with negative work done. During CD, the curve of the M_A versus θ graph is non-linear and can be modeled as a non-linear spring. Initially, there is positive work done as the moment is still positive at FF, however the remainder of CD is negative work done. During PP, the ankle changes direction releasing the energy stored in the non-linear spring. Additional work is required to propel the body forward. This could be achieved by a torque source. The net positive work required during PP is the difference between Areas 5-6 and Areas 3-4.

4.1.1.3 Swing Characteristics

During swing phase a small dorsiflexor moment is required to support the weight of the foot to clear the ground [4, 1]. The moment and angular velocity required is small, and thus the power and consequently work done are small as well. With the foot in the air, the dominant moment acting on the ankle joint is the plantarflexion moment caused by the weight of the foot [1]. Since the inertial moment is small compared with the moment required for horizontal acceleration during swing, the inertial moment is assumed to be neglected [23]. This means that the only counteracting moment is due to the muscle force

at the ankle, which is a conservative approximation. Consider a 50th percentile male with a height of 180 cm and a mass of 82.2 kg [105]. When the foot is horizontal, the moment due to the weight of the foot is maximum as is the case for flaccid drop foot. Table 4.3 compares two anthropometric sets. Conservatively, the required moment per unit body mass should be 0.02 Nm/kg.

Table 4.3: Comparison of swing moment calculations.

	Set 1 [23]	Set 2 [105]
Location of COM relative to TCJ	0.1368 m	0.1365 m
Mass of Foot	1.192 kg	1.010 kg
Moment with foot horizontal	1.60 Nm	1.35 Nm
Moment/kg	0.019 Nm/kg	0.015 Nm/kg

Next, a model to implement an AAFS is developed.

4.1.2 AAFS Model

4.1.2.1 Model Assumptions

As previously reviewed, populations with ankle-foot gait deficiencies have altered kinematic and kinetic gait patterns resulting in differing work patterns from a young healthy adult work pattern. The challenge lies in improving the gait-deficient work patterns to those of healthier individuals. Since the healthier individuals may have lower physical capacity compared with young healthy adults, matching the shape and size of deficient work patterns to those of young healthy adults would be considered the ideal goal. It is understood that the level of functional achievement of each patient may be less the ideal functional goal (that of YHA). A tunable AAFS device could adjust to meet the requirements for the specific patient's goals. Assuming that the maximum ankle muscle moment that can be produced by the gait-deficient patient is considered the deficient moment, in order to correct the kinematics, the moment deficit must be corrected. The ideal goal is to correct the deficient kinetics to achieve young healthy adult ankle kinematics in the patient. Successful methods of moment correction include functional electrical stimulation (FES) where ankle muscles are electrically stimulated during the gait cycle [51, 106] and a robotic orthosis where forces and/or torques were machine-applied [107]. Studies of the effect of passive AFOs have also shown success in improving ankle moment patterns resulting in limited kinematic improvements [54, 78]. In a study by Ferris [108], a spring placed posterior to the tibia to provide a plantarflexion moment to resist dorsiflexion allowed the wearer to

reduce their biological ankle stiffness by reducing soleus, medial gastrocnemius, and lateral gastrocnemius muscle activation.

The required moment, or the augmentation moment, M_Q, to correct the moment deficit could be provided by the AAFS. Based on the ankle stiffness characteristics previously mentioned, the AAFS can be assumed to act as a variable rotational spring during the entire gait cycle with a torque source during PP. The natural position of the ankle is the neutral (NT) position and therefore it would be ideal if the variable rotational spring returned the ankle to NT after it is deformed. During CP from HC to FF, the variable rotational spring would deform along the required spring stiffness profile performing negative work. During CD from HC to NT, the negative work done would be returned as positive work done, or dorsiflexion assistance. During CD from NT to HO, the variable rotational spring would deform again along the required spring stiffness profile for this gait period, performing negative work. During PP from HO to NT, the negative work done would be returned as plantarflexion assistance. Finally, during PP from NT to TO, the variable rotational spring would deform along the spring stiffness profile required to lift the foot during the swing phase, similar to Ossur's Foot-Up previously reviewed. Since the spring stiffness profile is only required to change while passing through the NT position, the device could be simplified. The spring is assumed to absorb and release energy without losses. During PP, the torque source activates to compensate for the remaining plantarflexion moment deficit.

4.1.2.2 Modified Link Segment Model

Introducing the AAFS device into the link segment model above, results in a modified link segment model shown in Figure 4.7. The linear acceleration of the center of mass, the force due to gravity, and the ground reaction force are a_F, $m_F g$, and F_{G_Y}, respectively. The force reaction at the talocrural (ankle) joint, A, is represented by R_{A_Y}. Since all forces are considered those of young healthy adults, the muscle moment at A is represented by a combination of the deficient muscle moment, M_D, and the augmentation moment, M_Q. The angular velocity and angular acceleration of the foot are ω_F and α_F, respectively. The dashed lines represent the moment arms of each force with respect to the center of mass.

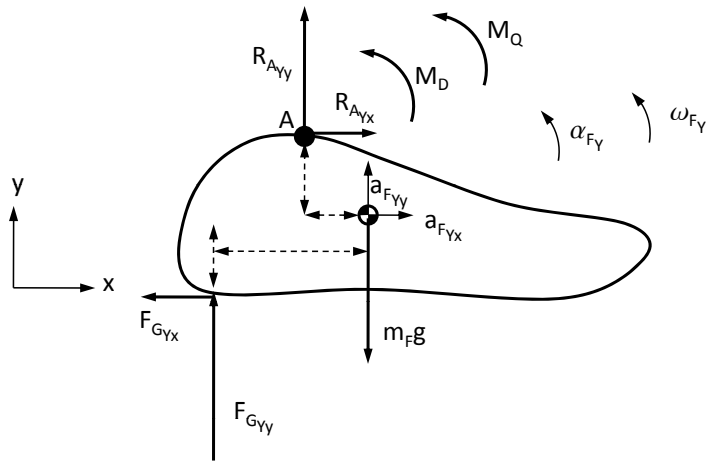

Figure 4.7: Modified link segment model of the foot showing x and y coordinates of forces.

Calculations are performed discretely, and therefore let k represent each time step. The summations of moments are as follows:

$$M_{Y_k} = M_{D_k} + M_{Q_k} \tag{4.7}$$

where M_Y is the desired moment for young healthy adults, M_D is the deficient ankle muscle moment and M_Q is the required augmentation moment.

$$M_{Q_k} = M_{S_k} + M_{T_k} \tag{4.8}$$

and,

$$M_{S_k} = K_{R_k}\theta_{Y_k} \tag{4.9}$$

where M_S is a function of the spring stiffness, K_R and the desired young healthy adult kinematics, θ_Y. M_T is applied directly as needed, and will also be a function of θ_Y.

It is useful to outline the sequence of the AAFS function throughout the gait cycle. This is illustrated in Figure 4.8.

Referring back to Figure 4.6, the cycle begins at HC where the foot is positioned into neutral (NT). A spring stiffness K_{R1_k} is used and the spring is deflected until it reaches FF (CP) providing plantarflexion moment resistance, M_{S1_k}. Upon FF, the spring energy is released until NT is reached (mid CD) providing a dorsiflexion moment assistance, M_{S1_k}.

As the shank continues to roll over the ankle, a new spring stiffness K_{R2_k} is used and the spring is deflected until HO occurs (terminal CD) providing a dorsiflexion moment resistance, M_S2_k. Upon HO, the spring energy is released providing a plantarflexion moment assistance, M_{S2_k} during PP up to the NT position. Upon reaching the NT position (mid PP), another spring stiffness K_{R3_k} is used and the spring is deflected until it reaches TO (terminal PP) providing a slight plantarflexion moment resistance, M_{S3_k}. As mentioned earlier, this energy when released by the spring upon TO, will lift the foot back to the neutral position during swing, preceding HC of the next gait cycle. During PP, a torque source, T_k, is applied to provide the necessary plantarflexion moment deficit, M_{T_k}, for push-off.

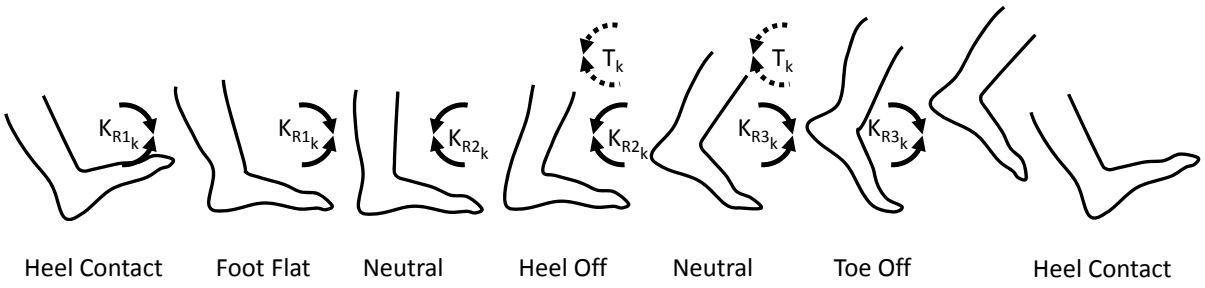

Figure 4.8: Sequence of spring stiffness profile changes and torque source activation throughout one stride. Moment direction due to the resistance of ankle rotation via spring stiffness profile, K_{R_k} is indicated by arrows and the torque source is indicated by, T_k.

4.1.2.3 Populations

The three populations of interest in this thesis are the fit and healthy elderly people, sprain-injured individuals, and drop foot patients. Clinical sagittal-plane ankle angle and moment data were available for fit and healthy elderly people and drop foot patients. For individuals with sprain-injured ankles, the required sagittal joint stiffness would be much less than the stiffness requirements of a drop foot patient. Therefore, designing the device with drop foot patient stiffnesses as an upper limit, would satisfy the stiffness requirements of sprain-injured individuals.

Consider the following data sets: mean ankle angle and moment for fit and healthy elderly people labelled "Elderly" [1]; ankle angle and moment for a stroke subject labelled "Drop Foot 1" [106]; mean ankle angle and moment for subjects with hemiplegia labelled "Drop Foot 2" [54]; and mean ankle angle and moment for Charcot-Marie-Tooth patients labelled "Drop Foot 3" [109] (see Appendix A for data sets). The stance work patterns for these data sets are compared with young healthy adults labelled "YHA" [1] (see Appendix

A) in Figures 4.9 through 4.12. The gait cycle beginning and end are indicated by "B" and "E", respectively. The area of work done by young healthy adults lies behind (overlaps) the area of work done by the gait-deficient population. The net work done for each population is listed in Table 4.4.

Table 4.4: Summary of normalized net work done for the stance phase.

Population	Normalized Net Work Done (J/kg)
Elderly	0.093
Drop Foot 1	-0.014
Drop Foot 2	-0.050
Drop Foot 3	-0.027

As previously mentioned, the net work done during stance for young healthy adults is positive. Of the listed populations above, only the elderly exhibit positive net work whereas drop foot patients exhibit negative net work done.

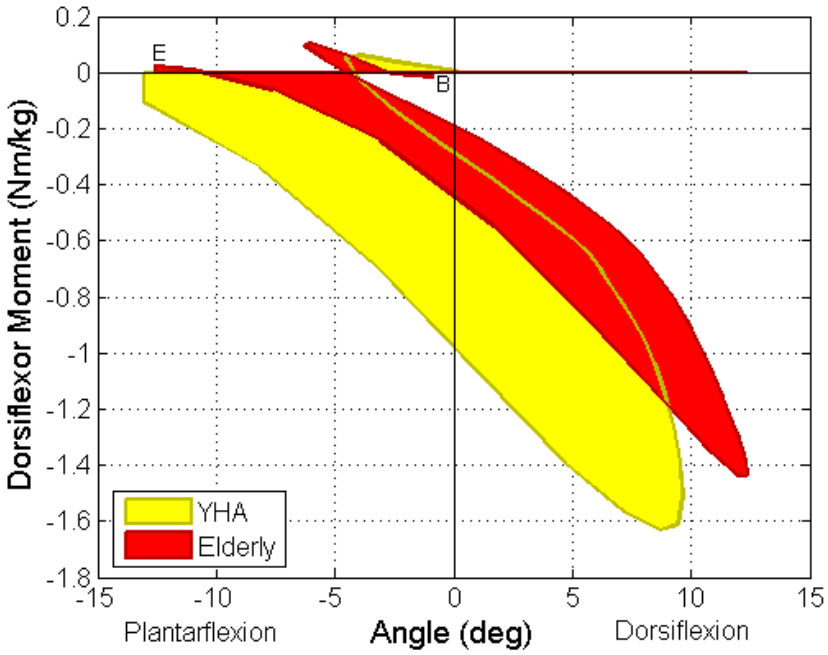

Figure 4.9: Normalized net work during stance for elderly [1] versus young healthy adults [1].

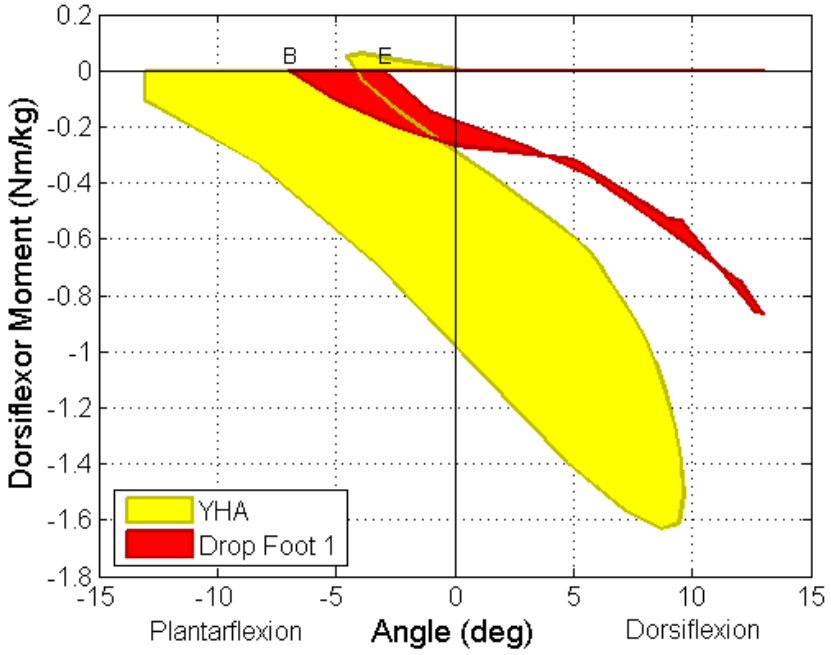

Figure 4.10: Normalized net work during stance for Drop Foot 1 patient [106] versus young healthy adults [1].

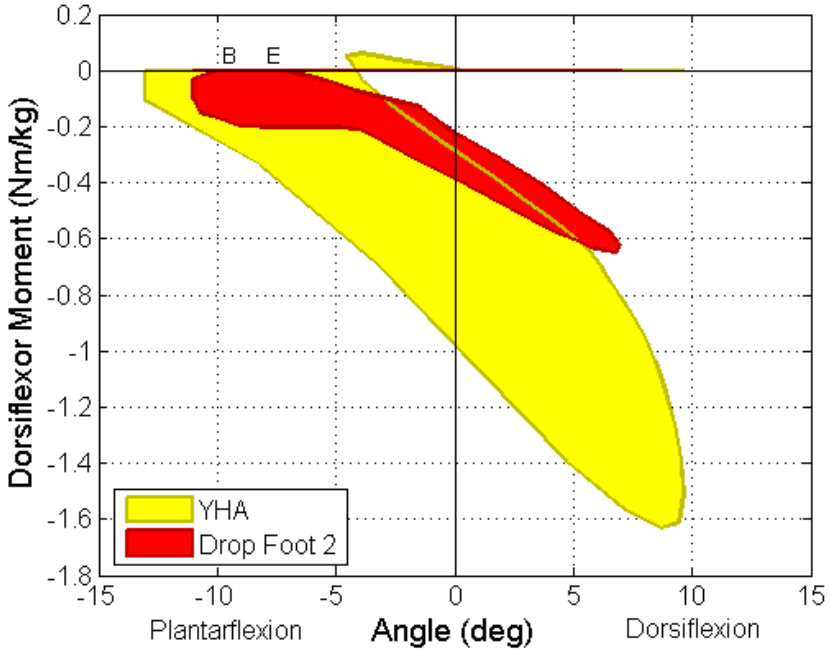

Figure 4.11: Normalized net work during stance for Drop Foot 2 patients [54] versus young healthy adults [1].

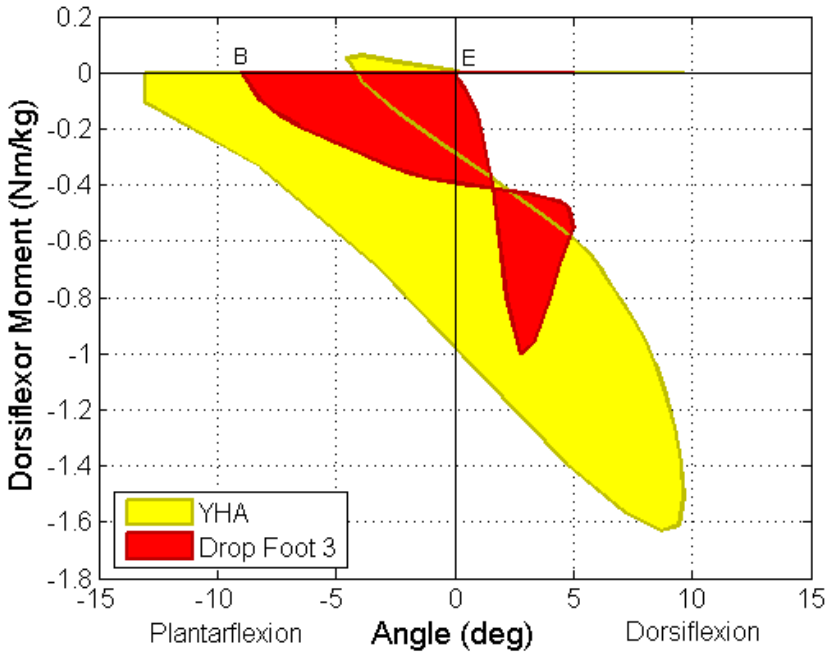

Figure 4.12: Normalized net work during stance for Drop Foot 3 patients [109] versus young healthy adults [1].

4.1.3 Functional Simulation of an AAFS Device

4.1.3.1 Analysis of Spring Characteristics

The deficit in moment at each time step, k, in the gait cycle reveals the augmentation moment, M_Q, required by the AAFS. As previously mentioned, this moment is a combination of the moment due to the resistance of a rotational stiffness spring, K_{R_k}, and the moment due to a torque source, T_k during PP. In particular, the rotational stiffness required was divided into three gait periods: HC to FF to NT, NT to HO to NT, and NT to TO to NT as previously illustrated in Figure 4.8. Since the goal is to achieve young healthy adult kinematics, graphing the augmentation moment, M_Q, versus YHA angle, θ_Y, determines the required dynamic stiffness of the spring. The moment deficit versus YHA angle curves for the gait periods of HC to FF during CP and NT to HO during CD are shown in Figure 4.13. The gait period from NT to TO is not shown since the rotational stiffness, K_{R_3}, is assumed to be linear to achieve the swing dorsiflexion moment required at TO found in Subsection 4.1.1.3.

During the gait period HC to FF (CP), the common trend between the populations is a linear curve at a different slope for each population. This implies that a rotational spring with a different constant spring rate for each population is required. During the

analysis of the elderly moment deficit, an aberration occurs at the end of CP where the deficit is negative resulting in an unusable linear best fit curve. To compensate, this point was removed and a linear best fit was applied to the remaining points.

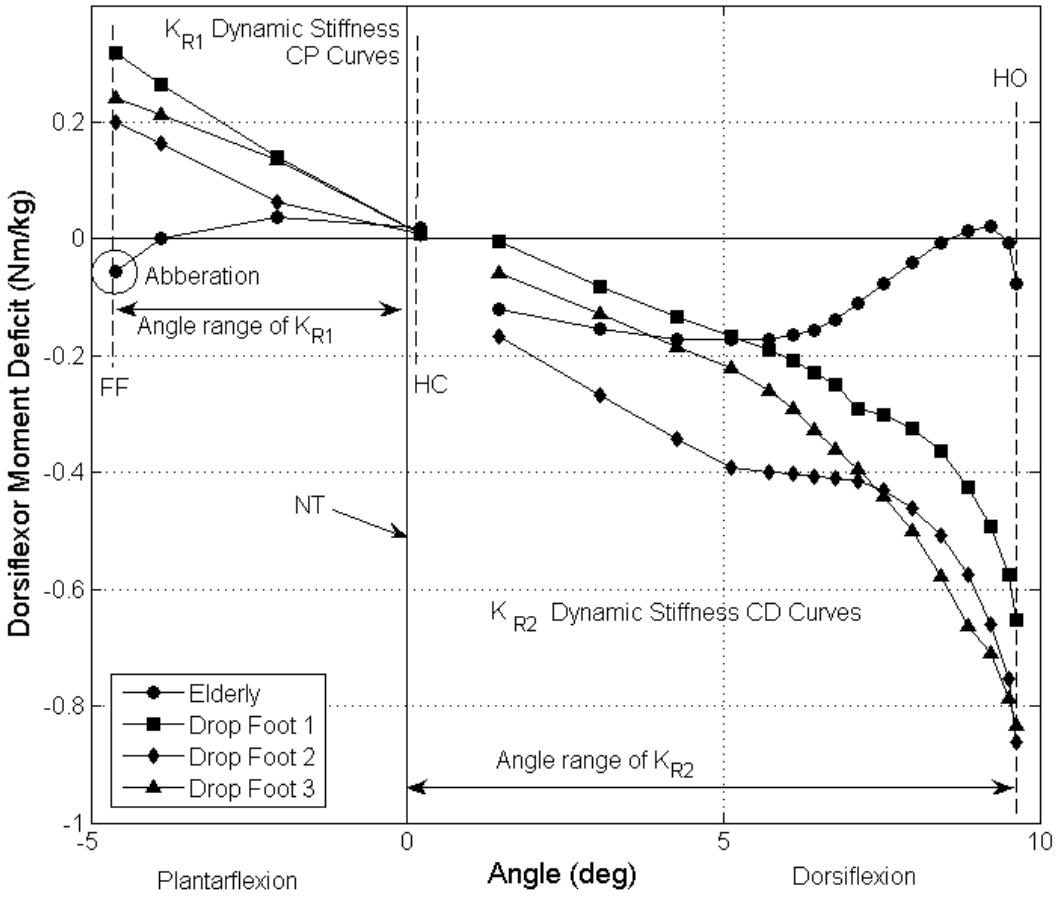

Figure 4.13: Normalized moment deficit versus young healthy adults angle during stance for deficient populations compared with young healthy adults. Data were obtained from [1],[106],[54] and [109].

During the gait period NT to HO (mid to late CD), the trend is not obvious. Each pattern can be characterized with a different non-linear spring. This could be difficult to implement in a device that does not allow controlled change of impedance. If an infinitely controllable spring is used and compensation by the patient were avoided, a curve fit is not necessary. However, since compensatory strategies may be possible by the patient, a simpler design would involve a linear rotational spring. Therefore, for each population, a linear best fit curve passing through the origin is applied and the resulting slope, or stiffness, is utilized to modify the work patterns. The origin was selected since it corresponds to

the neutral position, and therefore when the foot is not in the neutral position, the linear rotational spring would tend to force the foot back into the neutral position. A summary of linear stiffnesses is described later in Subsection 4.1.4.2.

4.1.3.2 Application of the AAFS Device

The modification of deficient work patterns are the functional requirements of the AAFS in the sagittal plane. YHA kinematics are prescribed and deficient moments are modified by M_S and M_T using the model above. First the stiffnesses K_{R1}, K_{R2}, and K_{R3}, are implemented, followed by the input of the torque source, T, to compensate for the remaining moment deficit during PP. By using this approach, the person with deficient gait is provided the work done (or energy) by the AAFS to have the same or similar work done of young healthy adults. Net work per unit body mass for the modified parameters with the application of the AAFS is calculated with the approach in Subsection 4.1.1.2, and compared with young healthy adults. Finally, the ratios of the deficient work patterns without the AAFS and with the AAFS are compared with the work pattern of a YHA. The results are discussed next.

4.1.4 Results and Discussion

4.1.4.1 Augmented Moments in Populations with Deficient Gait

The resulting modified curves from the simulation are shown in Figures 4.14 to 4.17 where the area of work done by young healthy adults lies behind (overlaps) the area of work done by the gait-deficient population modified by the augmentation moment.

Table 4.5 summarizes the normalized net work ratios with and without the application of the AAFS for each population compared with young healthy adults. A ratio of 1.0 after the modification with the AAFS would mean the AAFS would enable the deficient-gait adult to have the same net work as a young healthy adult. As mentioned previously, the negative values indicate net negative work indicating orthotic assistance is needed. The net work after modification with the AAFS is effectively restored to within 8% of a young healthy adult.

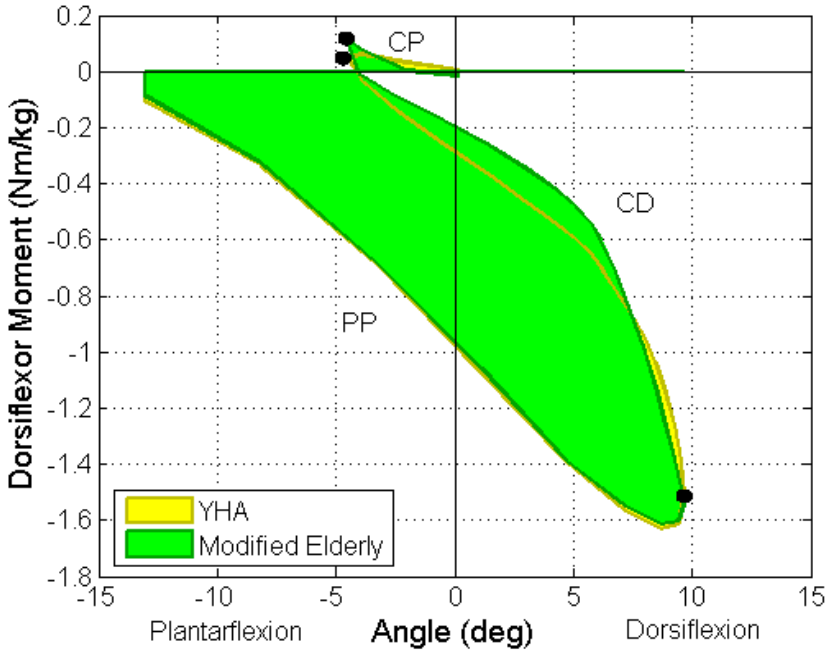

Figure 4.14: Normalized net work during stance for modified elderly versus young healthy adults. Data were adapted from [1]. Angle data are for young healthy adults [1].

Table 4.5: Comparison of normalized net work ratios of deficient populations to young healthy adults.

Population	Normalized Net Work Ratio	
	Before Modification Without AAFS	After Modification With AAFS
Elderly	0.436	1.049
Drop Foot 1	-0.067	0.926
Drop Foot 2	-0.232	1.019
Drop Foot 3	-0.125	0.942

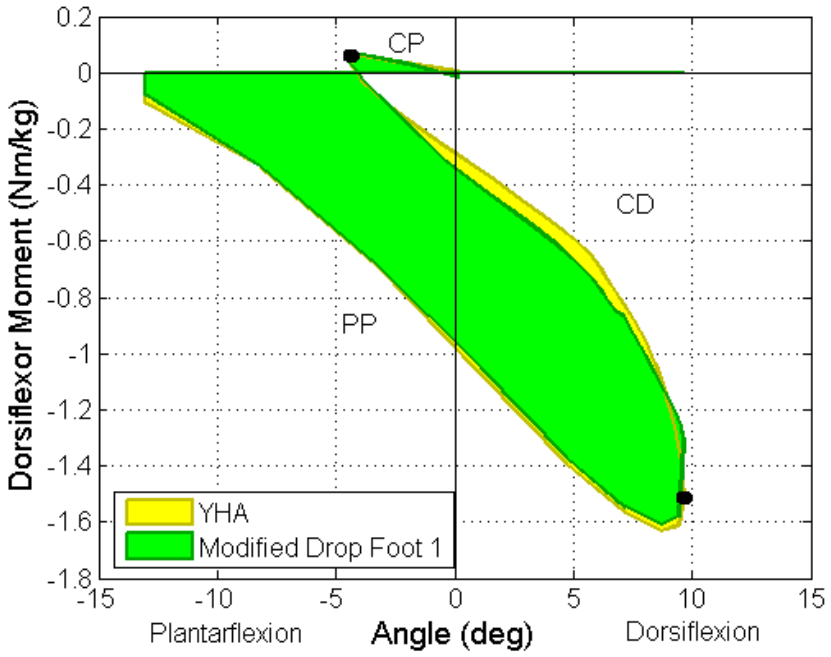

Figure 4.15: Normalized net work during stance for modified Drop Foot 1 patients versus young healthy adults. Data were adapted from [106] and [1]. Angle data are for young healthy adults [1].

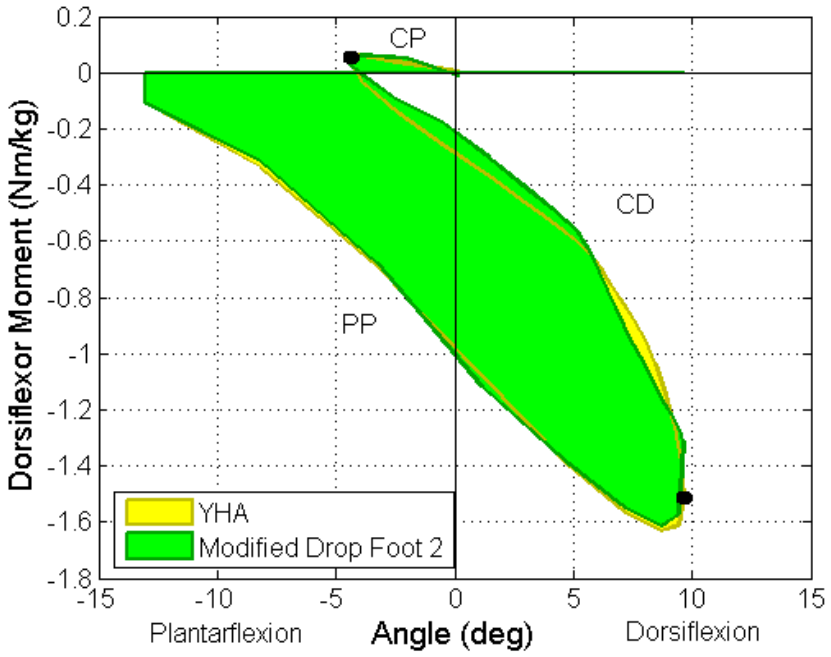

Figure 4.16: Normalized net work during stance for modified Drop Foot 2 patients versus young healthy adults. Data were adapted from [54] and [1]. Angle data are for young healthy adults [1].

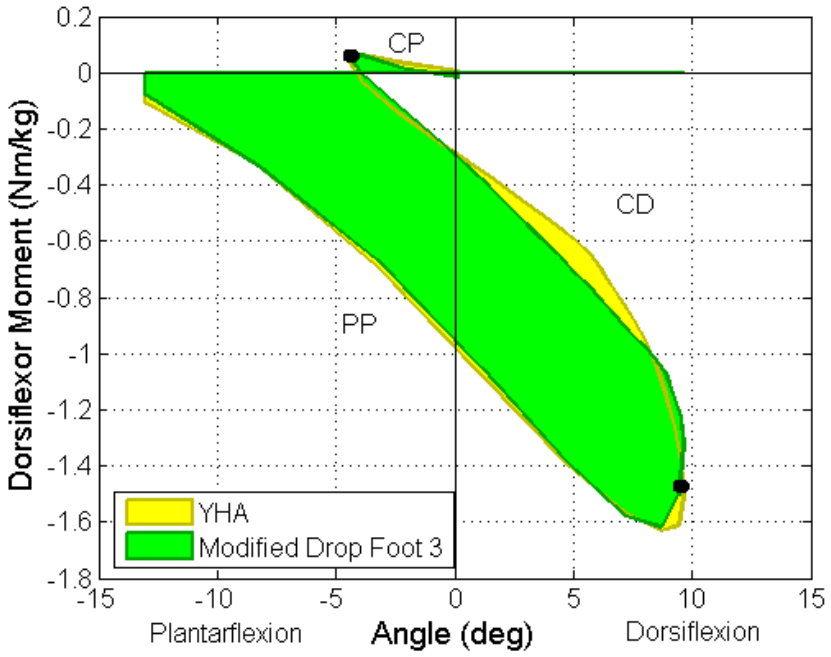

Figure 4.17: Normalized net work during stance for modified Drop Foot 3 patients versus young healthy adults. Data were adapted from [109] and [1]. Angle data are for young healthy adults [1].

4.1.4.2 Linear Rotational Spring

Table 4.6 summarizes the required spring constants for the different gait periods for each population. For the design of the AAFS, the upper rotational stiffness limit should be 0.070 Nm/kg/deg θ up to 10 deg and the lower rotational stiffness limit should be 0.002 Nm/kg/deg θ up to 20 deg. For a patient body mass of 90 kg, the upper and lower values are 6.3 Nm/deg θ up to 10 deg and 0.18 Nm/deg θ up to 20 deg.

Table 4.6: Summary of spring stiffnesses computed for deficient-gait populations.

Population		Spring Stiffness per Gait Period (Nm/kg/deg θ)		
	Gait Phases	CP-CD	CD-PP	PP-SW
	Gait Period	NT(HC) $\rightarrow$ FF $\rightarrow$ NT	NT $\rightarrow$ HO $\rightarrow$ NT	NT $\rightarrow$ TO $\rightarrow$ NT
	Stiffness	K_{R1}	K_{R2}	K_{R3}
Elderly		0.004	0.011	0.002
Drop Foot 1		0.069	0.047	0.002
Drop Foot 2		0.042	0.069	0.002
Drop Foot 3		0.055	0.066	0.002
Max Angle (θ)		5	10	20

The linear spring assumption for the CP and CD phases resulted in discrepancies between the modified deficient work done patterns and normal work done pattern as can be seen in Figures 4.14 to 4.17. Since the moment versus angle curves between the deficient-gait patients and young healthy adults are not coincident during these phases, the kinematics would not be completely normal; however, they would be significantly improved.

4.1.4.3 Torque Source

Figure 4.18 illustrates the required torque for each deficient population. Each curve follows a similar ramp pattern of positive and negative slope as the torque source is applied from a dorsiflexed angle upon HO to a plantarflexed angle upon TO. Peak torque is needed near mid-PP around the neutral position. This may be beneficial in designing the AAFS since geometry during PP could vary the torque source. The maximum plantarflexion torque required by the torque source is 0.72 Nm/kg. For a maximum patient body mass of 90 kg, the maximum plantarflexion torque required by the torque source is 65 Nm. The maximum angular velocity during PP is 3.6 rad/s, or 206 deg/s [1], and therefore the maximum power required by the torque source is 2.6 W/kg or 234 W for a 90 kg patient.

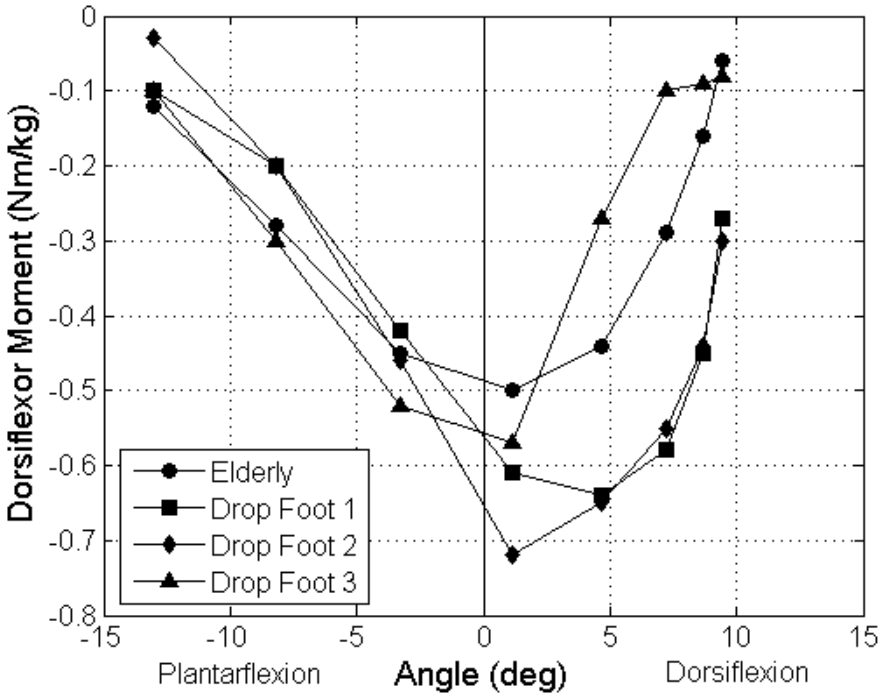

Figure 4.18: Torque source requirement for modified populations during powered plantarflexion.

4.1.4.4 Compensation Moment

The overall simulation showed improvement in stance work patterns for the above populations. With a linear rotational spring assumption for the CP and CD phases, the exact deficit moment was not provided by the AAFS and therefore exact kinematics during these phases would not be observed. It may be possible for the body to compensate for these differences. It is therefore important to reveal the differences between the modified moment patterns throughout the stance phase with those of young healthy adults. Figures 4.19 through 4.22 show the compensation moments for each population. By applying these compensation moments while using the AAFS, a user could potentially achieve the gait pattern of young healthy adults.

The compensation moment lies within +/-0.2 Nm/kg for each population. Minimal differences are seen during PP (45% to 60% gait cycle) with the active torque source. The CP phase (0% to 5% gait cycle) and CD phase (5% to 45%) are discussed in more detail as follows. First, elderly people are examined more closely in Figure 4.19. During CP, the compensation moment is nearly zero, however it increases to a plantarflexor moment as terminal CP is reached. This indicates the device is providing more dorsiflexion moment than required and thus the elderly patients are assisted. During CD, the compensation

moment is initially plantarflexor up to 0.1 Nm/kg which requires the patient to use their own plantarflexors slightly more than without the AAFS. However, the opposite is true during the latter portion of CD where the compensation moment is dorsiflexor indicating the need for less plantarflexor strength.

Drop foot patients are examined next in Figures 4.20 through 4.22. All three graphs show similar patterns and thus will be discussed together. During CP, the compensation moment is nearly zero which indicates a good match of functional requirements by the device. During CD, the compensation moment is mostly dorsiflexor indicating less plantarflexion moment required by the patient. During terminal CD, there is a cross over to a plantarflexor compensation moment resulting in the only portion where additional strength is required by the subject.

The compensation moment required is minimal compared with the augmentation moment required to achieve young healthy adult kinetics. Even if the compensation were not supplied, significant improvements in kinematics would be seen. Based on the above results, the sagittal plane, or anterior-posterior, functional requirements for the AAFS were determined.

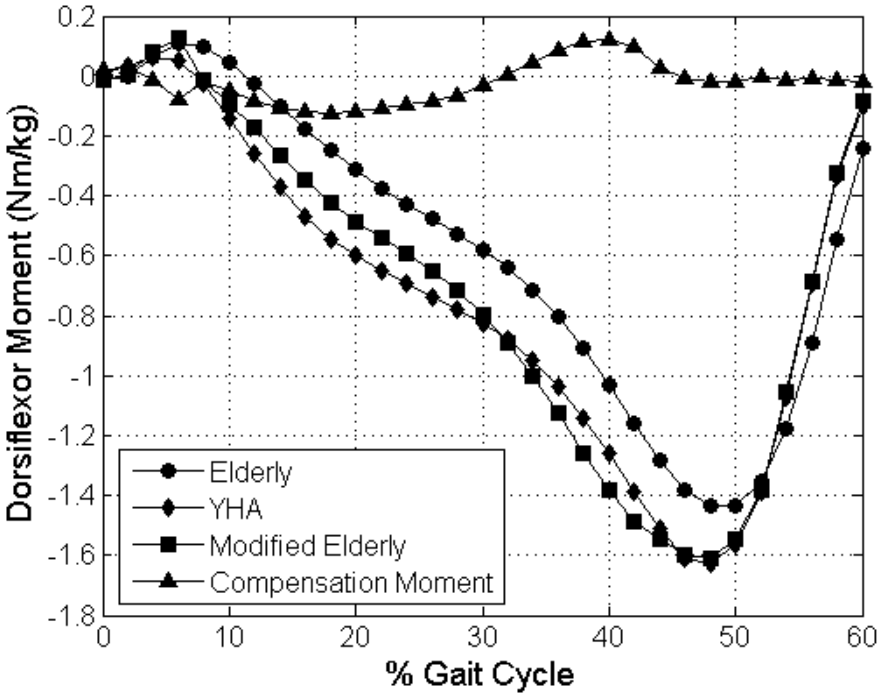

Figure 4.19: Compensation moment versus percentage gait cycle for elderly people.

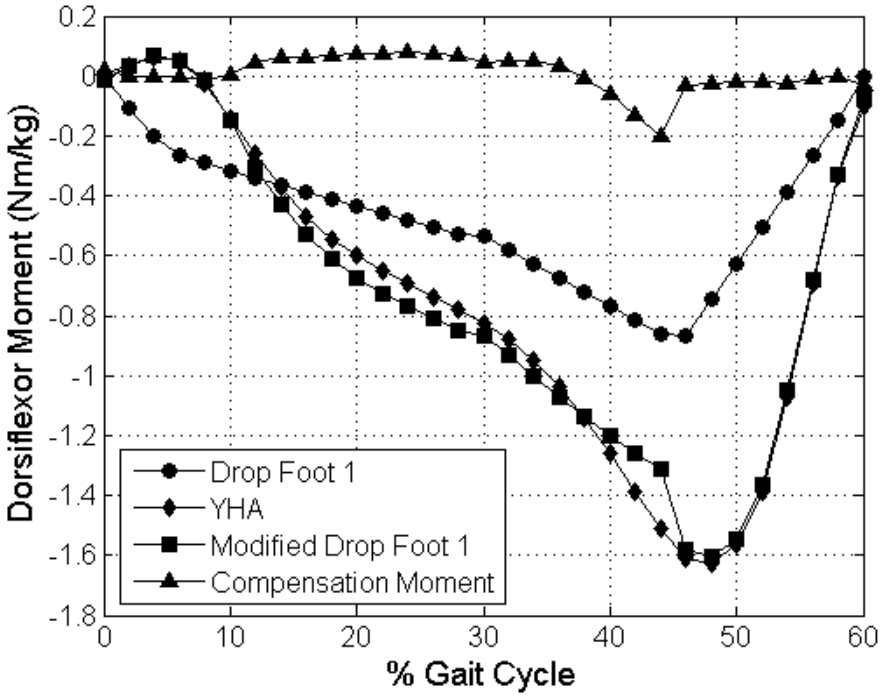

Figure 4.20: Compensation moment versus percentage gait cycle for Drop Foot 1 patients.

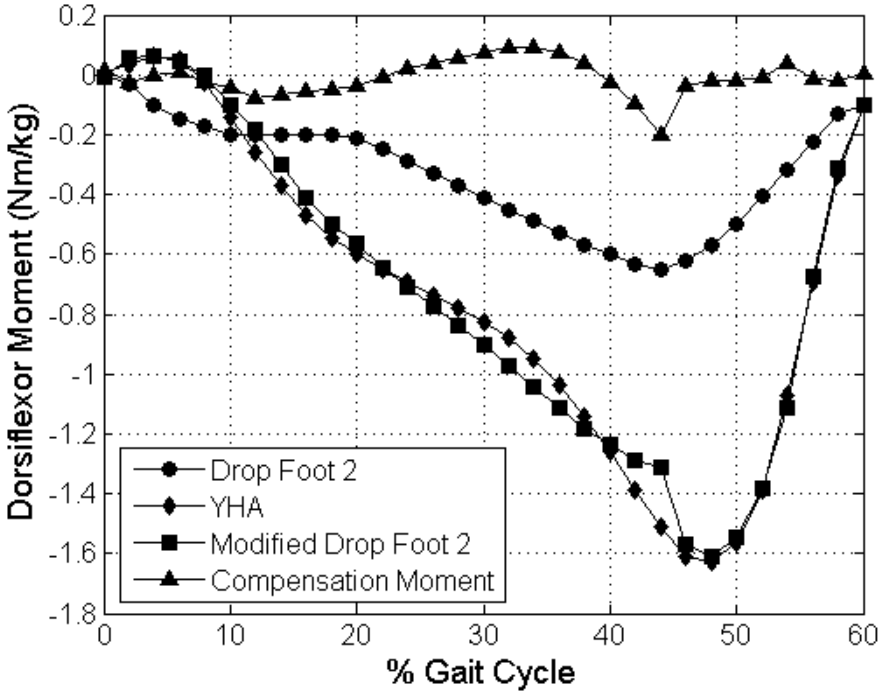

Figure 4.21: Compensation moment versus percentage gait cycle for Drop Foot 2 patients.

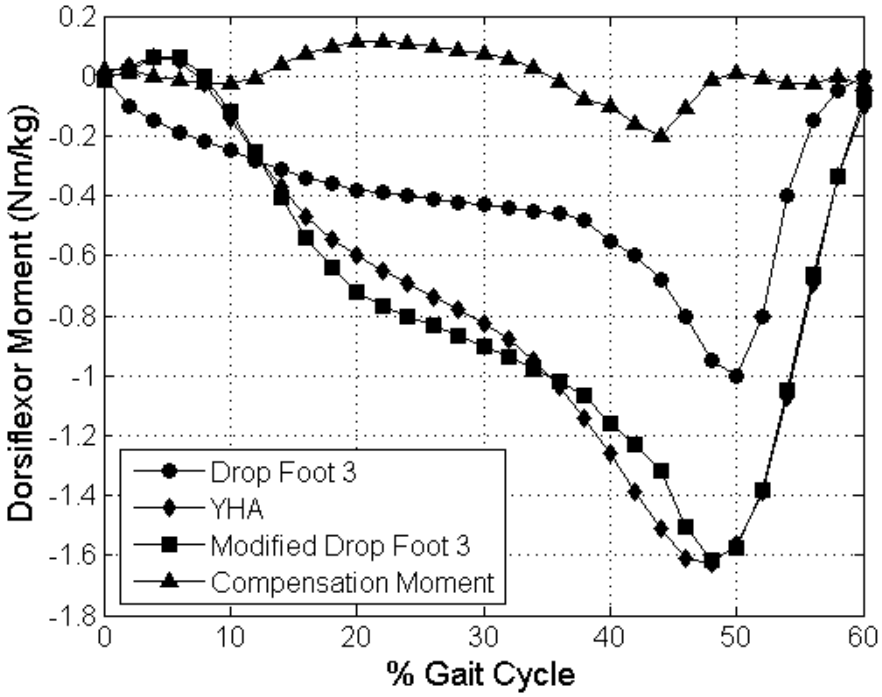

Figure 4.22: Compensation moment versus percentage gait cycle for Drop Foot 3 patients.

4.2 Frontal Plane (Medial-Lateral) Functional Requirements

Unlike the sagittal plane (anterior-posterior direction) requirements, the frontal plane (medial-lateral direction) requirements are not cyclical in nature. As previously discussed, supination and pronation of the ankle is important for stability and injury prevention. Stiffening the ankle in the frontal plane can increase stability by preventing the foot from rotating past its medial or lateral borders, or by damping mediolateral fluctuations in foot movement. Based on the literature review in Chapter 2, there are four selected events where stiffening the ankle with an AAFS is desired. These are:

1. High impact landings where forces are greater than 1.1 times the patient's body weight.

2. Fluctuations in stability where abnormal mediolateral COP shifts occur.

3. Sudden and/or high torque supination or pronation of the foot where torques are greater than 10 Nm [24] and/or angular speeds are greater than 200 deg/s (conservative estimate of angular speed to cause injury based on studies by [62, 65, 69]).

4. Misaligned supination or pronation upon HC or TO.

Stiffening could imply stopping the motion completely, or damping the motion. However, the neutral position is the ideal stable position for the foot, so returning the foot to neutral is highly desirable. Logically, a spring would be suitable for this application. Not only is a spring safe by being compliant, it would react quickly within milliseconds. As an upper limit, 20 Nm is selected to stiffen the ankle based on sudden inversion studies of [60, 62, 63, 64]. At a maximum supination or pronation angle of 10 deg β during gait, the upper spring stiffness is 2 Nm/deg β for a 90 kg patient, and therefore 0.022 Nm/kg/deg β.

4.3 Concluding Remarks

The AAFS functional requirements in the sagittal plane (anterior-posterior direction) were determined using the M_A versus θ work approach. The adjustment of joint rotational stiffnesses in the CP and CD phases were altered with a linear rotational spring. This resulted in discrepancies between the moment versus angle curves of the gait-deficient populations and young healthy adults. An analysis of the moment deficit differences showed that compensation moments required by the gait-deficient individual were reasonable. A linear rotational spring was used to store energy prior to the swing phase to provide an assistive dorsiflexor moment upon HO. The upper stiffness of the linear rotational spring limit should be 0.070 Nm/kg/deg θ up to 10 deg and the lower rotational stiffness limit should be 0.002 Nm/kg/deg θ up to 20 deg. The corresponding values for a 90 kg patient are 6.3 Nm/deg and 0.18 Nm/deg, respectively. For PP, a torque source was supplied in a negative then positive pattern to restore plantarflexion power. The maximum plantarflexion torque and power required are 0.72 Nm/kg and 2.6 W/kg, respectively. For a 90 kg patient, the maximum plantarflexion torque and power required is 65 Nm and 234 W, respectively.

The medial-lateral functional requirements were also determined based on specified events during the gait cycle. A linear rotational spring was chosen to best meet these requirements with upper stiffness of 0.022 Nm/kg/deg β. The functional requirements established in this chapter combined with the design criteria in Chapter 3 form the foundation to design an AAFS. This is explored next in Chapter 5.

Chapter 5

Design of an Active Ankle-Foot Stabilizer

In the previous two chapters, the design criteria and functional requirements of the AAFS were determined. In this chapter, several design concepts are explored, followed by an in-depth analysis of potentially viable designs and their feasibility.

5.1 Design Concepts

Based on the functional requirements, the AAFS design consists of a linear rotational spring and a torque source in the sagittal plane, and a linear rotational spring in the frontal plane. The following sections discuss design concepts for both of these aspects of the AAFS beginning with the torque source.

5.1.1 Torque Source

A torque source at the ankle and foot presents a difficult challenge. As previously reviewed in Subsection 2.3.2, current technologies and the level of actuation as they compare to the plantarflexion assist requirements of the AAFS (Subsection 4.1.4.3) are summarized in Table 5.1.

All of the AAFOs in Table 5.1 have high bulk and weight in common and therefore do not satisfy the criteria of an AAFS. The plantarflexion torque required by the AAFS is similar to the Pneumatic Muscle Actuator AAFO. The plantarflexion power required by the AAFS is much higher than the Series Elastic Actuator AAFO, however the AAFO was

only designed for 50% assistance of young healthy adult requirements. In an attempt to develop a torque source for an AAFS, some concepts are explored below along with their individual challenges explained.

Table 5.1: Summary of previously reviewed plantarflexion assist devices and level of actuation compared with plantarflexion assist requirements of AAFS.

Device	Level of Actuation
Robotic Tendon [7]	Plantarflexion Power, 1.54 W/kg
Series Elastic Actuator [91]	Plantarflexion Torque, 1.62 Nm/kg Plantarflexion Power, 1 W/kg
Pneumatic Muscle Actuator [5]	Plantarflexion Torque, 0.7 Nm/kg Plantarflexion Work, 0.28 J/kg of positive work at 1.0 m/s and 0.31 J/kg of positive work at 1.5 m/s
AAFS	Plantarflexion Torque, 0.72 Nm/kg Plantarflexion Power, 2.6 W/kg

5.1.1.1 Explored Concepts

Underfoot Spring with Bellow The first PP assist concept is an underfoot spring with bellow shown in Figure 5.1. The design consists of an underfoot structure containing two mechanical locks, a bellow, and a spring. A cable attached to the spring extends proximally towards a shank cuff and passes through a return spring mechanism.

Figure 5.2 outlines the sequence of operation of the concept. Upon HC, the spring is mechanically locked (indicated by the dark square) under the heel while a bellow is compressed during CP. The pressure generated underfoot is used to extend the spring. Once FF occurs, the distal lock is engaged leaving the spring extended. Upon HO, the proximal lock is disengaged and the spring releases its energy resulting in plantarflexion assistance. Extension arms medial and lateral of the shank rest on the malleoli at the TCJ to prevent the shank cuff from sliding down.

Since the proximal end of the cable is fixed to the shank, the length of the cable becomes critical. For instance, upon HC the foot is in the neutral position and the lock is engaged. In order to lock the cable effectively, the slack in the cable must be eliminated. This implies

that the length of the cable is equal to the distance between the lock mechanism and the shank attachment point. However, complications arise from FF to HO where the cable is required to stretch during dorsiflexion. To avoid this issue, a slider lock mechanism with a return spring can be implemented.

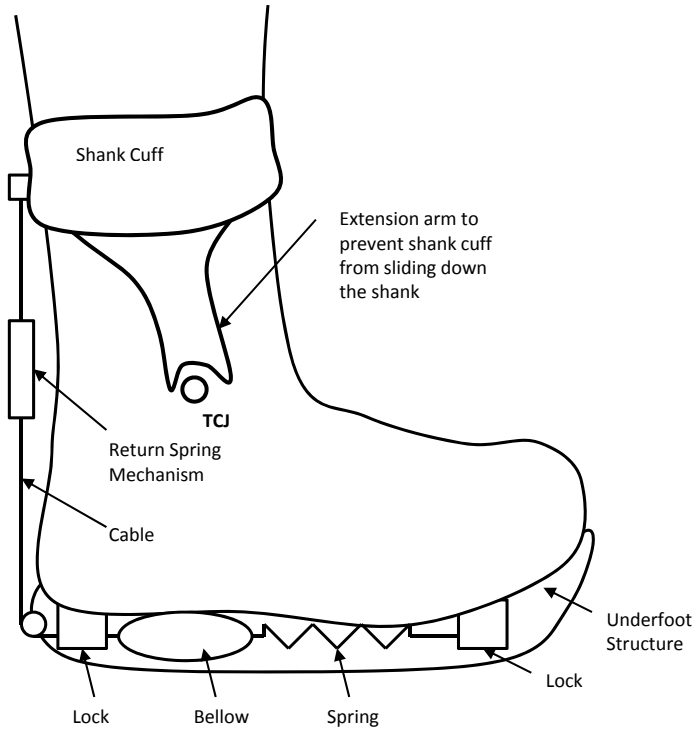

Figure 5.1: Concept design layout of Underfoot Spring with Bellow on right ankle and foot.

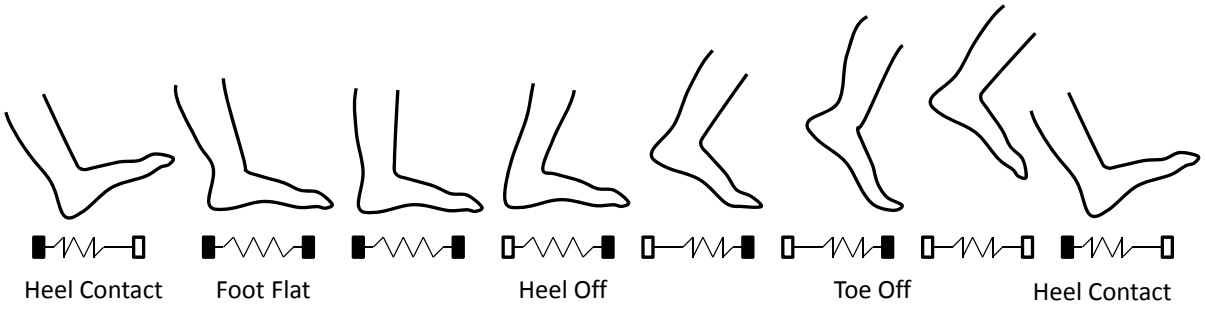

Figure 5.2: Sequence of operation of Underfoot Spring with Bellow. A lock when engaged is shown as a dark square and the lock when disengaged is shown as a light square.

Since the spring is loaded from the neutral position, the release of spring energy upon

HO should also return the foot to the neutral position. By returning to the neutral position, the issue of resetting the spring mechanism from plantarflexion is avoided. Upon release, the spring would produce a maximum force which then tapers off as the spring reaches its rest length. The linear pattern does not follow the negative and positive slope ramps required for the torque source. It can be argued that since during PP, a short burst of energy is needed, the linear release of a spring could still provide improvement in gait and therefore this concept shows promise.

Another challenge is determining the pressure required to produce the desired torque. For a 90 kg patient, the maximum torque is 65 Nm. With a conservative moment arm of 7 cm from the TCJ, the maximum force required is 930 N for a subject of 180 cm height. In the study by [84], an underfoot bellow was able to produce a pressure of 169 kPa. In order to extend a spring to reach 930 N, an area of 0.058 m^2 is required. This would translate to a square area of 7.62 cm $\times$ 7.62 cm which is a large surface area to place under the foot as proprioception would be diminished. If there is too much resistance from the bellow, the knee moment is adversely affected [85]. The solution is an external air supply which can input higher pressure to extend the spring with minimal area. The introduction of an air supply may greatly limit device portability by increasing size and weight.

Magnetorheological Fluid Spring Catapult A potential electromechanical solution is an MRF Spring Catapult concept inspired by a prosthetic ankle design [110]. The design concept (Figure 5.3) consists of a hinged AFO with a shank cuff and foot plate as a base device combined with MRF Spring Catapult mechanism posterior to the ankle. The MRF Spring Catapult mechanism incorporates an MRF lock in series with a series elastic actuator. The premise of the catapult is to wind up the spring in the series elastic actuator prior to HO. Between HO and TO, the spring energy is released providing plantarflexion assist.

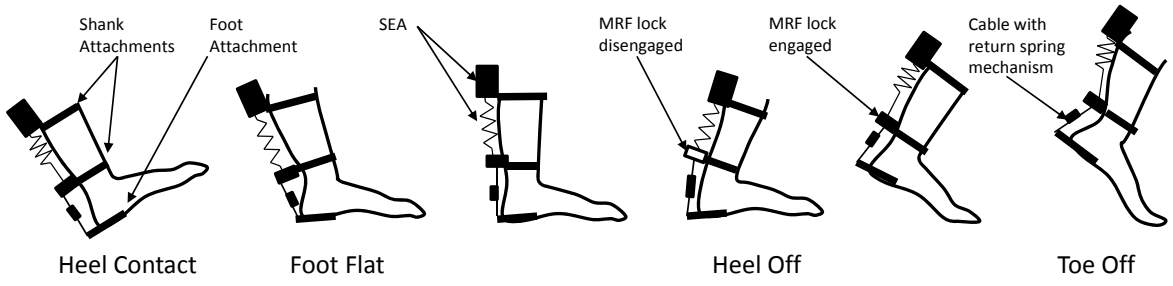

Figure 5.3: Sequence of operation of Magnetorheological Fluid Spring Catapult.

The operation sequence of the MRF Catapult is shown in Figure 5.3. Upon HC, the

MRF lock is engaged at the distal shank attachment. A cable in series with a return spring mechanism runs from the MRF lock to the heel attachment. Proximal to the MRF lock is the series elastic actuator which is extended during CP and CD. With the MRF lock engaged, the rotation of the ankle is not effected. During CD, the cable is stretched taught and the return spring is extended to its maximum length. Upon HO, the MRF lock is released allowing the extended series elastic actuator spring to return to its rest length. This is not the ideal ramp-up ramp-down torque source; however, as with the previous concept, the short burst is beneficial for plantarflexion assist. Since there is an issue of resetting the spring after TO, the spring is designed to release to the neutral position. This will avoid the foot from being held in plantarflexion during swing.

The main advantage of this design concept is the ability to store energy in the spring via the motor prior to HO without effecting the CP and CD gait phases. This could potentially reduce both power and size requirements of the motor for the series elastic actuator resulting in an overall compact torque source. The major drawback to using an MRF lock is safety when there is a power failure. The MRF lock would release and cause the spring to be released propelling the subject forward. A safety mechanism would have to be implemented.

Improved Pneumatic Muscle Actuator Concept In an attempt to achieve the desired negative and positive slope torque pattern of the torque source, PMAs are considered in this concept. AAFO designs with PMAs by Ferris et al. [5] and their drawbacks have been previously discussed in subsection 2.3.2. For example, one of the issues with their design configuration was the presence of abnormal kinematics (i.e., premature plantarflexion) during CD.

Consider a PMA attached to pin joints on the shank and foot posterior to the ankle with an articulated AFO similar to Ferris et al. [5] in Figure 2.24b. To avoid passive stretching of the PMA, the natural length of the PMA should be the longest length between the shank and foot pin joints during the gait cycle. This length occurs upon HO when the foot is in its maximum dorsiflexed position. In this configuration, the PMA would be free to kink and bow when the PMA is not at its natural length. This presents a similar issue to Ferris' designs where the PMA bowing outward adds to bulk. To avoid bowing, a corrective mechanism could be implemented. For example, a slider mechanism attached to a return spring could allow the PMA to be recoiled and maintain a minimal profile.

The more prevalent challenge, however, is addressing the negative and positive slope characteristic of the torque pattern required for the AAFS. Consider a bank of Festo (Mississauga, ON) Fluidic Muscle PMAs posterior to the ankle. The smallest diameter is

10 mm and thus could best satisfy the discrete profile of an AAFS. Pressure, force and percentage contraction are all critical aspects of sizing a PMA. Assume that the maximum pressure available is 100 psi or 690 kPa. From the functional analysis, the maximum torque required is 65 Nm about the neutral position. If the range of motion during PP is from 10 deg dorsiflexion to 15 deg plantarflexion, the total range is 25 deg. Assuming a moment arm from the TCJ to the PMA is 7 cm, the maximum force required is 930 N (as mentioned above) at neutral with a total PMA contraction of 3.08 cm during PP.

Now, consider 10 mm PMAs with a maximum contraction of 10%. With a maximum contraction of 3.08 cm, the nominal length of the PMA would 30.8 cm. The peak moment for the torque source occurs around neutral, which corresponds to a contraction of 1.22 cm. According to Figure 5.4, the peak moment for the torque source occurs at 4% contraction [111]. At the maximum pressure specified, the peak force attainable by the PMA is just over 300 N which means that three 10 mm diameter PMAs are required to attain 930 N. Figure 5.4 shows the positive and negative slope force profile required through contraction during PP. The corresponding required pressure profile is determined from the graph as shown by the pressure curves.

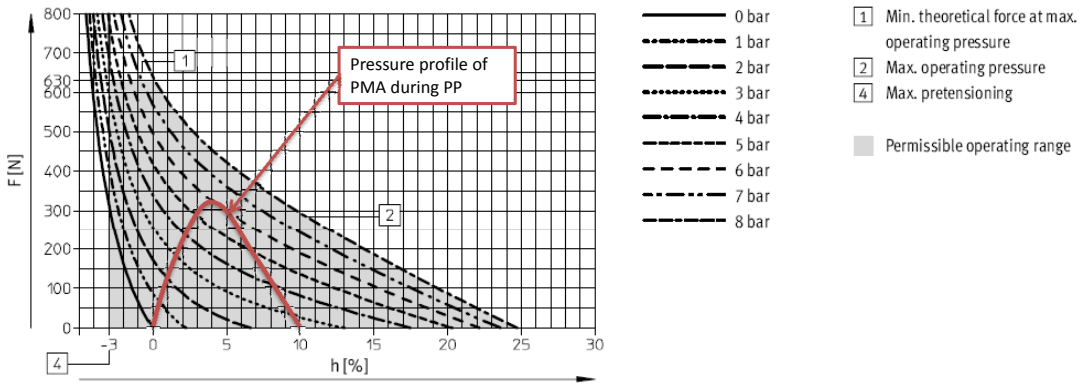

Figure 5.4: Pressure profile of Festo 10 mm PMA during powered plantarflexion [111].

The use of three 10 mm PMAs may be too bulky for an AAFS. Consider the next size up which is the 20 mm diameter PMA with a maximum contraction of 20%. With a maximum contraction of 3.08 cm, the nominal length of the PMA is 15.4 cm. According to Figure 5.5, the peak moment for the torque source occurs at 8% contraction [111]. At the maximum pressure specified, the peak force attainable by the PMA is just over 900 N which means that a single 20 mm diameter PMAs is required. Figure 5.5 shows the positive and negative slope force profile required through contraction during PP. As with the 10 mm PMA, the required pressure profile is thus determined.

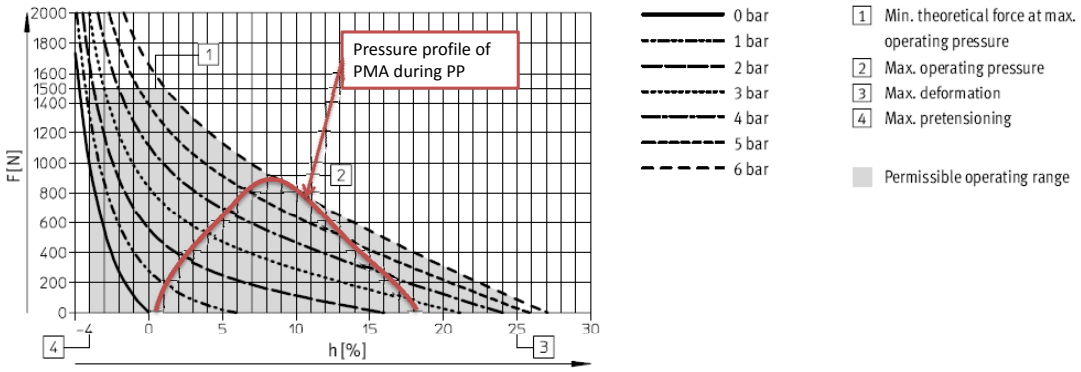

Figure 5.5: Pressure profile of Festo 20 mm PMA during powered plantarflexion [111].

The 20 mm diameter PMA with a length of 30.8 cm would not satisfy the design criteria of the AAFS since the PMA would pass posterior to the calf and thus protrude further posterior than desired. A comparison of both PMA configurations is provided in Table 5.2. In both cases, a compact and portable air supply is not available.

Table 5.2: Summary of pneumatic muscle actuator configurations as a torque source.

	Configuration 1	Configuration 2
PMA Diameter (mm)	10	20
Nominal Length (cm)	15.4	30.8
Total % Contraction throughout PP	10	20
% Contraction at Peak Force	4	8
Number of PMAs	3	1

Combination Thus far, the torque source and rotational spring were considered separate entities of the AAFS. The idea of combining the two components should be explored. An example is a bidirectional direct drive torque source with a passive spring in series to continuously adjust the ankle joint rotational stiffness. For instance, consider a posterior leafspring (PLS) AFO on an individual. During gait, the PLS would provide resistance when deviating from the neutral position. The amount of resistance varies in each direction with each patient. Since a passive PLS AFO would not be able to adjust to these variances, supplying a variable direct torque could actively adjust the effective resistance of the PLS AFO. Although not explicit, these principles are similar to the SEA AFO by MIT and ultimately are subject to the same limitations. Similar configurations could be made for a PMA instead of an SEA as the active element, with similar limitations.

5.1.1.2 Consideration for Design of AAFS without Torque Source

A torque source that can provide 65 Nm at 206 deg/s can be considered unsafe. In addition to adding bulk and weight to the ankle, the issue of control arises. Since the torque source would provide a short burst of assistance, ensuring that the user's intent is to progress forward is critical. For example, if the patient is walking and decides to stop upon HO, the device could still launch the patient forward increasing the risk of falling or injury. With a complex control algorithm this can be avoided. However, adding a bulky and heavy device may hinder natural PP rather than assist. It may be possible that the human body can compensate for kinematic and kinetic changes during PP due to the correction of CP and CD, and thus improvement in PP may be seen without external assistance. Ideally, a viable actuator should be developed to provide torque assistance safely within the design criteria.

The use of linear rotational springs in the functional analysis has also allowed for some assistance during PP because the CD spring releases its energy. Of course, without the torque source, the kinematics of the PP phase would change. However since PP is a short burst, the kinematics may improve regardless, since the ankle would be in a more natural kinematic position due to gait correction in the earlier phases. The linear rotational spring is explored next.

5.1.2 Linear Rotational Spring

5.1.2.1 Variable Shape Leafspring AFO

The first concept of a linear rotational spring uses variable shape leafsprings placed posteriorly and medially to control the motions of the ankle and foot. For a leafspring, few parameters can control the bending stiffness, typically the length, width, and thickness. Sugar et al. [112] patented adjustable stiffness leaf spring actuators that vary the length via a roller mechanism, rotating the orientation of the leafspring by 90 deg, and varying the material properties along the length of the leafspring.

Since the leafspring is considered a beam, the cross-sectional shape greatly affects the area moment of inertia and consequently the bending stiffness. For example, if the beam is a flat leafspring, the area moment of inertia is:

$$I_0 = \frac{bh^3}{12} \tag{5.1}$$

Figure 5.6 shows a design layout of the Variable Shape Leafspring AFO. There are two leafsprings, one posterior to control sagittal plane rotational stiffness, and one lateral to

control frontal plane rotational stiffness. A leadscrew actuator is on the proximal end of each leafspring. The actuator is a leadscrew and motor assembly which presses on the leafspring, changing its cross sectional shape from flat to arced, increasing its area moment of inertia. The use of a leadscrew allows precise control of bending stiffness with only one variable.

The concept is not limited to an arc shape. For example, the leafspring could be a flattened diamond that changes to a tall diamond shape or a ellipse that changes to a circle. Since the shape change only occurs at the neutral position, the out of plane forces due to the bending of the leafspring are minimized. Considering the magnitude of bending forces required, the holding forces on the shape changing mechanism would be very high, which could increase the risk of leafspring failure. Failure analysis on these components and the leafspring would have to be performed to ensure the bending resistance characteristics are met. With these drawbacks, this concept is not considered further.

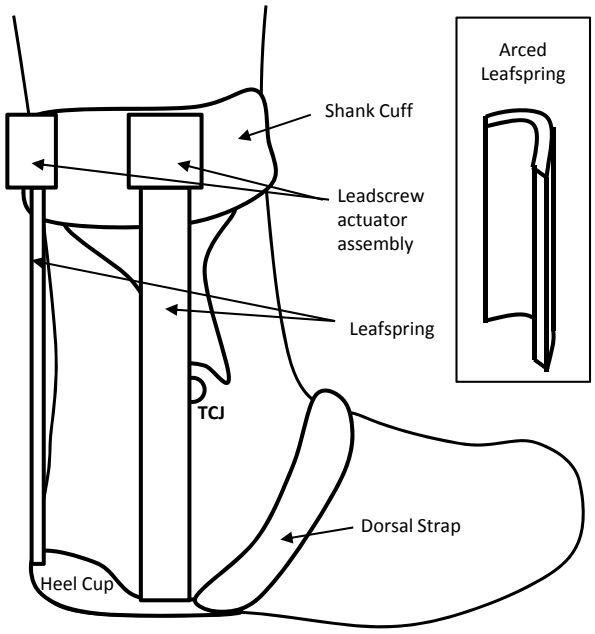

Figure 5.6: Concept design layout of Variable Shape Leafspring AFO on right ankle and foot (lateral view).

5.1.2.2 Series-Elastic Actuator Leafspring AFO

Another concept is a Series-Elastic Actuator (SEA) leafspring AFO which employs a wave leafspring to replace the conventional helical spring in [6] as shown in Figure 5.7. As in [6] a leadscrew and motor actuate the device which ideally is implemented posteriorly and laterally to the ankle. The advantage of using such a configuration is the improvement in bulk reduction around the ankle joint. The bulk from the motor assembly is held more proximal to the ankle. The wave design allows for both extension and compression of the spring. To prevent the leafspring from bowing outward when compressed, a flexible sleeve would need to be implemented to contain the leafspring. The geometry would need to be optimized in order to prevent jamming in the sleeve as well as bending near the attachment points possibly with rigid end links. Although an improvement from [6], the weight and power requirements would be similar and therefore this concept is not considered further.

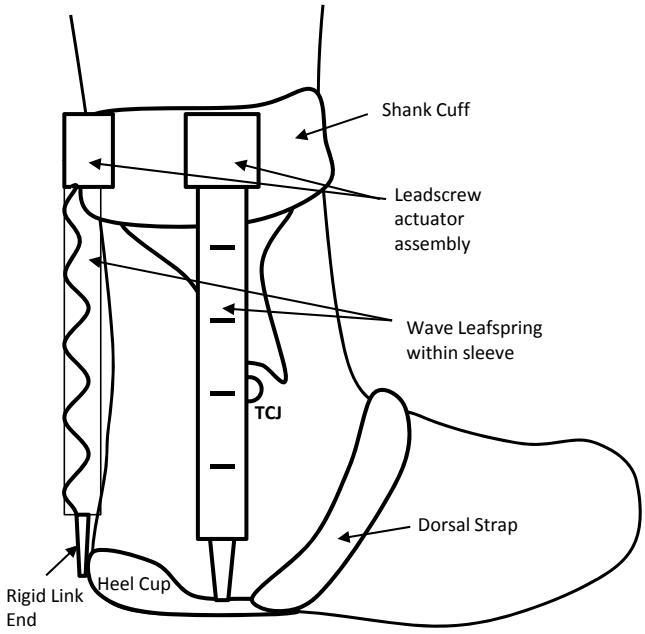

Figure 5.7: Concept design layout Series-Elastic Actuator Leafspring AFO on right ankle and foot (lateral view).

5.1.2.3 Variable Stiffness Rotational Actuator AFO

A novel concept Variable Stiffness Rotational Actuator (VSRA) AFO is shown in Figure 5.8. The actuator principle involves a spring with a constant spring rate with a variable end point. The end point travels along a circular arc to change the deflection characteristics of the spring. The end point rotation actuator could be actuated electromechanically or pneumatically. The primary focus of this design is the sagittal plane (anterior-posterior direction) which is the dominant plane of interest; however, in the medial-lateral direction a passive leafspring could be implemented.

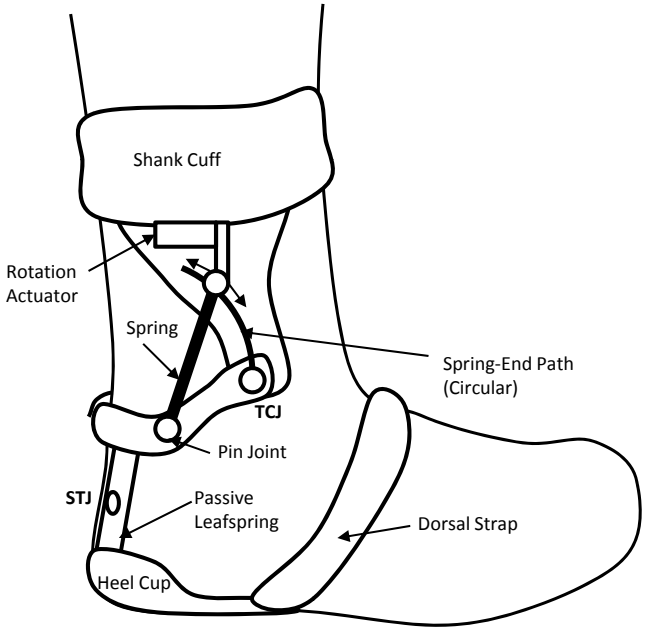

Figure 5.8: Concept design layout of Variable Stiffness Rotational Actuator AFO on right ankle and foot (lateral view).

The design concept has many advantages including the ability to: adjust the spring stiffness only while the foot in the sagittal plane is passing the neutral position, have little to no actuator force required when changing the end position, and potentially have minimal power requirements since the device would not be continually actuated. Finally the spring rest length would correspond to the ankle neutral position which makes this a safer device. The drawbacks are that the device may require an articulated AFO (both TCJ and STJ) to ensure undesired moments are not produced about the STJ, and a suitable spring-end actuator would need to be explored. Despite the disadvantages to this design, this concept

may be an improvement over existing AAFOs because it could be less bulky and heavy and have lower power requirements which could best satisfy the design criteria. The design concept warrants further exploration which is described in Section 5.2.

5.2 Design Feasibility of a Variable Stiffness Rotational Actuator AFO

The Variable Stiffness Rotational Actuator (VSRA) AFO design was selected as a potential design for the AAFS. The following describes the VSRA AFO in more detail along with a feasibility analysis.

5.2.1 Design Layout of VSRA AFO

The design layout of the VSRA AFO is illustrated in Figure 5.9. The design consists of a hinged AFO with two actuators. The first actuator is the VSRA to provide control of the TCJ. For the purpose of symmetry, a VSRA is placed medially and laterally of the ankle. Due to the limited area of the heel below the STJ joint and medial/lateral faces of the ankle, the second actuator is a passive leafspring to provide control of the STJ. Although the STJ control is not variable, it could still provide improvement in natural supination and pronation over a solid, single-hinged, or PLS AFO by allowing more frontal plane rotation.

The VSRA consists of a spring with a constant spring rate which acts in both compression and extension. During plantarflexion, the spring is compressed. During dorsiflexion the spring is extended. The Shank-End (labeled G) of the spring is positioned (β_0) along a circular path called the "Spring-End Path". β_0 is the angle between the spring axis (H to G) and the foot in neutral position (H to TCJ). Varying β_0 changes the spring deflection characteristics and results in a variable stiffness rotational spring. As mentioned previously, this repositioning only occurs as the ankle angle passes through neutral, where the spring is at its resting length, exerting little to no force, thus minimizing the actuating forces.

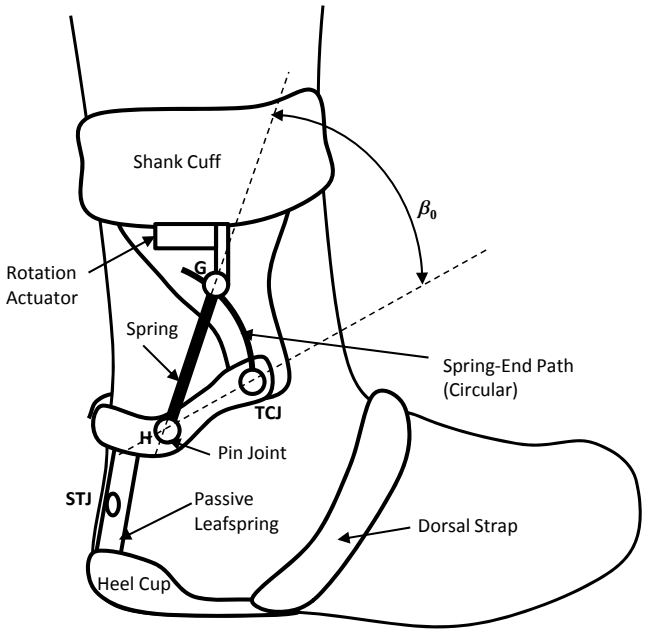

Figure 5.9: Design layout of variable stiffness rotational actuator AFO on right ankle and foot (lateral view and medial actuator hidden). The rotation actuator positions the spring-end, G, along the Spring-End Path.

5.2.2 Functional Requirements

As previously mentioned, the frontal plane (medial-lateral) functional requirements of the VSRA AFO are addressed with the passive leafspring posterior to the ankle. There is no variability in this spring and therefore, the actuator cannot be deactivated. As a result, the stiffness best suited for the patient would be implemented. For example, if the patient had weak supinators and pronators, a higher stiffness leafspring would be used to control frontal plane rotation. The opposite would be true for a patient with stronger supinators and pronators. The details of this component are discussed later.

The primary focus of the VSRA is to satisfy the sagittal plane (anterior-posterior) functional requirements of the AAFS. To evaluate the VSRA, the following model is developed, followed by results and discussion.

5.2.2.1 VSRA Model

The geometric layout of the design concept is shown in Figure 5.10. The TCJ and H are labeled and are assumed to be articulated pin joints. Point G on the shank is a pin point

which is adjustable along a circular path with radius r equal to the distance from the TCJ to point H. The origin point of the spring is the H. As illustrated, by adjusting the position of G along the circular path (Spring-End Path), the compression or extension of the spring can be controlled. As determined in the functional requirements, the position of G is only changed as the ankle passes though neutral. The effect is a continuously variable rotational spring.

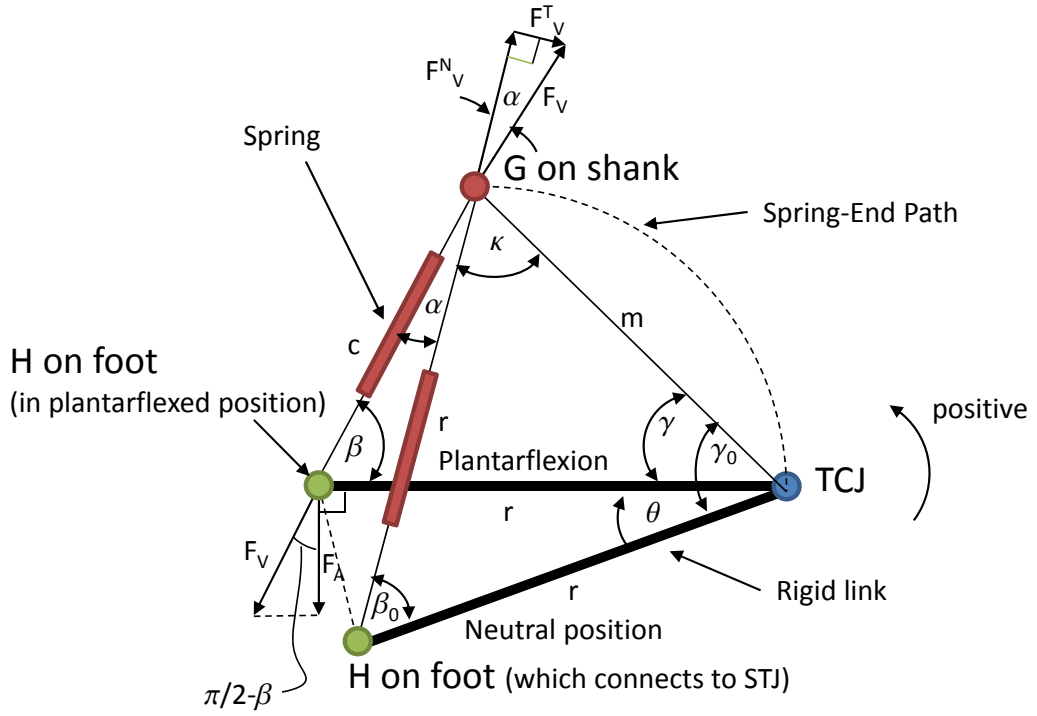

Figure 5.10: Planar view of geometric layout of Variable Stiffness Rotational Actuator in the sagittal plane. The point G is positioned along the Spring-End Path. The actuator in neutral and plantarflexed positions are shown.

The input parameter to the actuator is β_0. The distance of m can then be calculated with the cosine law as follows:

$$\begin{aligned} m^2 &= r^2 + r^2 - 2rr\cos(\beta_0) \\ m^2 &= 2r^2 - 2r^2\cos(\beta_0) \\ m^2 &= 2r^2(1 - cos\beta_0) \\ m &= \sqrt{2r^2(1-\cos\beta_0)} \end{aligned} \tag{5.2}$$

The angle opposite to the spring is determined by the sine law as:

$$\begin{aligned} \frac{\sin\gamma_0}{r} &= \frac{\sin\beta_0}{m} \\ \gamma_0 &= \sin^{-1}\left(\frac{r\sin\beta_0}{m}\right) \end{aligned} \tag{5.3}$$

As an example of how varying θ affects the actuator, placing the foot in plantarflexion is illustrated. Upon plantarflexion, the angle γ is:

$$\gamma = \gamma_0 - \theta \tag{5.4}$$

The resulting pin-to-pin (H to G) length of the deflected spring is the distance c where:

$$\begin{aligned} c^2 &= m^2 + r^2 - 2mr\cos\gamma \\ c &= \sqrt{m^2 + r^2 - 2mr\cos\gamma} \end{aligned} \tag{5.5}$$

Ultimately, the value of α is required to determine the spring force as follows:

$$\kappa = \pi - \beta_0 - \gamma_0 \tag{5.6}$$

$$\begin{aligned} \frac{\sin\beta}{m} &= \frac{\sin\gamma}{c} \\ \beta &= \sin^{-1}\left(\frac{m\sin\gamma}{c}\right) \end{aligned} \tag{5.7}$$

In the triangle formed by *c*-*m*-*r* where r is TCJ-H in plantarflexion, γ, κ, and β are known. The remaining angle α is calculated as follows:

$$\alpha = \pi - \beta - \gamma - \kappa \tag{5.8}$$

The resulting spring force, F_V is as follows:

$$F_V = K_S(r - c) \tag{5.9}$$

The moment produced by the spring about the TCJ is:

$$M_V = rF_V \cos(\pi/2 - \beta) \tag{5.10}$$

The normal and tangential forces on the slider mechanism (Spring-End Path) are:

$$F_V^N = F_V \cos\alpha \tag{5.11}$$

$$F_V^T = F_V \sin\alpha \tag{5.12}$$

These equations were computed for a radius, r, of 40 mm, 60 mm, and 100 mm. 40 mm is considered the best case scenario to minimize the posterior protrusion of the device. 100 mm is considered the worst case scenario where a longer length would no longer satisfy the posterior profile requirements of an average-sized foot and ankle. The spring stiffness for each configuration was calculated using the model above for the desired rotational stiffness as determined by the sagittal plane (anterior-posterior) functional analysis. Since the TCJ would be a pin joint, the minimum β_0 was chosen as 10 deg to allow clearance for the pin. The maximum β_0 is determined below.

5.2.2.2 Results

The optimal range of β_0 was found to be within 65 deg since the effect on the rotational stiffness was minimal beyond 65 deg. The results of the kinetic analysis revealed the following design parameters as listed in Table 5.3.

Table 5.3: Summary of variable stiffness rotational actuator parameters.

Parameter	Configuration		
	1	2	3
Pin-to-Pin Length (mm)	40	60	100
Spring Free Length (mm)	30	50	90
Spring Working Length (mm) (@ 20 deg plantarflexion)	18	32	60
Spring Working Length (mm) (@ 10 deg plantarflexion)	24	41	75
Spring Working Length (mm) (@ 10 deg dorsiflexion)	36	59	105
Spring Rate (N/kg/mm)	1.66	0.736	0.265
Spring Rate (@ 90 kg) (N/mm)	149	66.3	23.9

The corresponding moment, normal force, and tangential force plots per spring for each configuration are shown in Figures 5.11 to 5.13 for $\beta_0 = 65$ deg, and 5.14 to 5.16 for $\beta_0 =$

10 deg. The range of ankle rotation shown is 20 deg plantarflexion to 10 deg dorsiflexion and values are shown as normalized and at 90 kg.

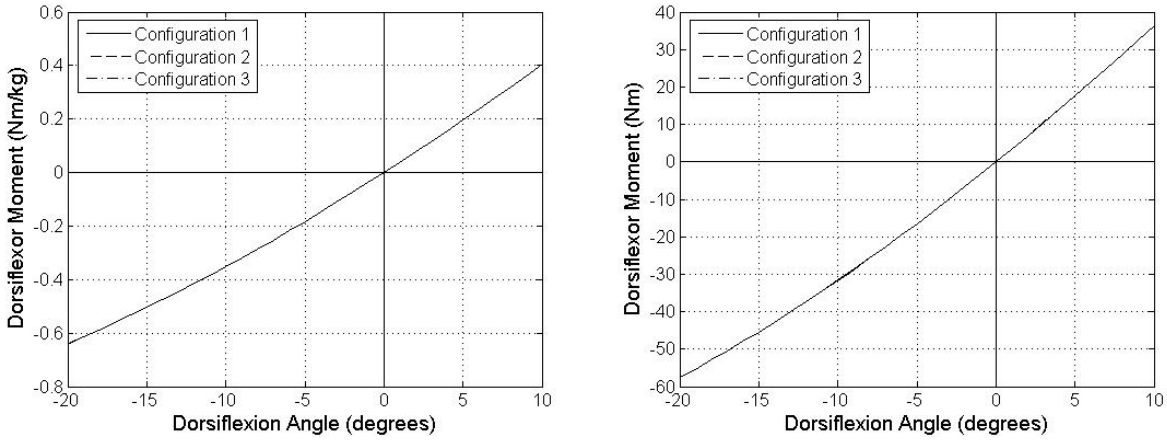

(a) (b)

Figure 5.11: Dorsiflexor moment versus dorsiflexor angle of VSRA for $\beta_0 = 65$ deg: a) normalized and b) at 90 kg.

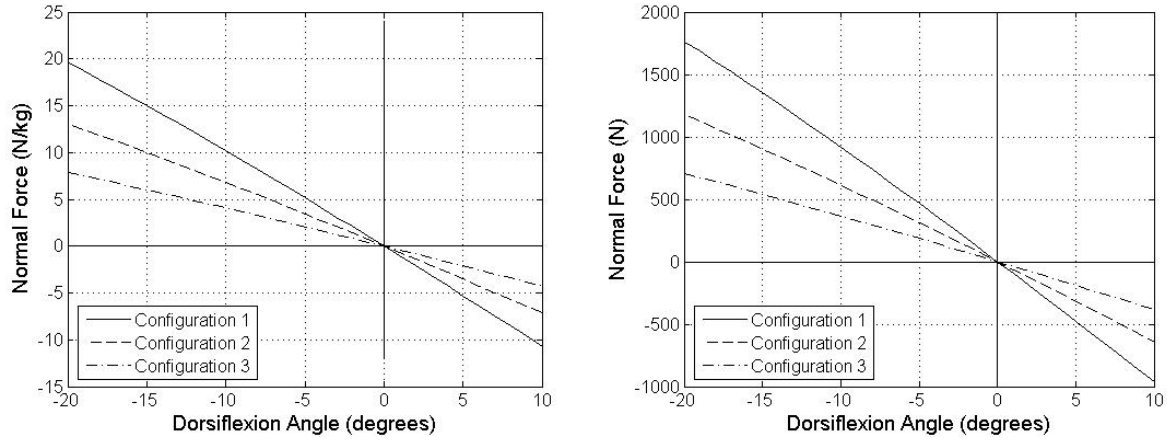

(a) (b)

Figure 5.12: Normal force on circular arc versus dorsiflexor angle of VSRA for $\beta_0 = 65$ deg: a) normalized and b) at 90 kg.

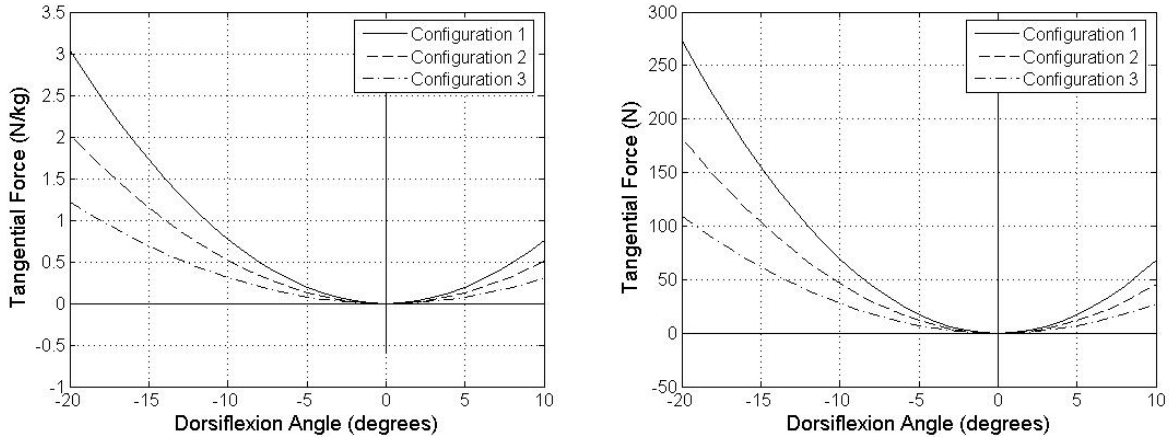

(a) (b)

Figure 5.13: Tangential force on circular arc versus dorsiflexor angle of VSRA for $\beta_0 = 65$ deg: a) normalized and b) at 90 kg.

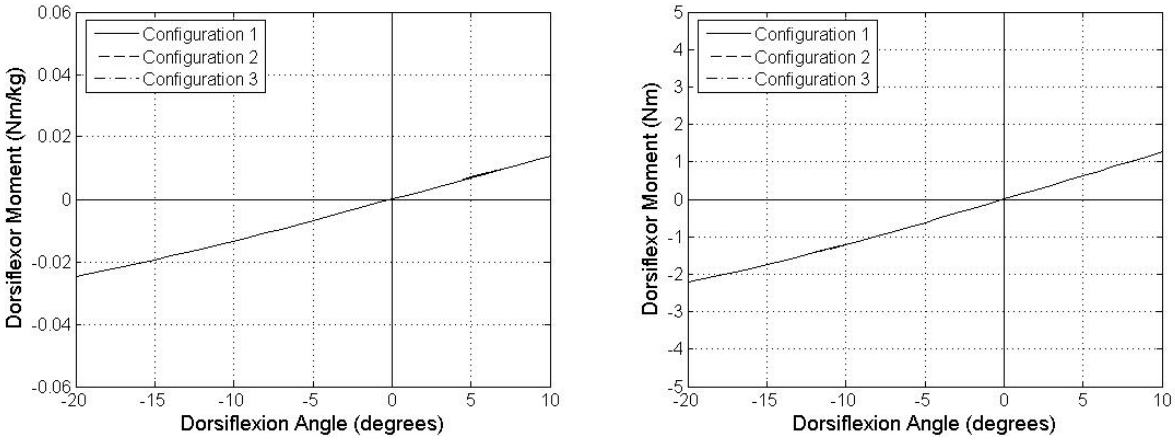

(a) (b)

Figure 5.14: Dorsiflexor moment versus dorsiflexor angle of VSRA for $\beta_0 = 10$ deg: a) normalized and b) at 90 kg.

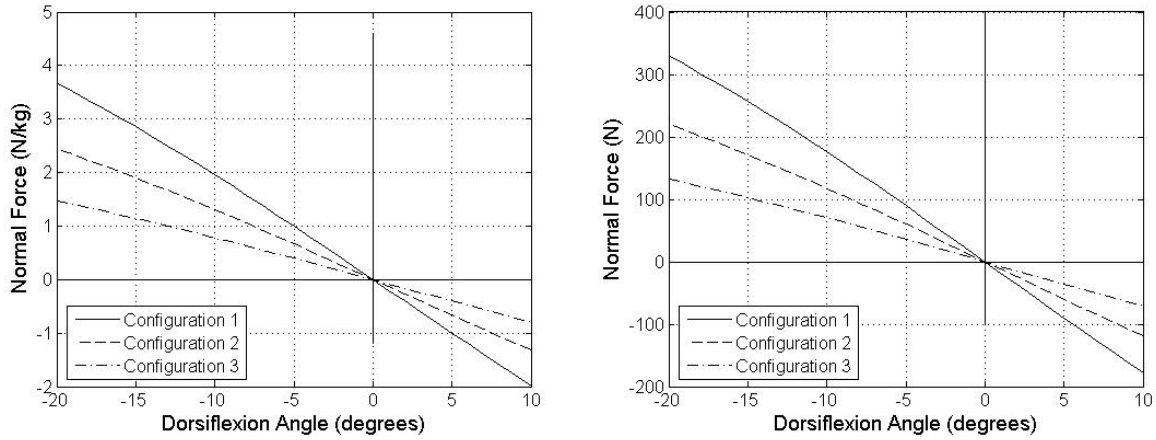

(a) (b)

Figure 5.15: Normal force on circular arc versus dorsiflexor angle of VSRA for $\beta_0 = 10$ deg: a) normalized and b) at 90 kg.

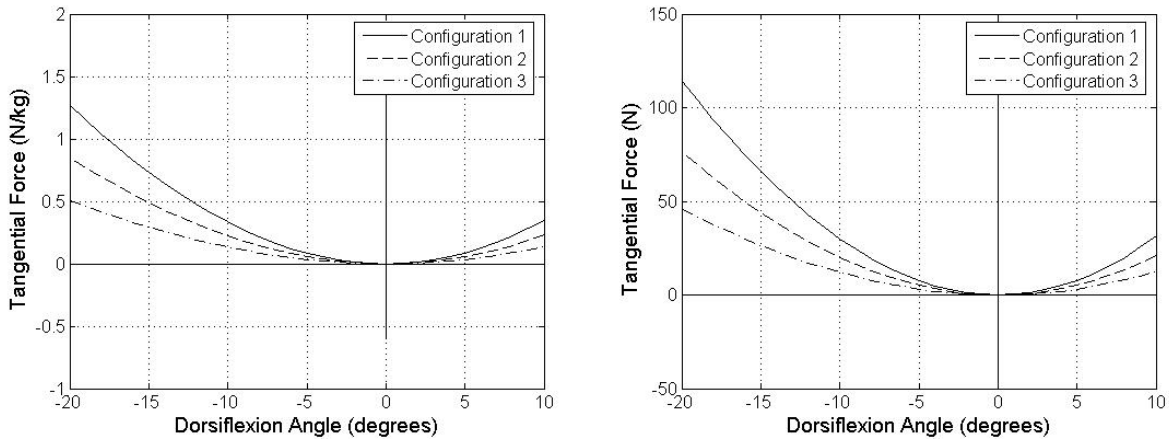

(a) (b)

Figure 5.16: Tangential force on circular arc versus dorsiflexor angle of VSRA for $\beta_0 = 10$ deg: a) normalized and b) at 90 kg.

Figure 5.17 shows the effect of modifying β_0 from 10 deg to 65 deg. This is similar for all configurations. The behaviour of the VSRA AFO was thus determined.

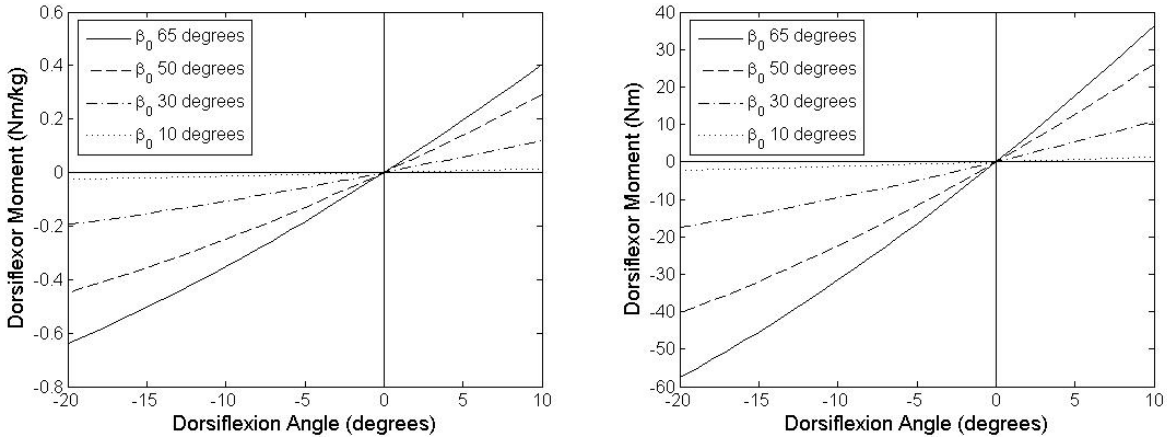

(a) (b)

Figure 5.17: Effect of varying β_0 from 10 deg to 65 deg on VSRA rotational stiffness (slope): a) normalized and b) at 90 kg.

Based on the functional requirements throughout the gait cycle, three different rotational stiffnesses are required for each patient. These correspond to the selection of β_0. Table 5.4 summarizes the rotational stiffnesses determined for the populations in the previous chapter and the corresponding angles β_0.

Table 5.4: Summary of β_0 selections for populations of interest.

Population	K_R (Nm/kg/deg)			β_0 (deg)		
	1	2	3	1	2	3
Elderly	0.004	0.011	0.002	43	21	10
Drop Foot 1	0.069	0.047	0.002	65	48	10
Drop Foot 2	0.042	0.069	0.002	45	65	10
Drop Foot 3	0.055	0.066	0.002	54	62	10

5.2.2.3 Discussion

The moment and force plots revealed trends between configurations. First, the moment plots at each angle of β_0 are essentially coincident for each configuration (Figures 5.11 and 5.14). This is the desired output of the VSRA and the spring stiffnesses were therefore selected to produce this result. Second, as the spring length is increased, the normal and

tangential forces are decreased. The normal forces (Figures 5.12 and 5.15) vary linearly with TCJ angle, θ, whereas the tangential forces (Figures 5.13 and 5.16) vary parabolically. The tangential force corresponds to the holding force along the slider arc mechanism to keep the Spring-End, G, at the desired position (i.e., β_0 when the TCJ is in the neutral position). This is advantageous because when the position of G is changed at the neutral position, the actuation device will see minimal forces, since the spring is near its rest length and exerts little force. Based on the above, it is possible to achieve the required rotational stiffness of the AAFS to satisfy its sagittal plane (anterior-posterior) functional requirements. The next sections consider the design issues to meet the design criteria.

5.2.3 Design Criteria

The actuator forces and moments above along with the spring parameters of the VSRA determined in Table 5.3 are now considered to satisfy the design criteria of the AAFS.

5.2.3.1 VSRA Spring

The main component to consider in the VSRA AFO is the spring. Based on the spring characteristics summarized in Table 5.3, a suitable spring design with a maximum diameter of 10 mm was investigated. Although the forces in the spring significantly reduce as its length increases, the working heights and spring rates required result in extremely high stresses, resulting in failure for a 90 kg patient [113]. Attempts to reduce the loads with multiple springs still resulted in an infeasible spring design since there was interference between the springs and the mechanism. Increasing the spring diameter to 30 mm to accommodate the high stresses was also infeasible. Further complications arose with the length to diameter ratio increasing, increasing the risk of spring buckling. The possibility of using a die spring was explored, however a suitable spring could not be developed for this device based on the functional requirements within the desired design criteria. In particular, a spring of diameter over 30 mm placed medial and lateral of the ankle would be very bulky and possibly heavy.

5.2.3.2 Rotation Mechanism

In addition to the challenges of the spring design, the rotation mechanism to rotate the spring is explored. The mechanism consists of a slider or roller circular track where point G is positioned (Figure 5.9). Initially, an electromechanical actuator combined with a linkage system is considered. A motor is attached in series to a leadscrew which in turn

is attached to a pinned nut. In essence, a linear actuator is created. The pinned nut is attached to point G via a linkage and pin joint. The linear motion of the leadscrew actuator translates into a circular motion via the linkage system. A potential mechanical issue with this actuator system could be jamming. To avoid this, another possibility is to use a flexible leadscrew which is bent along the circular arc for direct actuation. Since the normal and tangential holding forces are high when the spring is deflected, the actuator mechanism must withstand these high forces. Also, there would be high loads on the pins.

The leadscrew would also have to be non-backdrivable to prevent the Spring-End G from sliding while the spring is deflected as opposed to actively holding the Spring End with the motor torque. As a result, reaction time would be increased. The device is required to change stiffness upon passing neutral position even during maximum angular velocity in the PP phase. If the change occurs within +2 deg to -2 deg of TCJ rotation, the required reaction time is 20 ms which is consistent with the design criteria. The reaction time will dictate the translation speed of the spring-end along the arc. The longer the spring rest length, r, the larger the arc length (Spring-End Path) (Figure 5.10). Therefore, even though forces can be reduced by increasing the spring length, the speed requirements on the arc slider mechanism increases. Based on the study in [97] on leadscrew design, meeting this requirement would be extremely difficult, since reducing the lead angle of the leadscrew significantly reduces the efficiency of the leadscrew actuator.

The rotation mechanism would also be the only source of noise for the device. Since the motor only actuates as the foot passes through the neutral position in the anterior-posterior direction, the device noise is minimized. With effective lubrication, friction between all the components can also be minimized resulting in an overall quiet AAFS.

The operation of the device while passing through neutral also minimizes the motor power source requirements. A smaller battery and motor could potentially be used increasing the portability of the device.

5.2.3.3 Passive Leafspring

The passive leafspring to control the STJ can vary in configuration. A basic flat spring attached to the VSRA spring foot support to the heel is the simplest form. The bending characteristics of the leafspring would consequently dictate medial-lateral stiffness control. Implementing multiple leafsprings can result in staged medial-lateral stiffness control to gain some stiffness variability. For example, within +/- 4 deg of supination/pronation a flexible leafspring could be active. Beyond +/- 4 deg, a second set of outer leafsprings could be activated as the central leafspring presses against the outer leafspring. The result is a

non-linear staged variable stiffness behaviour. Instead of a second set of outer leafsprings, rubber stoppers could also be implemented.

Since the forces transferred from the heel through the leafspring to the VSRA foot support are high, a high risk of buckling can occur. For example, if the leafspring is highly flexible, the probability of buckling increases resulting in undesired loss of medial-lateral control. The patient's supination and pronation ability would have to be considered before a suitable leafspring could be implemented.

5.2.3.4 General Discussion

The above analysis revealed key difficulties faced in designing the device within the design criteria limits. The benefits of such a device could not outweigh the cost in bulk, weight, and complexity. Therefore, the design was deemed infeasible.

Concepts similar to this electromechanical approach were explored, but conventional electromechanical actuators were unfit for an AAFS. Removing bulk and weight from the ankle and foot appeared to be a logical design step. Cables or PMAs were considered; however, the same problems persisted, particularly the use of an articulated joint to support the forces of these actuators. Therefore, a completely novel approach was explored.

5.3 Design Feasibility of an Airbeam AFO

The forces involved in the AAFS are very high for a low profile configuration. It is reasonable to infer that the other linear rotational actuator concepts would observe similar forces since the desired profile and size of the concepts are similar. As a result, conventional electromechanical portable actuators are not suited for the application of an AAFS. Since ERF, MRF, and hydraulic actuators are typically used in damping applications, a novel pneumatic approach using an airbeam was considered. Although an air source is required, the development of a portable air source is not in the scope of this research, and thus will not be considered.

5.3.1 Background

Airbeams are made from synthetic fibers that are woven or braided into a circular cross section, and have an internal pressurized bladder [114]. The pressurized air provides structural capacity both by pretensioning the fabric and through its behavior as a confined gas

[114]. In particular, bending stiffness is achieved from the interlacing configuration of the braided fibers [115]. The orientation of the fibers when the tube is inflated produces a stiffened beam. Unlike a PMA, an airbeam does not necessarily contract or expand in length, but rather expands to a maximum diameter when fully inflated. The optimal fiber orientation is 54 deg relative to the longitudinal axis of the airbeam, however additional axial fibers are placed along the length to increase bending stiffness [116, 117]. The air pressure inside the tube controls the overall bending stiffness and also prevents localized kinking of the beam [116, 118].

The simplest modeling approach of an airbeam is to assume Euler-Bernoulli bending [119]. An Euler-Bernoulli beam under three point bending will have a maximum bending stiffness of:

$$K_R = \frac{M_{max}}{\theta_{max}} = \frac{4EI}{L} \tag{5.13}$$

where E is the Young's modulus of the beam, I is the area moment of inertia of the beam, θ_{max} is the angle at the end points of the beam, and L is the length of the beam. Since the pressure in the airbeam does not appear in this equation, more complex models have been developed [114, 120, 115, 115, 118]. Airbeams are currently under research by the US Military, NASA, and private corporations such as Vertigo Inc. who have conducted finite element modeling and experimentation to characterize airbeams. They are typically large in diameter and used as structural supports in shelters. An example is in Figure 5.18 showing an inflated airbeam supporting a motor vehicle. Vertigo Inc. carries off-the-shelf airbeams of 25.4 cm (10 in) diameter.

Figure 5.18: Hanging test of vehicle supported by airbeam [121].

Another example of airbeams that are more suitable for an AAFS in terms of size are

airbattens. Air battens are used in sailing to stiffen a main sail to improve sail performance to capture wind. Upon deflation, the airbatten can be furled which is an important advantage over conventional battens. Some commercial manufacturers include Airbattens LLC. C-Tech Ltd, and HDT Engineered Technologies. A C-Tech airbatten is shown in Figure 5.19.

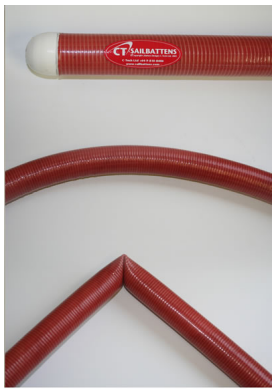

Figure 5.19: Image of C-Tech airbatten [122].

5.3.2 Layout of Airbeam AFO

The design concept of an Airbeam AFO is shown in Figure 5.20. Airbeams are strategically placed around the ankle to resist bending depending on the set pressure. The overall rotational stiffness is thus controllable. The design consists of rigid or semi-rigid shank and foot attachments to which the proximal and distal ends of the airbeams are attached, respectively. The shank attachment is a cuff which wraps around the shank with extension arms that sit on the malleoli corresponding to the TCJ. The cuff prevents the attachment from riding up the shank, and the extension arms prevent the attachment from sliding down the shank. The foot attachment consists of a heel cup with a strap over the dorsal surface of the foot to maintain its position. The simplest configuration of the airbeams is a single airbeam posterior to the ankle to control anterior-posterior ankle stiffness, and an airbeam lateral to the ankle to control medial-lateral ankle stiffness. The posterior airbeam is the dominant airbeam.

5.3.3 Functional Requirements and Design Criteria

The Airbeam AFO is an exoskeleton surrounded by inflated airbeams. The only active components are the airbeams and by determining the characteristics of each airbeam, the

overall behaviour of the device can be established. First, consider the operation of the device throughout the gait cycle.

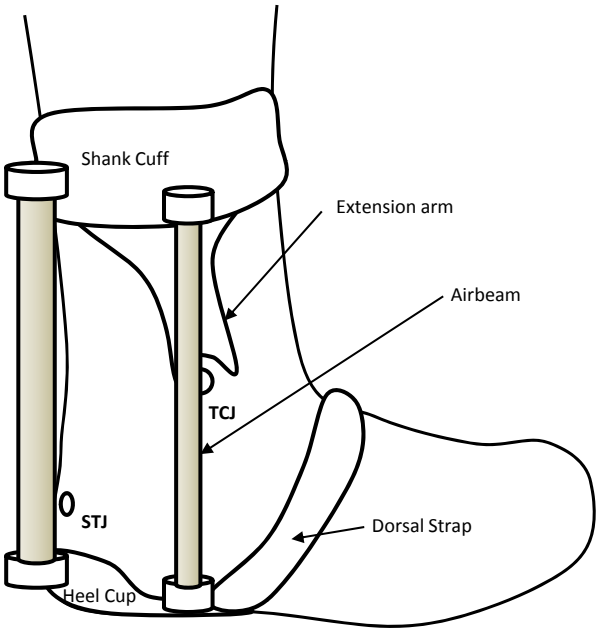

Figure 5.20: Concept design layout of Airbeam AFO on right ankle and foot (lateral view).

5.3.3.1 Actuation of Airbeam AFO

The Airbeam AFO requires an air supply which feeds the airbeams with the ability to control each internal pressure. For the sagittal plane (anterior-posterior direction), the posterior airbeam is inflated to a particular pressure as the foot passes through the neutral position. This selected pressure corresponds to the pressure that provides the desired linear rotational stiffness profile [116] as the airbeam is deflected into plantarflexion or dorsiflexion. Once the pressure is set, the airbeam is sealed via a valve which locks the air inside. To achieve K_{R1}, K_{R2}, and K_{R3} throughout the gait cycle, corresponding initial pressures P_1, P_2, and P_3, respectively, are implemented.

In the medial-lateral direction, the medial and lateral airbeams are inflated when one or more of the four gait cycle events selected in the previous chapter take place. Similar to the anterior-posterior direction, the airbeams are inflated to the selected pressure and sealed resulting in the desired stiffness.

The air supply and control components are discussed in Section 6.1. First, the feasibility of an airbeam(s) to meet the functional requirements and design criteria are discussed.

5.3.3.2 Concept Prototypes

With the assistance of the Prosthetics and Orthotics Lab and the Rehabilitation Engineering shop at The Ottawa Hospital Rehabilitation Centre, some proof of concept airbeam prototypes were built to demonstrate the behaviour of an airbeam. The construction of prototypes were as follows:

1. Latex rubber inner tube (approximately 10 cm long)
2. Braid layer (Carbon Fiber or Polyethylene Terephthalate)
3. Nylon 210 denier fabric outer shell
4. Schrader valve inlet with Delrin end cap
5. Jubilee end clamps

Figure 5.21 shows two typical examples of the prototypes. The first prototype did not include a braid layer, however bending stiffness was more appreciable with a braid layer as expected from the previous studies mentioned above. The different prototypes were inflated from 0 to 100 psi with a hand air pump. Using a compressive force transducer, the force required to bend an airbeam with the braid layer in a cantilever beam configuration approximately 20 deg was 10 N at 552 kPa (80 psi). This translates to a bending stiffness of 0.05 Nm/deg which is very low compared with the desired AAFS rotational stiffness of 6.3 Nm/deg. Upon reaching approximately 20 deg critical failure of the airbeam was observed where localized kinking occurred. The optimization of braid, pressure, and diameter are critical to achieve the desired level of stiffness. This is discussed next.

5.3.3.3 Feasibility of Airbeam AFO

Based on the initial concept prototypes, it is evident that the design and construction of an airbeam is complex. The US Military (U.S. Army Soldier Systems Center-Natick, MA), NASA (Jet Propulsion Laboratory-Pasadena, CA), HDT Technologies (Fredericksburg, VA) mentioned previously, have performed in-depth modeling and experimentation to characterize the parameters affecting airbeam bending stiffness. Since an airbeam is only one component in the overall AAFS system, similar to a spring, HDT Engineered Technologies

was approached to manufacture the airbeam based on the sagittal plane (anterior-posterior) functional requirements determined earlier. The sagittal plane (anterior-posterior) requirements were chosen first since they involve higher forces and therefore are more challenging to meet relative to the frontal plane (medial-lateral) requirements. HDT Engineered Technologies are experts in commercial airbeam manufacturing including custom applications such as airbattens. Simulating various scenarios of pressure and diameter with an airbeam(s) of 10 cm long, a summary is shown in Table 5.5.

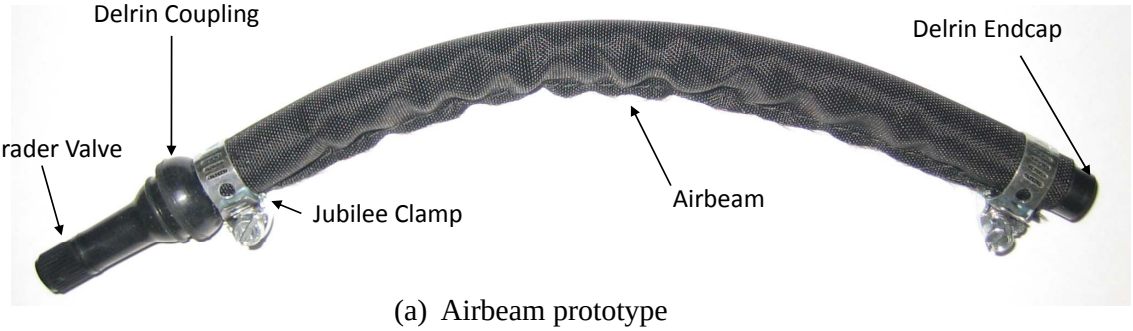

(a) Airbeam prototype

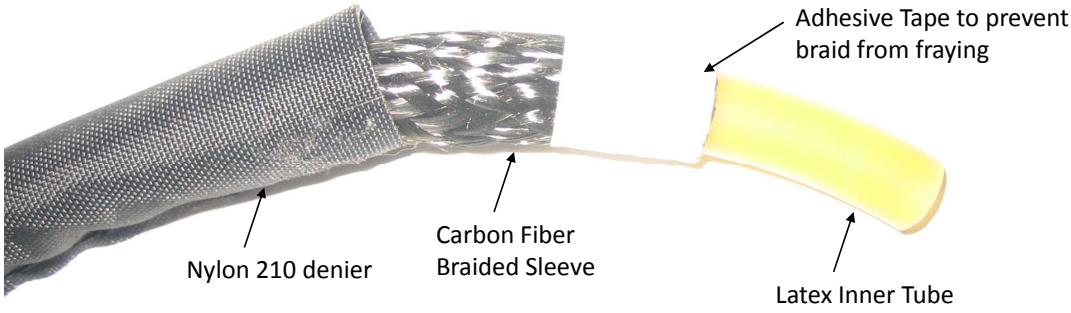

(b) Layers of airbeam prototype

Figure 5.21: Image of airbeam prototype built at The Ottawa Hospital Rehabilitation Centre, Rehabilitation Engineering Laboratory showing a) the overall prototype with clamps affixed to the beam, and b) the individual layers of the airbeam including the inner tube, braid layer, and outer shell.

Due to manufacturing constraints with the braiding layer, the minimum diameter beam that can be produced is 2.5 cm to achieve the desired bending stiffness [116]. The smaller the diameter, the higher the required pressure to prevent failure. To operate within a reasonable pressure range, say within 689 kPa or 100 psi, which could be produced by an

external air compressor, the minimum airbeam diameter would be 6.4 cm. This dimension does not meet the design criteria for an AAFS. In addition, the bending stiffness cannot be sustained for the desired range of motion in the gait cycle and therefore critical failure would be expected. The sudden buckling of an airbeam could potentially be dangerous to a patient not expecting such an event.

Table 5.5: Summary of airbeam scenarios [116].

Scenario	# of Beams	Max Pressure (kPa (psi))	Diameter (cm (in))	Deflection (degrees)
1	1	345 (50)	7.6 (3)	5
2	1	517 (75)	7.6 (3)	8
3	2	517 (75)	6.4 (2.5)	8
4	3	4826 (700)	2.5 (1)	10

Another issue to consider is the effect of external pressure on the airbeams since maintaining the cylindrical shape is critical in sustaining bending stiffness. For example, if the patient wears a shoe which places localized pressure on a section of the airbeam, the result could alter the bending stiffness characteristics of the airbeam and possibly induce undesired localized kinking through pinching. Therefore, the Airbeam AFO is not a viable solution.

5.4 Design Feasibility of a Pneumatic Sock AFO

The next pneumatic actuated concept is a Pneumatic Sock AFO. Unlike the Airbeam AFO, which relies on the structural stiffness of the cylindrical shape, the pneumatic sock operates on the principles of an airspring. The design concept is discussed next.

5.4.1 Pneumatic Sock Background

An airspring is an actuator which uses pneumatic pressure to absorb and release energy similar to a spring. An example is an airspring that is used in vehicle suspensions shown in Figure 5.22. Encasing the air in a semi-flexible shell similar to a bellow, the air pressure increases as the volume decreases. The increasing air pressure results in increased resistance to motion similar to compressing a helical spring.

5.4.2 Layout of Pneumatic Sock AFO

The concept of the Pneumatic Sock AFO is a series of fabric shells surrounding the ankle and foot with an inner sock lining the ankle and foot. Between the fabric shells and the inner sock are bladders which inflate to different pressures to provide varying joint rotational resistance similar to an airspring. Figure 5.23 illustrates the initial layout; a more detailed description is discussed in the sections that follow. As shown, two sets of bladders and fabric shells are placed around the ankle to control the anterior-posterior and medial-lateral directions. The bladders are affixed to the anterior, posterior, medial and lateral faces of the inner sock. The fabric shells are affixed to the inner sock at the TCJ and STJ. A model is developed next to evaluate the Pneumatic Sock AFO on its ability to meet the functional requirements.

Figure 5.22: Image of bellow type airspring [123].

5.4.3 Functional Requirements and Design Criteria

The introduction of a Pneumatic Sock AFO on the ankle and foot can be difficult to model. To simplify the modeling approach, the device is divided into anterior-posterior and medial-lateral elements. Furthermore, each of these elements is divided into bladder and fabric shell elements. The following develops a modified link segment model of the shank and foot segments with the Pneumatic Sock AFO followed by a model of the individual bladder and fabric shell elements.

5.4.3.1 Model of Pneumatic Sock AFO on Shank and Foot Segments

Model Background The model for the Pneumatic Sock AFO has the same underlying assumptions as the functional requirements modified link segment model. The model is developed considering the posterior bladder only for now. Upon plantarflexion, the posterior bladder inflates creating the airspring effect. The same principle is applied for the anterior, medial, and lateral bladders and fabric shells where dorsiflexion, supination (right foot), and pronation (right foot), respectively are resisted.

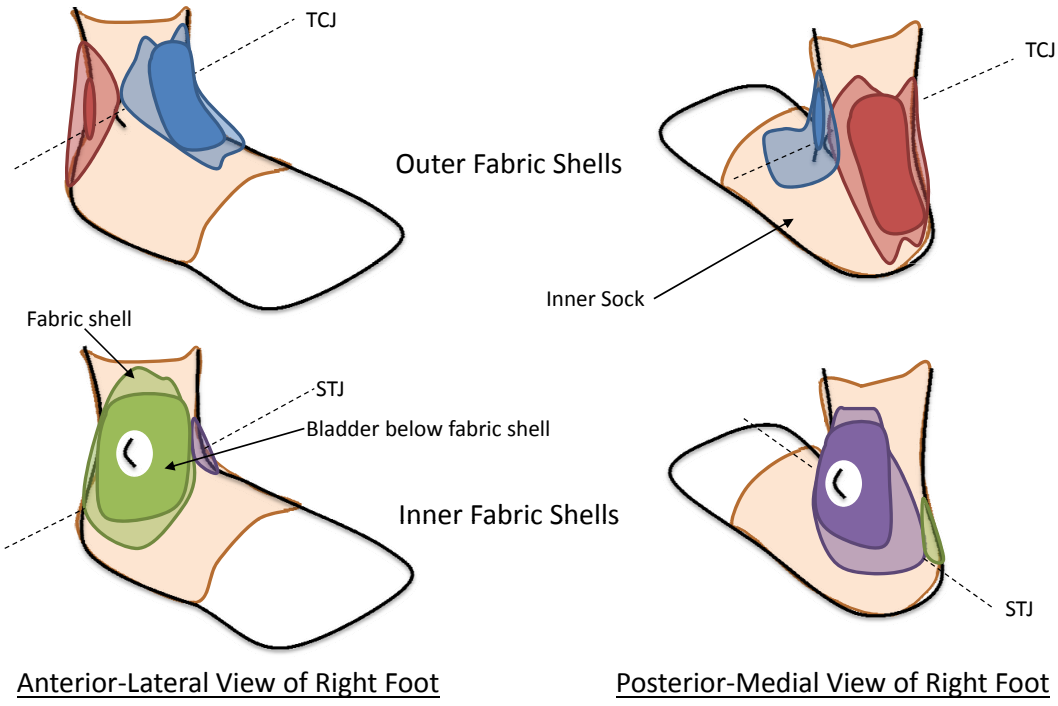

Figure 5.23: Layout of pneumatic sock AFO.

As such, the goal is to use the Pneumatic Sock AFO to augment the deficient ankle muscle moment only without disturbing the other moment balances. Therefore, any additional forces added must balance each other and leave only the augmentation moment. To achieve this, external forces are assumed to be those of a young healthy adult so that the resulting muscle moment reaction, M_A, at the joint is that of a young healthy adult as well. The pneumatic pressure bladders act to provide torque assistance to the existing muscle moment for the shank and foot segments. The fabric shell of each bladder wraps around the ankle and foot and is affixed to the inner sock at the joint axes to ensure no moments are produced by the tension in the fabric (represented by F_H). As discussed in the literature review, this method of joint control is three-point fixation. The fabric is always under tension so that the bladder expands towards the segment of interest resulting in a force F_B. F_B is modeled as a point force acting at a moment arm, r_B; however, F_B acts as a result of a distributed force due to the pressure in the bladder acting over the contact area of the segment, where the moment arm, r, is the center of pressure, COP, of the contact area. The frictional force would also be distributed; however, it is assumed to act at the COP as well. Since the device is made of fabric and bladders, it is considered massless compared with the foot. A modified link segment model illustrating the above

concepts is presented next.

Modified Link Segment Model The modified link segment model of the foot and shank segments, with the posterior bladder and fabric shell, are shown in Figure 5.24; a posterior view shows the contact areas of the bladder on each segment. The linear accelerations of the shank and foot center of masses are represented by a_S and a_F, respectively. The force due to gravity is represented by $m_S g$ for the shank and $m_F g$ for the foot. The ground reaction force is represented by F_G. The external force and moment at the knee joint, K, are represented by F_K and M_K, respectively. The force due to the bladder is represented by F_B with a corresponding friction force of F_f, acting through the COP of each segment contact area. The force from the fabric shell, F_H, passes through the joint axis, A, at the attachment points of the fabric shell. Furthermore, the modified link segment models of the individual foot and shank segments are shown in Figure 5.25. The force and deficient moment reaction at the talocrural (ankle) joint, A, are represented by R_A and D_A, respectively. The dashed lines represent the moment arms of each force with respect to the joint axis, A.

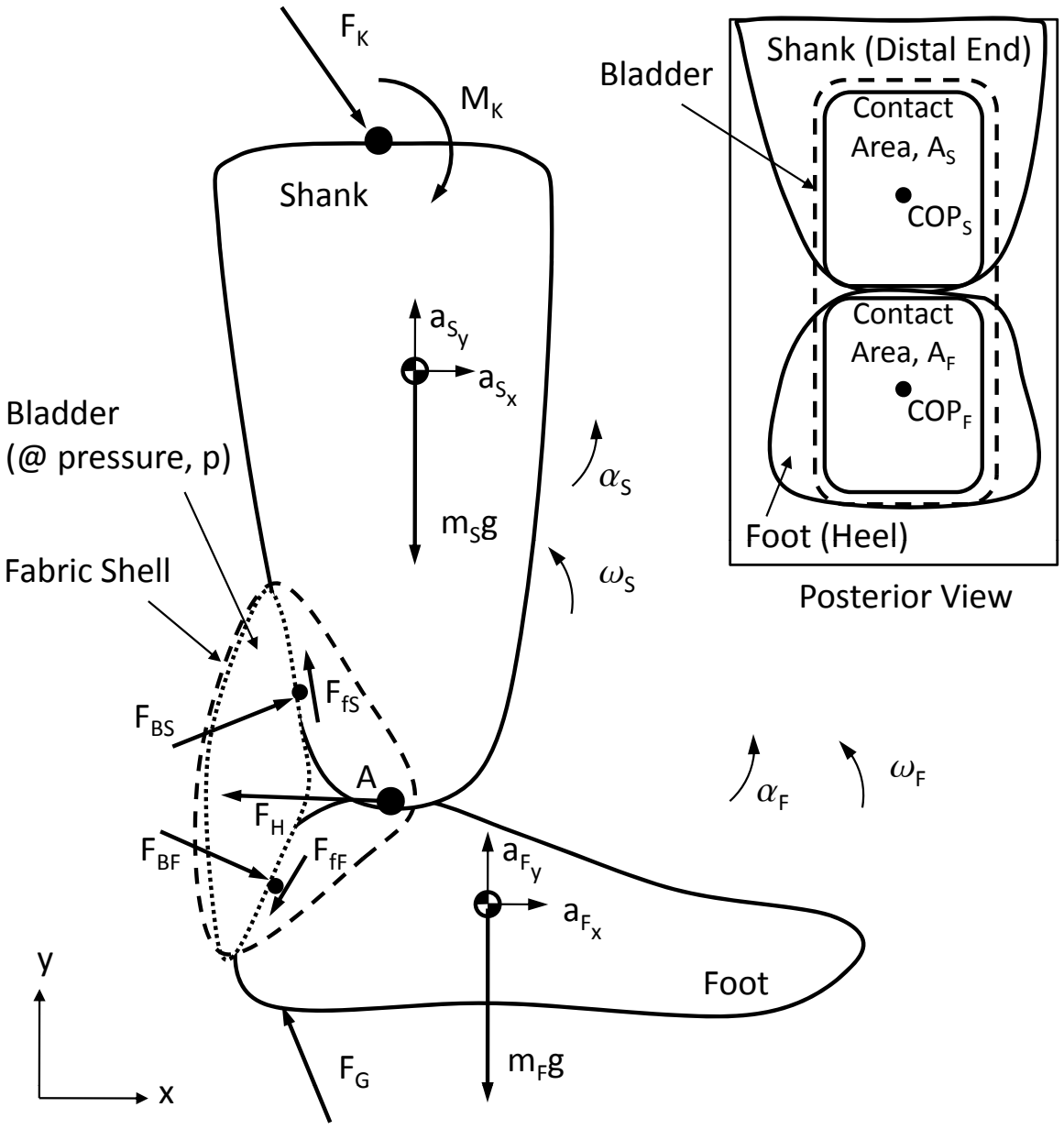

Figure 5.24: Modified link segment model of shank and foot with Pneumatic Sock AFO posterior bladder and fabric shell shown. A posterior view of the contact area, A, of the bladder on each segment, and their center of pressure, COP, are indicated.

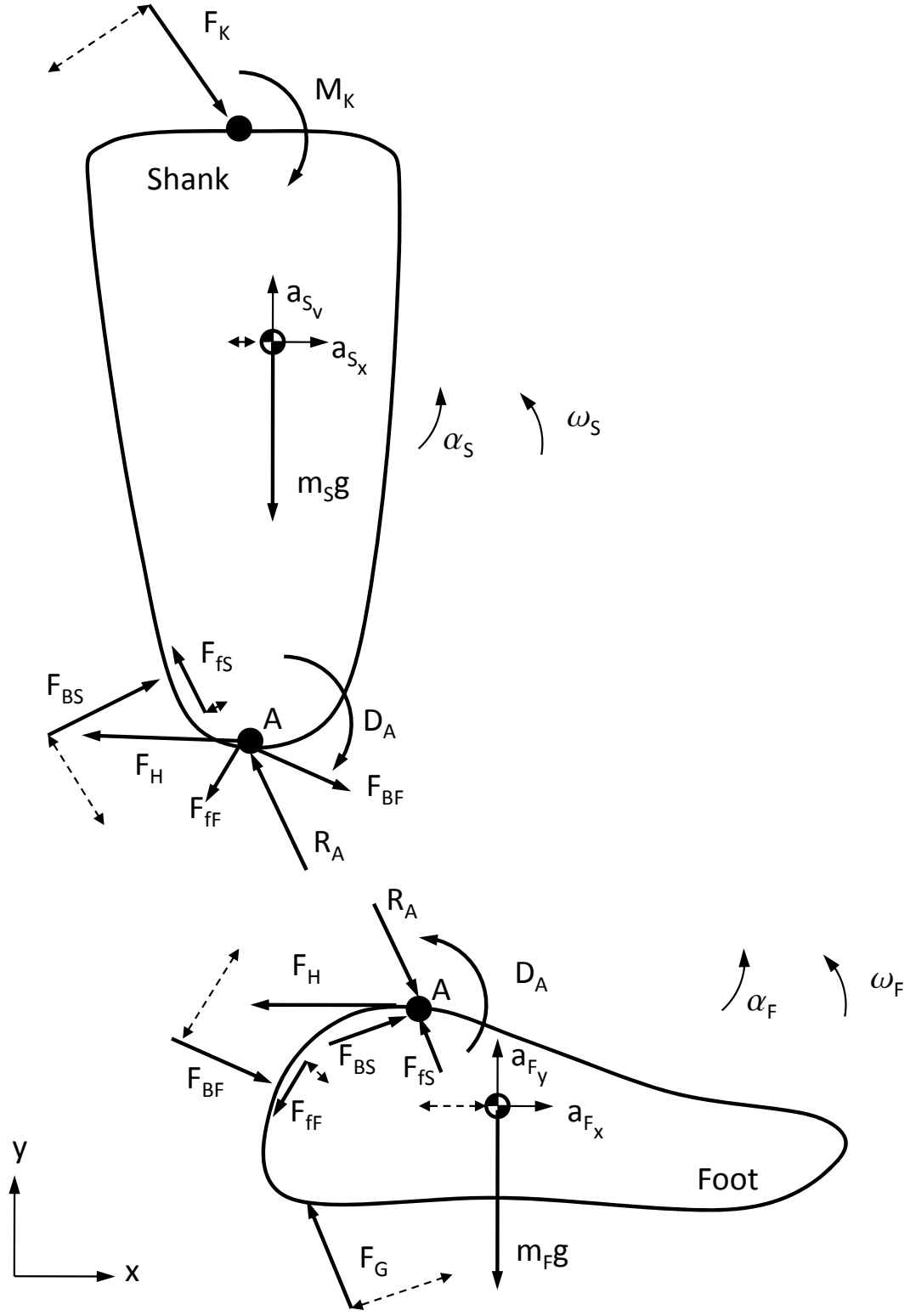

Figure 5.25: Modified link segment model of shank and foot segments with Pneumatic Sock AFO forces.

Referring to Figure 5.25, force and moment balances can be performed on the foot. Performing a force balance on the foot in the x direction reveals:

$$\begin{aligned} \sum F_x &= m_F a_x \\ R_{A_x} - F_{G_x} + F_{BF_x} - F_{fF_x} + F_{BS_x} - F_{fS_x} - F_{H_x} &= m_F a_x \\ R_{A_x} - F_{G_x} &= m_F a_x \end{aligned} \tag{5.14}$$

Performing a force balance on the foot in the y direction reveals:

$$\begin{aligned} \sum F_y &= m_F a_y \\ -R_{A_y} + F_{G_y} - m_F g - F_{BF_y} - F_{fF_y} + F_{BS_y} + F_{fS_y} + F_{H_y} &= m_F a_y \\ -R_{A_y} + F_{G_y} - m_F g &= m_F a_y \end{aligned} \tag{5.15}$$

Performing a moment balance on the foot about A reveals:

$$\begin{aligned} \sum M_A &= I_{A_F} \alpha_F \\ -m_F g r_{m_F g} - F_G r_{F_G} + F_{BF} r_{F_{BF}} + F_{fF} r_{F_{fF}} + D_A &= I_{A_F} \alpha_F \end{aligned}$$

but,

$$-m_F g r_{m_F g} - F_G r_{F_G} + M_A = I_{A_F} \alpha_F$$

therefore,

$$M_A = D_A + F_{BF} r_{F_{BF}} + F_{fF} r_{F_{fF}} \tag{5.16}$$

where $M_A - D_A$ is the augmentation moment provided by the Pneumatic Sock AFO.

A similar analysis for the shank reveals:

$$M_A = D_A + F_{BS} r_{F_{BS}} + F_{fS} r_{F_{fS}} \tag{5.17}$$

For the anterior bladder and the frontal plane (medial and lateral) bladders, a similar analysis can be performed.

5.4.3.2 Bladders

Figure 5.26 illustrates a model of an individual bladder sandwiched between the inner sock and outer fabric shell. The external forces acting on the bladder are the reaction forces of the shank and foot segments, F_{BS} and F_{BF}, respectively; the resistive force of the fabric shell, F_H; and frictional forces between the bladder and surrounding contact surfaces, F_f. The moment arms, r, are symmetrical about the joint axis passing through the midlength of the bladder and therefore, the forces F_{BS} and F_{BF} are equal in magnitude.

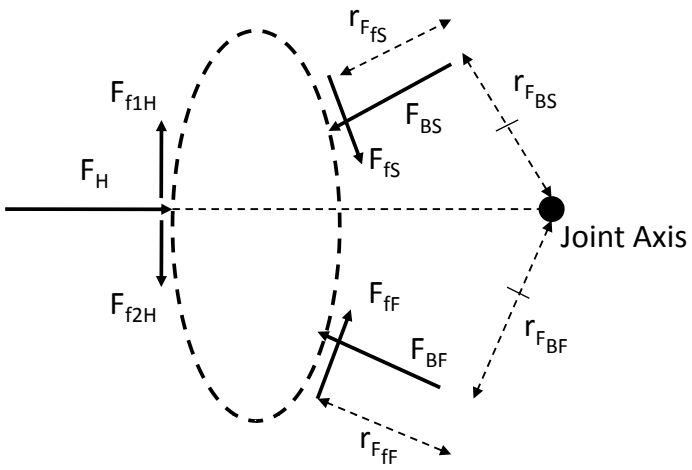

Figure 5.26: Simplified free body diagram of bladder.

Assuming that the fabric shell is fixed to the joint axis which is a static pivot point, the pressure in the bladder evenly builds against the fabric shell and body segments as the bladder is inflated. In this case, all forces must balance each other where:

$$\vec{F}_H + \vec{F}_{f1H} + \vec{F}_{f2H} + \vec{F}_{BF} + \vec{F}_{fF} + \vec{F}_{BS} + \vec{F}_{fS} = 0 \tag{5.18}$$

Since the device uses air pressure to produce the required stiffness, the size of each bladder and their corresponding working pressures must be determined. Consider an average-sized male ankle and foot with a foot length of 27.3 cm and a foot breath of 9.9 cm [105, 23] as shown in Figure 5.27. As a conservative approach, the maximum functional requirements that occur for a patient body mass of 90 kg is imposed. Based on this ankle and foot size restriction, the maximum bladder size on the anterior and posterior surfaces is 14 cm high by 4 cm wide. The midlength of the bladder is aligned with the TCJ on both surfaces and therefore the corresponding moment arm, r_B, is 3.5 cm for each segment which is aligned to the COP of the bladder contact area on each segment. The maximum bladder

size on the medial and lateral surfaces is 10 cm high by 5 cm wide. The corresponding moment arm, r_B, is 2.5 cm for each segment.

A complication arises from the overlapping of fabric shells. If the medial and lateral bladders are placed first with their respective outer shells, the TCJ is no longer exposed to attach the anterior and posterior outer shells. The solution is a hole in the medial and lateral bladders that corresponds to the TCJ. A diameter of 3 cm is selected as a conservative size for this hole and therefore the resulting moment arm, r_B, is 3.14 cm instead of 2.5 cm. The bladder sizes on the foot and ankle are shown in Figure 5.27.

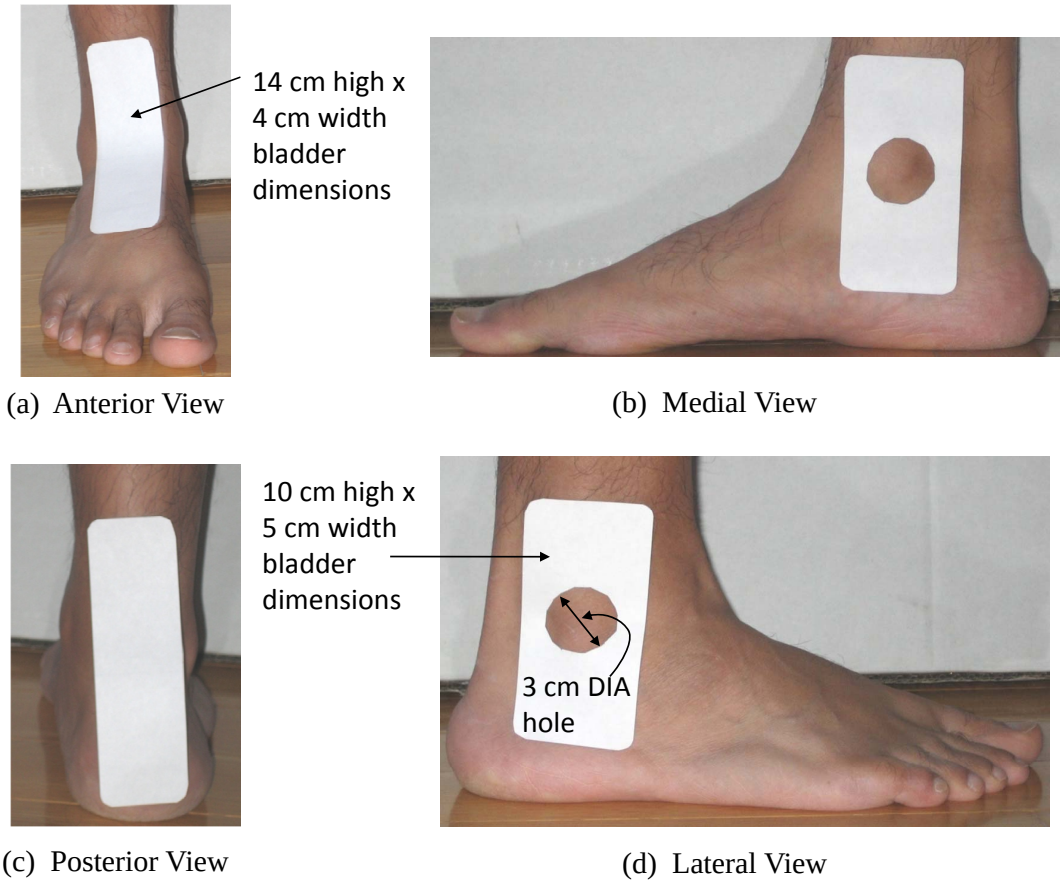

(a) Anterior View (b) Medial View

(c) Posterior View (d) Lateral View

Figure 5.27: Images of average-sized male right ankle and foot with anterior, posterior, medial, and lateral bladder sizes shown.

The geometry of the bladders determines the operating pressure of the bladders. There are two cases to consider when pressurizing the bladders. The first is a friction-free case where the movement of the body segments and fabric shells are free to move against the bladders without a friction force acting on them. The second case is when friction is present, where the friction is acting against the direction of rotation. This is advantageous

because the frictional force contributes to the resistive moment produced by the AAFS device. The frictional force due to the bladder force is:

$$F_f = \mu F_B, \tag{5.19}$$

where μ is the coefficient of friction and F_B is the normal force produced by the inflated bladder. The coefficient of friction depends on the contact surface interfaces. Appropriate bladder materials would be natural gum or neoprene because of their high pressure tolerance and elongation [124]. The inner sock and fabric shells are assumed to be made of nylon since nylon is a commonly used material and coefficient of friction values are available. A coefficient of friction between nylon and rubber is not reported; however, the coefficient of friction between nylon and nylon is 0.15 to 0.25, and the coefficient of friction between rubber and dry asphalt is 0.5 to 0.8 [125]. Since nylon would be expected to resist sliding less than dry asphalt, a coefficient of friction of 0.375 is assumed to demonstrate the differences between pressures. The assumed coefficient of friction (0.375) is the mean between the highest nylon-nylon coefficient of friction (0.25) and the lowest rubber-dry asphalt coefficient of friction (0.5).

$$\begin{aligned} M_A - D_A &= F_B r_B + F_f r_f \\ M_A - D_A &= F_B r_B + \mu F_B r_f \\ M_A - D_A &= F_B (r_B + \mu r_f) \\ M_A - D_A &= pA(r_B + \mu r_f), \end{aligned} \tag{5.20}$$

where $M_A - D_A$ is known from the functional requirements, p is the bladder pressure, A is the area of the bladder on each segment (i.e., half the bladder height by the full bladder width), r_B is the moment arm of the bladder force about the joint axis, and r_f is the moment arm of the frictional force about the joint axis. Based on the sizing of an average-sized ankle, a conservative length of r_f in the sagittal plane is 4 cm and in the frontal plane is 2 cm. Equation 5.20 is applied to each bladder for each segment. The results are summarized in Table 5.6 below.

Since all values are under the 689 kPa or 100 psi upper limit set previously, this design is feasible. Experimentation would need to be conducted to characterize the friction interaction between the actual surfaces in the prototype.

Table 5.6: Summary of bladder size and operating pressures.

Bladder	Height (cm)	Width (cm)	Maximum Pressure (without friction) (kPa (psi))	Maximum Pressure (with friction) (kPa (psi))
Anterior-posterior	14	4	643 (93)	450 (65)
Medial-lateral	10	5	297 (43)	239 (35)

The bladders are compliant but need to be constructed so that they tend to expand in one dimension. For example, the bladder should not grow along its height and width but rather in its thickness to press against the ankle and foot segments and the outer fabric shell similar to a bellow. In consultation with IRP Industrial Rubber Ltd. in Mississauga, ON [124], it was suggested that fabric reinforcements be placed around the perimeter of the bladder to restrict planar expansion. However, there are issues that must be resolved before bladder construction can begin. The first is the type of sealing used at the edges of the bladders. Typically, this is done through heat sealing or vulcanizing adhesive. The issues with vulcanizing adhesive is the requirement of a large band around the perimeter to ensure a good seal. At 100 psi, there is a high probability of the seal bursting. Therefore, burst pressure tests are suggested before actual device testing can take place. It was strongly suggested that a custom molded bladders be constructed to ensure that the bladders behave as intended without the possibility of bursting. However, this option is highly expensive since a custom mold is necessary for each bladder configuration. Provisions for an inlet valve (e.g., Schrader valve) for each bladder would also be required for inflation and deflation.

5.4.3.3 Fabric Shell

The outer layer of the Pneumatic Sock AFO is the fabric outer shell. The attachment points of the shells are at the joint axes and therefore the shells wrap around the shank and foot segments such that the bladder lies between the shell and segments. The critical characteristic of the fabric shell is its tensile strength. To calculate the tension force in the fabric, a pulley model is used, as shown in Figure 5.28. An example of the posterior fabric shell wrapped around the right shank and foot is shown in Figure 5.29. The posterior bladder is sized according to Figure 5.27.

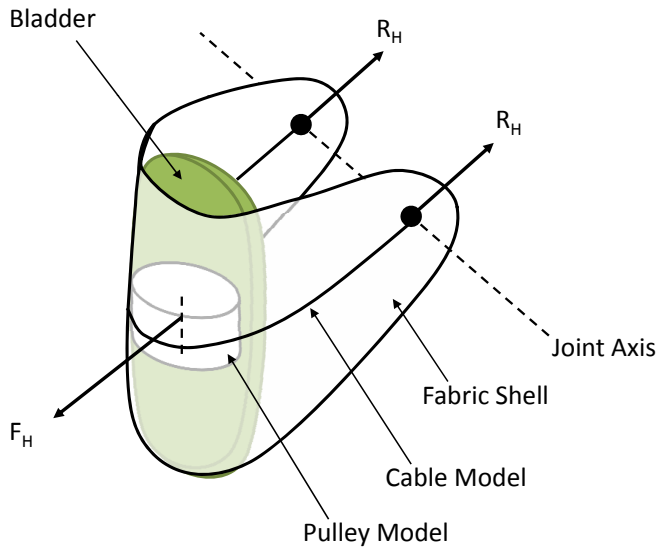

Figure 5.28: Model of tension in fabric shell wrapped around bladder and shank-foot segments (not shown) using pulley and cable system.

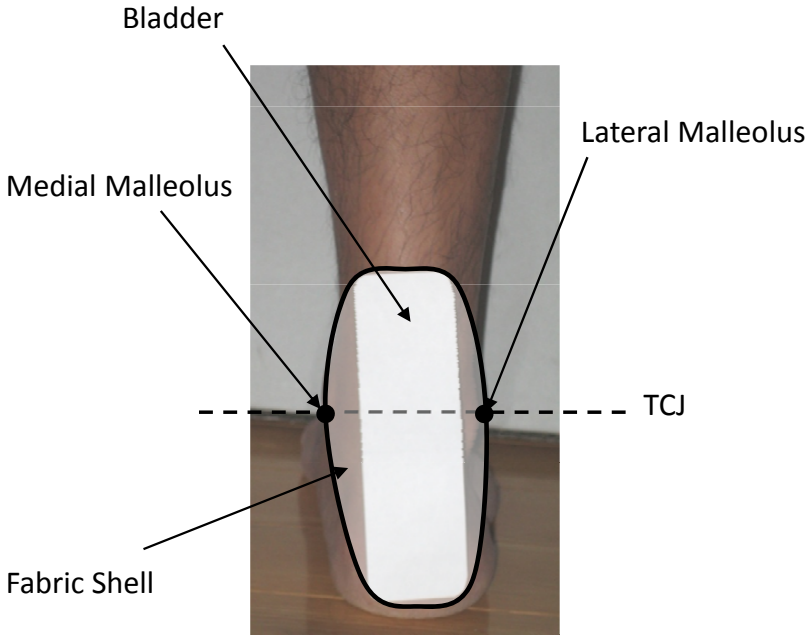

Figure 5.29: Posterior view of posterior fabric shell wrapped around average-sized right shank and foot with posterior bladder shown.

Assuming the bladder acts as a frictionless pulley and the fabric shell acts as a cable wrapping around the pulley which is affixed to the joint axes, the tension in the fabric shell is half of the total force of the bladder on the shell where:

$$F_T = R_H = \frac{F_H}{2} \tag{5.21}$$

For the anterior-posterior fabric shells, the maximum force is the product of the maximum pressure in the bladder (643 kPa or 93 psi) and the maximum area of the bladder (14 cm by 4 cm). Therefore, a maximum tension force of 1800 N exists. Introducing a friction coefficient of 0.375 (as mentioned previously), the tension force increases to 2500 N. To meet this requirement, Cordura 1000D with a minimum width of 2.7 cm is selected as a suitable fabric [126].

The shape of the shells is also important to consider. Each fabric shell must fully encompass its corresponding bladder. The shells cannot be too tight on the ankle and foot since this can cause difficulties for donning and doffing. As depicted in Figure 5.28, the ideal fabric shell shape would be similar to a folded diamond where the center portion would fully encompass the bladder and the tapered ends would ensure that all tensile forces pass through the joint axis. As mentioned above, since the medial and lateral bladders have holes to accommodate the shell overlapping, the medial and lateral fabric shells would also have holes. The fabric shells have to be reinforced with stitching at the edges of the shell and the hole to avoid fraying and possible failure of the fabric. The ideal material candidate would be Bonded Nylon 6,6 from COATS, which is currently used in the Prosthetics and Orthotics Laboratory at The Ottawa Hospital Rehabilitation Centre. However, mechanical strength testing should be performed on the final stitched product.

Individual testing of the stitched fabric shells would need to be performed to ensure that failure would not occur. The ability to don and doff comfortably would also need to be investigated with the final product.

5.4.3.4 Inner Sock

The base layer of the Pneumatic Sock AFO must be comfortable and able to conform to the ankle and foot effectively. Many human factors are important to consider such as breathability, moisture wicking, and abrasion. To address all of these aspects, a passive mild compression ankle sock is the ideal candidate. The Otto-Bock Malleo Sensa was chosen because of its elastic, breathable, and moisture-wicking properties (Figure 5.30).

There are many behavioural aspects of the Malleo Sensa that can effect its performance. For example, since the fabric outer shells are attached directly to the inner sock, the high

forces can cause stretching and possibly weaken the elastic characteristics of the fibers. A possible solution is to use velcro strapping (Figure 5.30) to reinforce the inner sock fibers at the attachment points. The issue with velcro strapping is the ability to fix and remove the straps to not interfere with the outer fabric shells or the donning and doffing the device. The attachment of the bladders and fabric outer shells to the inner sock will also affect the inner sock behaviour. If these are stitched to the inner sock, there will be localized stress at the attachment points. If adhesive is used, the stress can be distributed more evenly; however, the strength of the adhesive must be investigated. Initial performance testing of the inner sock should be conducted.

Figure 5.30: Image of Malleo Sensa sock from Otto-Bock showing velcro strapping (modified from [127]).

5.4.3.5 Application of Pneumatic Sock AFO

Based on the above analysis, the application of the Pneumatic Sock AFO on an average-sized male right ankle and foot is shown in Figure 5.31. The bladder forces, F_B, on the shank and foot segments for the anterior, posterior, medial, and lateral are shown with their corresponding moment arms. The frictional forces would act perpendicular to the bladder forces on the surface of the shank and foot.

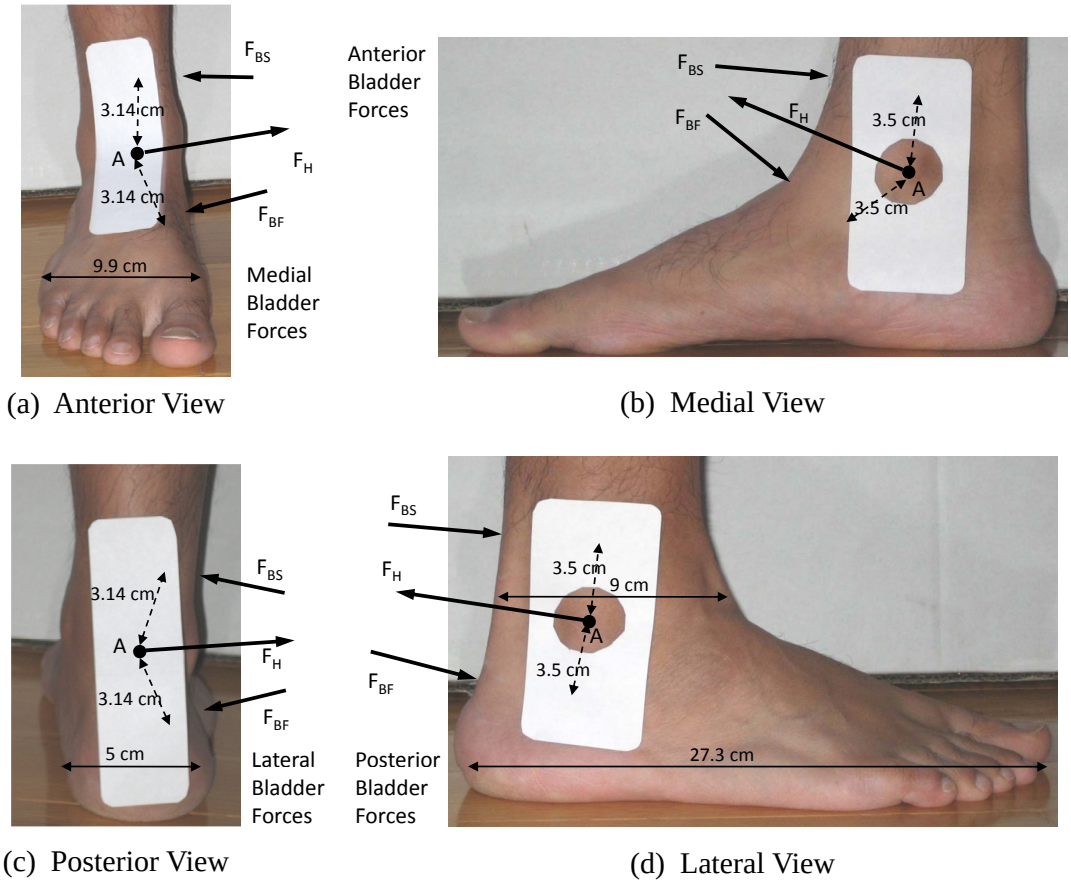

(a) Anterior View (b) Medial View

(c) Posterior View (d) Lateral View

Figure 5.31: Images of average-sized male right ankle and foot with anterior, posterior, medial, and lateral bladder and fabric shell forces shown. The frictional forces, F_f, (not shown for clarity), would be perpendicular to the bladder force, F_B, at the surface of the shank and foot.

5.4.3.6 Actuation of Pneumatic Sock AFO

Once the above manufacturing difficulties can be overcome and a viable Pneumatic Sock AFO prototype can be constructed, the actuation of the device over the gait cycle to satisfy the functional requirements must be investigated. Since the above analysis has been established for the maximum functional requirements for a 90 kg patient, it is reasonable to analyze the behaviour of the device within these operating parameters by assuming some basic characteristics of the bladders. The determination of the actual characteristics would require experimentation. For instance, assume for simplicity that the bladder acts frictionless. In order to produce a linear rotational spring, the augmentation moment must vary proportionally with angle as the foot is rotated relative to a joint axis. If the moment

arm, r_B, of the bladder force, F_B is considered constant about the joint axis, and the contact area, A, of the bladder against the body segment is also constant, the result is a proportional graph of bladder pressure versus angle as shown in Figure 5.32. Therefore, to produce the rotational spring effect as the foot is rotated about a joint axis, the bladder, which is in the direction of rotation, is inflated directly proportional to angle of rotation.

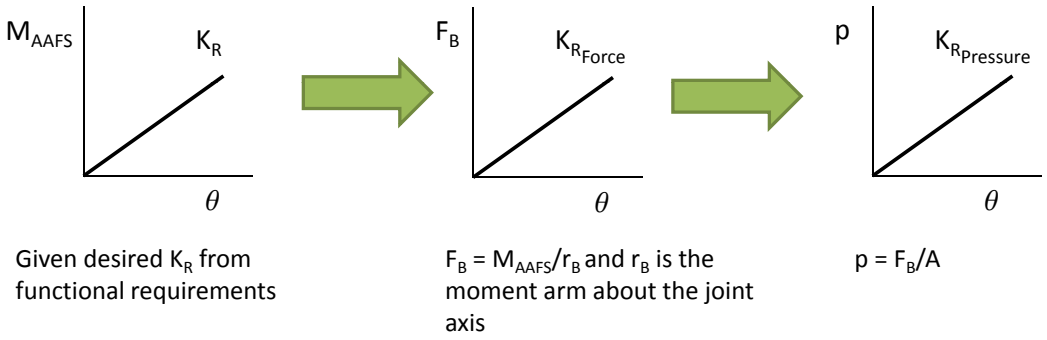

Figure 5.32: Conversion of linear rotational stiffness K_R to pressure stiffness $K_{R_{Pressure}}$ for frictionless Pneumatic Sock AFO. The angle θ can represent dorsiflexion, plantarflexion, supination, or pronation.

Consider the sagittal plane (anterior-posterior) functional requirements. Three rotational stiffnesses are required: K_{R1}, K_{R2}, and K_{R3}. K_{R1} is required during the CP phase, which involves only the posterior bladder to be inflated to resist plantarflexion. K_{R2} is required during CD, which involves only the anterior bladder to be inflated to resist dorsiflexion. K_{R3} is required to store energy for the swing phase; however, unlike a spring, the posterior bladder can be directly inflated during swing phase to actively lift the foot. The advantage of this type of actuation is that plantarflexion resistance during terminal PP can be eliminated, which allows the patient to push off unhindered.

The anterior bladder of the Pneumatic Sock AFO could provide torque upon HO, which would be a safe torque source. Instead of reducing the pressure from HO to NT (the release phase when the spring is following stiffness K_{R2}), the bladder could remain inflated at an appropriate pressure to provide an assistive plantarflexion moment. Further investigation is required.

Based on the frontal plane (medial-lateral) functional requirements, inflation of the bladder in the direction of rotation is needed in response to the four selected gait events. Again, the pressure can be directly controlled to adjust the rotational stiffness. The medial and lateral bladders can be inflated individually or together depending on the level of control required.

5.4.3.7 General Discussion

The concept of a Pneumatic Sock AFO is promising. The device itself would be discrete and comfortable with the use of an inner sock, fabric shells, bladders and air pressure. Based on the model developed, the functional requirements are expected to be satisfied; however, there are many issues that need to be addressed. The inner sock would be under high tension requiring reinforcement by velcro strapping which would be difficult to implement. The high tension in the inner sock would require reinforcement. The bladders would also be difficult to produce because of their small size and potential to burst due to the pressure requirements; custom molded bladders would have to be investigated. The fabric shells would require mechanical testing to ensure they would withstand the tension produced by the bladder forces.

Extensive experimentation would need to be conducted on each of the Pneumatic Sock AFO components to characterize their behaviour, including the potential of using the anterior bladder as a torque source. Ultimately, this information could then be used to construct a viable prototype and characterize the behaviour of the overall device. The actuation of the device was explored based on behavioural assumptions of the device. In addition to the mechanical aspect, it is prudent to explore the control aspects of the device. These are discussed in Chapter 6.

5.5 Concluding Remarks

In this chapter, several design concepts of the torque source and linear rotational spring were explored. Focus was placed on the linear rotational spring aspect of the AAFS and the VSRA concept was analyzed. Due to difficulties with the spring design and limitations of the rotation actuator, the VSRA design was deemed infeasible. A pneumatic approach was explored which included an Airbeam AFO concept. However, the required pressure and diameter of the airbeams to satisfy the functional requirements, could not satisfy the AAFS design criteria. A second pneumatic approach involving a novel Pneumatic Sock AFO was explored. Although most materials were determined, extensive experimentation is required to characterize the behaviour of each component and the overall device itself to ensure the design criteria and functional requirements can be satisfied; including its use as a torque source. Further investigation to develop a prototype is required. Once a prototype is built it will need to be tested. The development of testing methods is important to isolate the characteristics of an AAFS. This is discussed next in Chapter 6.

Chapter 6

Development of Testing Methods

6.1 Proposed Control Method for Pneumatic Sock

The Pneumatic Sock AFO is the favoured candidate for the AAFS. Assuming the challenges outlined in the previous chapter can be overcome, the next step would be to control the device. The following sections briefly outline a potential control scheme for the Pneumatic Sock AFO.

6.1.1 Control Layout

The control layout for the Pneumatic Sock AFO is shown in Figure 6.1. Attached to each bladder is a tube which supplies air. Each tube is connected to a pressure transducer which monitors and adjusts the pressure of the bladder based on a control input. The air is supplied from an air source of 100 psi (or 690 kPa) possibly from a compressor. The control input for the pressure transducers is from a data acquisition (DAQ) controller. Connected to the DAQ is a laptop computer with a software interface. The DAQ also receives input signals from external sensors to capture the state of the device. A detailed breakdown of each components in the control system follows.

6.1.2 Components

6.1.2.1 Data Acquisition Controller

The Data Acquisition Controller (DAQ) consists of a few modules from National Instruments used in conjunction with Labview software. The base module is a cDAQ-9174 that is

a CompactDAQ chassis with four slots and a USB computer interface (Figure 6.2a). Two modules are selected for input and output. The first is the NI 9215 four channel 16-Bit, +/-10 V simultaneous sampling differential analog input module (Figure 6.2b) and the second is the NI 9263 4-Channel, 16-Bit, +/-10 V, analog output module (Figure 6.2c). The four channel output was selected specifically for the four pressure transducers. A DAQ software package in Labview allows for a graphical interface to execute the control algorithm in realtime.

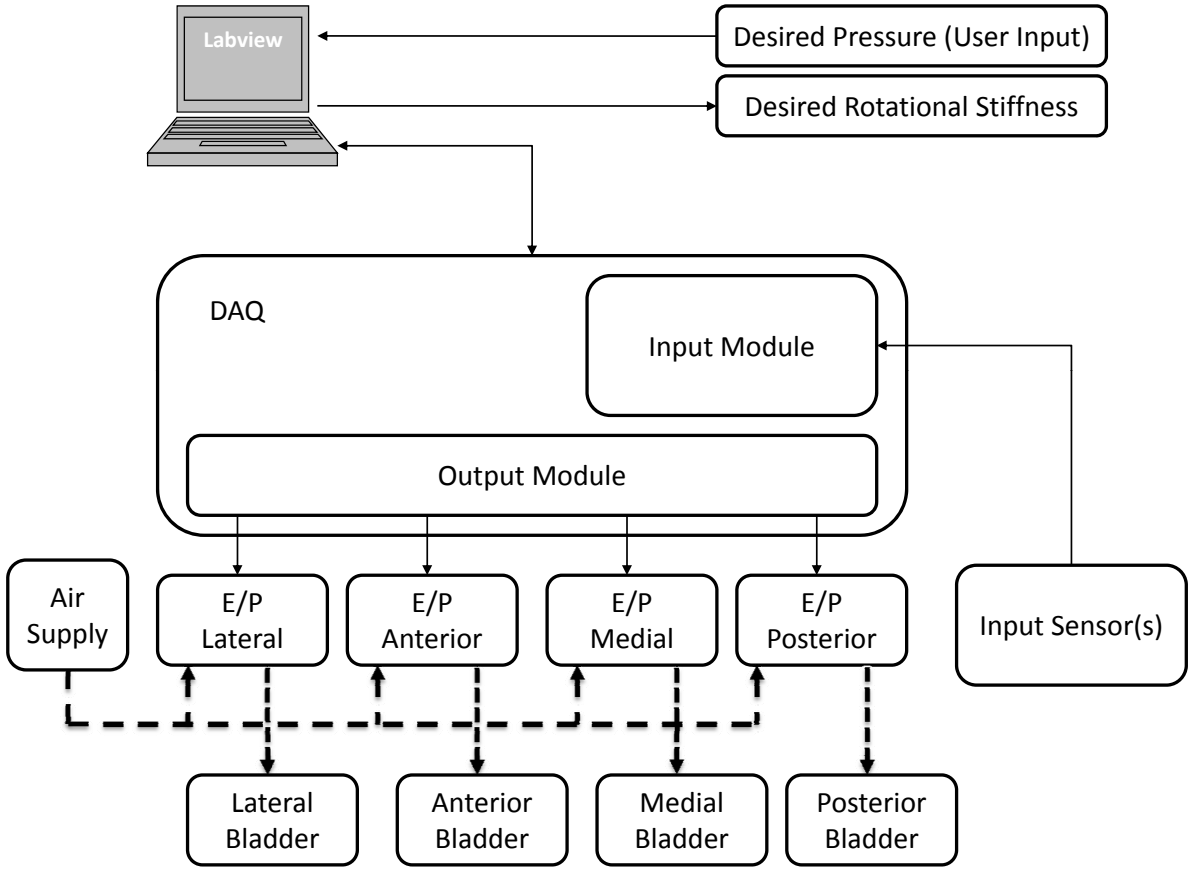

Figure 6.1: Control layout for pneumatic sock AFO. Air supply lines are represented by thick dashed lines and electrical control lines are represented by thin solid lines.

6.1.2.2 Pressure Transducers

The pressure transducers for this control scheme are T900X Miniature E/P (voltage to pressure) Transducer for Electronic Air Pressure Control from ControlAir Inc. They feature a self-correcting bimorph piezo actuator to maintain precise control of pressure. Model T900EHT uses a voltage control input from 0 to 10 V, a pressure range of 2 to 100 psi, and

a terminal block electrical connection. Upon calibration, the output pressure is directly proportional to the input voltage. A separate power supply is required. A typical T900X pressure transducer is shown in Figure 6.3. A wiring diagram is provided in Figure 6.4

(a) cDAQ-9174 (b) NI9215 (c) NI9263

Figure 6.2: Images of DAQ components from National Instruments Inc. [128, 129, 130]

Figure 6.3: Image of T900X pressure transducer from ControlAir Inc [131].

6.1.2.3 Input Sensors

The input sensors for this control scheme can be portable or non-portable; however, the former is preferred since the AAFS would then also be portable. Ideally, the sensor would directly detect the angle of dorsiflexion/plantarflexion and supination/pronation. The first two sensor types discussed are portable and the third sensor type is non-portable.

Flexible Goniometer A two-dimensional flexible goniometer can detect angle in both the sagittal and frontal planes. Particularly, the SG110 or the SG110A from Biometrics

Ltd. are examples of these goniometers shown in Figure 6.5. As the goniometer is flexed in either the sagittal or frontal plane, an analog voltage is outputted with either a positive or negative sign to indicate rotation direction. These outputs can be inputted into the DAQ and processed using the Labview software to determine the orientation of the foot.

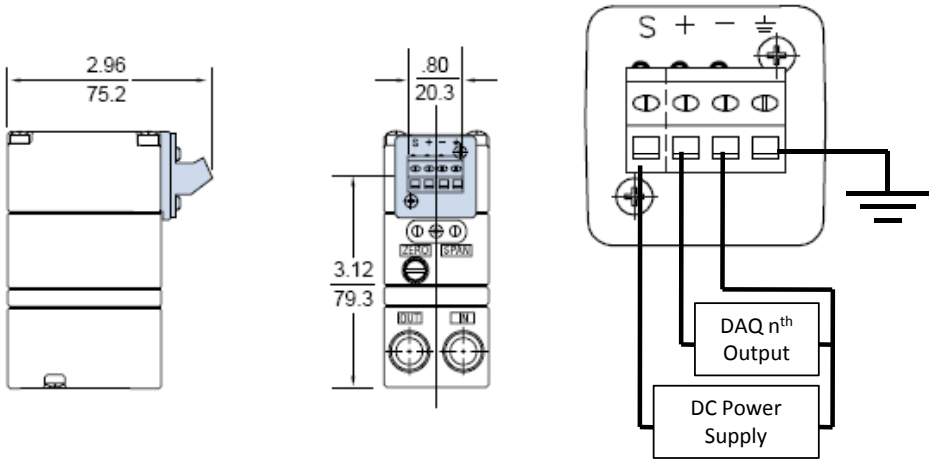

Figure 6.4: Wiring diagram for T900X pressure transducer with terminal block electrical connection (adapted from [132, 133]).

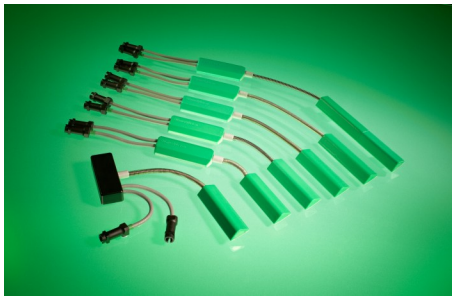

Figure 6.5: Image of two-dimensional goniometers from Biometrics Ltd [134]. SG110A is at the bottom.

Force Sensing Resistors Another potential input sensor is a force sensing resistor (FSR). Examples of these include single cell FSRs, which were used in [91], and more intricate multicell arrays that hold hundreds of FSRs, such as the F-Scan system (Figure 6.6). The drawback to these sensors is that they can only be used during stance since they rely on compression of the sensors to output a signal. For swing, a preprogrammed response after TO could be implemented to lift the foot to prevent drop foot and stabilize the foot

mediolaterally. A threshold would also have to be determined to distinguish between the stance and swing phases. During stance, the location of the COP could be mapped to a corresponding angle for each patient, since the sensor does not read the angle directly. For example, if the COP is shifted posteriorly, this could indicate dorsiflexion. A neural network or fuzzy logic controller could be implemented with the DAQ such that, as the patient would walk, the output to the DAQ would vary based on the COP location.

Figure 6.6: Image of an F-Scan in-shoe sensor pad from TekScan, Inc. [135]

Camera-based Motion Analysis System Another option for an input sensor is to use a camera-based motion analysis system for realtime kinematic measurement of gait. Using markers located on the foot and shank, the relative joint angles can be determined and input into the DAQ. This is an expensive option because the patient would need to walk in a gait laboratory in order to extract the desired data. Eventually, the motion capture system would be used during clinical testing to verify the efficacy of the device. Ultimately, a portable sensor option would be needed for the Pneumatic Sock AFO to be successful as an AAFS for daily use. Further investigation is required.

6.2 Mechanical Testing of AAFS

6.2.1 Test Structure and Configuration

Characterization of the AAFS device is important in testing whether the desired functional requirements are met. A proposed test rig is illustrated in Figures 6.7 and 6.8. The test rig consists of an average-sized male prosthetic shank and foot with a universal joint to permit two degrees of freedom. Although this does not correspond to the anatomical STJ, this is a good approximation. The device is donned on the prosthesis and the sole of the foot is fixed to the rotating foot plate. The axis of the rotating plate is aligned with the prosthetic joint. The angle of the foot can be selected via a locking pin system. The foot

can be aligned on the plate either anterior-posteriorly or medial-laterally depending on which direction of measurement is required.

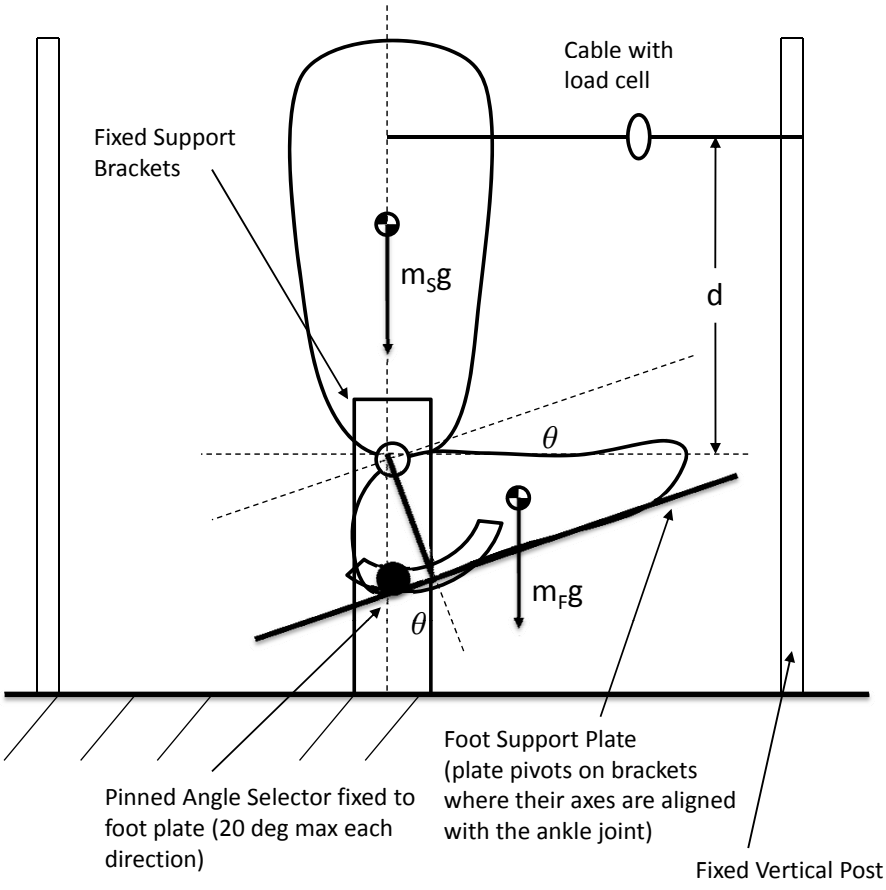

Figure 6.7: Side view of test rig layout for AAFS.

The shank is held vertical such that the force due to gravity of the shank passes through the joint axis. A cable with a load cell is attached to the shank on one end, and attached to a fixed post on the other. Initially, the shank is held vertical such that the force in the cable is zero. Upon release of the shank, the actuation force due to the AAFS can be measured. The moment produced by the AAFS, M_Q, at the angle selected at the foot is the product of the distance from the cable to the prosthesis joint and the force measured in the cable by the load cell.

$$M_Q = F_C d \tag{6.1}$$

The moment produced by the AAFS can be determined for various angles of the foot. Ultimately, the desired output would be a linear curve of moment, M_Q, versus ankle angle as determined previously for the functional requirements.

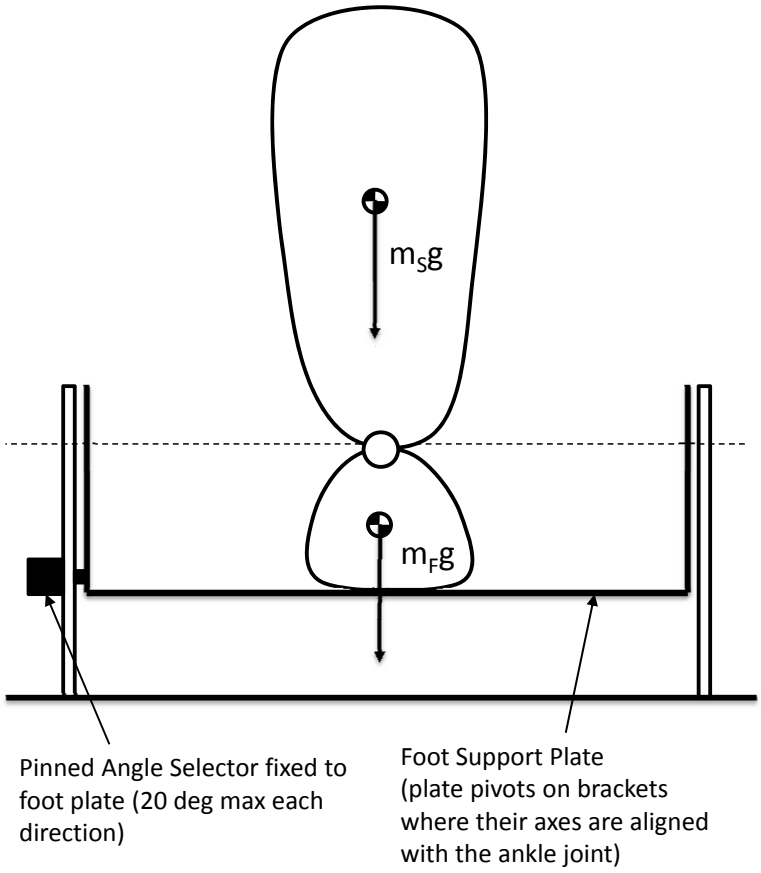

Figure 6.8: Front view of test rig layout for AAFS.

Next, using this test configuration, a test procedure for the stance and swing phase are developed for the Pneumatic Sock AFO.

6.2.2 Stance Test Procedure

6.2.2.1 Anterior-Posterior

For the testing of the anterior-posterior functions of the Pneumatic Sock AFO, the procedure is as follows:

1. Place the AAFS on the prosthesis and connect all sensors and air supply tubes as outlined in Section 6.1.
2. Place the prosthesis on the foot plate anterior-posteriorly and align the joint axis with the axis of the foot plate.
3. Rotate the foot plate to 2 deg dorsiflexion.
4. Position the shank vertically and connect the cable to the vertical post such that the force in the cable is zero when the AAFS is not activated.
5. Inflate the anterior bladder using its assigned pressure transducer via the Labview interface to a maximum of 93 psi (refer to Table 5.6).
6. Record the pressure and force, F_C, where $F_C d = K_R \theta$ for K_R = 2, 4, and 6.3 Nm/deg. 6.3 Nm/deg is the maximum stiffness requirement for the AAFS in the sagittal plane, and the other values of K_R can allow interpolation between pressure versus angle curves.
7. Repeat steps 3 through 6 for θ dorsiflexion = 4, 6, 8, and 10 deg.
8. Repeat step 7 for the posterior bladder with θ plantarflexion = 2, 4, 6, 8, and 10 deg.

6.2.2.2 Medial-Lateral

For the testing the medial-lateral functions of the Pneumatic Sock AFO, the procedure is as follows:

1. Place the AAFS on the prosthesis and connect all sensors and air supply tubes as outlined in Section 6.1.
2. Place the prosthesis on the foot plate medial-laterally and align the joint axis with the axis of the foot plate.
3. Rotate the foot plate to 2 deg supination.

4. Position the shank vertically and connect the cable to the vertical post such that the force in the cable is zero when the AAFS is not activated.

5. Inflate the medial bladder using its assigned pressure transducer via the Labview interface to a maximum of 43 psi (refer to Table 5.6).

6. Record the pressure and force, F_C, where $F_C d = K_R \beta$ for K_R = 0.5, 1.25, and 2 Nm/deg. 2 Nm/deg is the maximum stiffness requirement for the AAFS in the frontal plane, and the other values of K_R can allow interpolation between pressure versus angle curves.

7. Repeat steps 3 through 6 for θ dorsiflexion = 4, 6, 8, and 10 deg.

8. Repeat step 7 for the lateral bladder and β pronation = 2, 4, 6, 8, and 10 deg.

6.2.3 Swing Test Procedure

For the testing of the swing phase function of the Pneumatic Sock AFO, the procedure is as follows:

1. Place the AAFS on the prosthesis and connect all sensors and air supply tubes as outlined in Section 6.1.

2. Place the prosthesis on the foot plate anterior-posteriorly and align the joint axis with the axis of the foot plate.

3. Rotate the foot plate to 0 deg.

4. Position the shank vertically and connect the cable to the vertical post such that the force in the cable is zero when the AAFS is not activated.

5. Inflate the posterior bladder using its assigned pressure transducer via the Labview interface to a maximum of 93 psi (refer to Table 5.6).

6. Record the pressure and force, F_C, where $F_C d = m_F g c$ where m_F is the mass of the foot and c is the moment arm of $m_F g$ when the foot is in neutral and horizontal (i.e., worst case scenario).

7. Repeat steps 3 through 6 for plantarflexion θ = 5, 10, and 20 deg.

6.2.4 Pressure Profiles

The recorded pressures for each test would be plotted against angle for the anterior-posterior and medial-lateral directions. The resulting curves would be the pressure input profiles required by the pressure transducers to successfully achieve the rotational stiffness of the AAFS. Interpolation of these curves can be performed to calculate the pressure input profiles for any rotational stiffness within the upper limits set out in the functional requirements.

6.3 Concluding Remarks

In this chapter, testing methods for the AAFS were developed for the favoured design, a Pneumatic Sock AFO. A control scheme was outlined using a laptop computer, DAQ, input sensors, and output pressure transducers. Ultimately, the device is intended for portable use and thus all of these components would also need to be portable. Regardless of these challenges, the behaviour of the AAFS must be characterized when the bladders are inflated. A rig structure configuration, consisting of a prosthetic shank and foot, and test procedures were developed to characterize the stiffness behaviour in the sagittal and frontal planes according to the functional requirements previously determined. The aim of the characterization is to determine the pressure profile curves where a desired moment at a specified angle can be achieved with a corresponding input pressure.

Chapter 7

Conclusions and Future Work

7.1 Conclusions

Deterioration of the ankle and foot can occur as a result of conditions due to stroke or injury, affecting healthy gait. Upon review of populations with ankle-foot gait deficiencies, including the elderly, drop foot patients, and ankle-sprain injured individuals, it was shown that changes in kinematic and kinetic gait patterns exist. A review of current passive AFO and active AFO technologies revealed several limitations for satisfying the needs of each population. Passive AFOs were unable to deactivate and thus limited natural motion of the ankle. They were also unable to adjust to variations in gait. In order to address some of these limitations, active AFOs have been developed. These were designed for specific applications, including drop foot prevention, plantarflexion assist, and combinations of the two. Most active AFOs also limited frontal plane motion, which could lead to unnatural gait patterns. Unlike passive AFOs, active AFOs are not available on the commercial market and are only found in the literature. Active AFOs were generally bulky and heavy, which reinforced their rehabilitative purpose. A single device that could meet the requirements of these populations does not exist.

In this thesis, the feasibility of an Active Ankle-Foot Stabilizer (AAFS) was researched to correct deficiencies in gait for the above three populations. Design criteria were established to determine the device parameters, including a desired patient body mass goal of 90 kg, a maximum device mass of 2.5 kg, and a minimal profile to allow fitting into a shoe or boot. The AAFS functional requirements in the sagittal plane (anterior-posterior direction) were determined using a moment versus angle work approach that analyzed the moment deficit of deficient gait patterns for the CP, CD, and PP gait phases. The adjustment of joint rotational stiffness in the CP and CD phases were altered based on a linear

rotational spring. This resulted in discrepancies between the moment versus angle curves of the gait-deficient populations and young healthy adults. An analysis of the moment deficit differences showed that compensation moments required by the gait-deficient individual may be reasonable. A linear rotational spring was used to store energy prior to the swing phase to provide an assistive dorsiflexor moment upon HO. The upper stiffness of the linear rotational spring limit should be 0.070 Nm/kg/deg θ up to 10 deg and the lower rotational stiffness limit should be 0.002 Nm/kg/deg θ up to 20 deg. The corresponding values for a 90 kg patient are 6.3 Nm/deg and 0.18 Nm/deg, respectively. During PP, an increasing then decreasing torque was supplied to restore plantarflexion power. The maximum plantarflexion torque and power required are 0.72 Nm/kg and 2.6 W/kg, respectively. For a 90 kg patient, the maximum plantarflexion torque and power required are 65 Nm and 234 W, respectively. The frontal plane (medial-lateral direction) functional requirements were also determined based on specified events during the gait cycle. A linear rotational spring was chosen to best meet these requirements with upper stiffness of 0.022 Nm/kg/deg β.

The design approach explored both the torque source and linear rotational spring aspects of the AAFS. Torque source concepts were explored; however, the high moments required resulted in similar design challenges faced by previous investigators, including high bulk and external power source requirements. Exploration of the linear rotational spring aspect of the AAFS yielded a Variable Rotational Spring Actuator (VSRA) AFO design concept consisting of a linear spring which rotated one of its end points to vary the spring stiffness characteristics. The device was limited to adjusting joint stiffness in the sagittal plane, while a passive narrow leafspring was used, due to the minimal area of the posterior surface of the ankle and foot, to control frontal plane motion. Although the sagittal plane functional requirements could be met according to the VSRA model (Section 5.2.2.1), a suitable spring for the VSRA AFO could not be designed due to the high forces and large spring diameters required. The VSRA AFO was deemed infeasible, and a pneumatic approach was explored.

Two pneumatic approaches were investigated: an Airbeam AFO and a Pneumatic Sock AFO. The Airbeam AFO design involved individually inflated airbeams placed posterior and lateral to the ankle. Unfortunately, based on the functional and rotational stiffness requirements, the airbeams were required to operate at high pressures and have large diameters. The minimum diameter manufacturable exceeded the desired AAFS profile determined in the design criteria. Another issue with the Airbeam AFO was the influence of external forces on the surface of the beam. Since the airbeam relied on its cylindrical shape to maintain stiffness, external forces could potentially cause failure. Therefore, this design was infeasible and a second pneumatic approach was explored.

The Pneumatic Sock AFO consisted of an anterior, posterior, medial, and lateral blad-

der that surrounded the ankle and foot over an inner sock. The bladders were each surrounded by a fabric shell that was attached to the ankle at the joint axes. Inflation of the individual bladders could produce resistive moments and control ankle rotation. Although most materials were determined, experimentation is required to characterize the behaviour of each component and the overall device itself, to ensure that the design criteria and functional requirements can be satisfied. Unlike the torque source options explored previously in this research, the Pneumatic Sock AFO anterior bladder could provide a safe method for plantarflexion moment assistance. The Pneumatic Sock AFO is the favoured design for an AAFS; however, further investigation is required to develop a prototype.

Once a prototype of the Pneumatic Sock AFO is developed, the characterization of the AAFS can be explored. Testing methods were developed for this purpose including the outline of a control scheme, control components required, and testing procedures to characterize the stiffness behaviour in the sagittal and frontal planes according to the functional requirements previously determined. The aim of the characterization is to determine the pressure profile curves where a desired moment at a specified angle can be achieved with a corresponding input pressure.

7.2 Future Work

The Pneumatic Sock AFO has the potential to significantly improve deficient human gait. There are many challenges ahead before a viable device can be developed. These are discussed next.

7.2.1 Construction of Pneumatic Sock AFO

The construction of a Pneumatic Sock AFO prototype requires testing of the individual materials to ensure they can withstand the forces required to meet the AAFS functional requirements. Since the fabric shells are attached to the inner sock, the issue of reinforcement must be considered. Tensile tests at the joint axis attachment points on the inner sock are required to measure the changes in the sock structure due to tensile forces. Velcro strapping may have to be implemented to reinforce the sock structure. The bladders would also need to be custom molded to prevent bursting at the required pressures and to ensure that the bladder tends to expand in one dimension. As well, a suitable inlet valve must be integrated into the bladder, such as a Schrader valve, to allow air flow in and out of the bladder. The attachment method between the bladders and the inner sock would need to be investigated, such as the use of an adhesive or a stitched seam. The fabric shells would

have to undergo tensile testing to ensure tearing or fraying of the fabric does not occur. Finally, characterization of friction between the bladders and fabric shells, and bladders and inner sock, would need to be investigated for functional and failure analysis. Once a prototype has been constructed, characterization of the Pneumatic Sock AFO can be performed.

7.2.2 Characterization of AAFS

The characterization of the Pneumatic Sock AFO would be performed as outlined in Chapter 6. The test rig would be constructed with an average-sized male shank and foot placed on the foot plate. Experimentation with the sensors, including the FSRs and goniometer, would need to be performed to determine the best sensor option for control. Once the control components have been configured, testing can begin as outlined in the testing procedures.

7.2.3 Setting and Tuning AAFS Parameters

Before an AAFS can be implemented for a patient, the gait patterns of the patient must be determined. Using a camera-based motion capture and analysis system in conjunction with force sensors below the sole of the foot (such as a force plate), the angle and moment for the individual patient can be measured during level ground walking. The same functional simulation performed in Chapter 4 would then be implemented to determine the patient's optimal spring rates. Based on the AAFS characterization in Section 6.2, the pressure profiles to achieve the required rotational stiffness can be extracted and programmed into the AAFS system. Once these parameters are established, clinical gait trials could be conducted to verify that the device functions correctly and to further tune the parameters.

7.2.4 Portability of Pneumatic Source

Another challenge of the Pneumatic Sock AFO is the portability of the pneumatic source. Ultimately, the device would be worn for daily use, therefore, a portable air supply is required. This could be in the form of a miniature compressor worn in a backpack on the patient near the body center of mass. The power source to compress the air would also need to be considered, such as a battery pack.

Ideally, the air pressure could be supplied from an air reservoir located on the leg or lower back, which would be replenished by body movement. For example, an air bellow

placed under the foot could pump air into the reservoir during each stance phase, however this may adversely affect proprioception. Capturing the power produced during knee or arm swing movement could also be a possibility, either to drive a bellow or charge a battery.

References

[1] D.A. Winter. *The biomechanics and motor control of human gait: normal, elderly and pathological*. University of Waterloo Press, Waterloo, ON, 1991. xiv, 1, 3, 12, 13, 17, 18, 21, 23, 24, 25, 26, 28, 60, 61, 62, 63, 64, 65, 66, 67, 71, 72, 73, 74, 75, 77, 78, 79, 80, 81

[2] M. Shields. Use of wheelchairs and other mobility support devices. *Health Reports-Statistics Canada*, 15(3):37–42, 2004. 1

[3] D.A. Nawoczenski and M.E. Epler. *Orthotics in functional rehabilitation of the lower limb*. WB Saunders Co, 1997. 1, 2, 7, 29, 31, 33, 34, 36

[4] P. Bowker, D.L. Brader, D.J. Pratt, D.N. Condie, and A.W. Wallace. *Biomechanical basis of orthotic management*. Butterworth-Heinemann Ltd, 1993. 1, 4, 5, 6, 9, 10, 11, 12, 14, 15, 16, 17, 27, 28, 31, 32, 36, 67

[5] K.E. Gordon, G.S. Sawicki, and D.P. Ferris. Mechanical performance of artificial pneumatic muscles to power an ankle-foot orthosis. *Journal of Biomechanics*, 39(10):1832–1841, 2006. 1, 42, 43, 44, 50, 88, 91

[6] J.A. Blaya and H. Herr. Adaptive control of a variable-impedance ankle-foot orthosis to assist drop-foot gait. *IEEE Transactions on Neural Systems and Rehabilitation Engineering*, 12(1):24–31, 2004. 1, 28, 37, 38, 39, 40, 96

[7] J. Hitt, A.M. Oymagil, T. Sugar, K. Hollander, A. Boehler, and J. Fleeger. Dynamically controlled ankle-foot orthosis (DCO) with regenerative kinetics: Incrementally attaining user portability. In *2007 IEEE International Conference on Robotics and Automation*, pages 1541–1546, 2007. 1, 42, 43, 88

[8] J.O. Judge, S. Ounpuu, and R.B. Davis 3rd. Effects of age on the biomechanics and physiology of gait. *Clinics in Geriatric Medicine*, 12(4):659, 1996. 1, 22, 23

[9] N.B. Alexander. Gait disorders in older adults. *Journal of the American Geriatrics Society*, 44(4):434, 1996. 2, 22, 25, 26

[10] J. Perry. *Gait analysis: Normal and pathological function*. McGraw-Hill, 1992. 2, 3, 4, 8, 9, 10, 11, 12, 13, 14, 15, 16, 17, 27, 28

[11] R. Seymour. *Prosthetics and orthotics: Lower limb and spinal*. Lippincott Williams and Wilkins, 2002. 2, 29, 32, 33, 34, 35, 36

[12] Image of foot bones. `http://bodyseeksoul.com/3D/characters/all/ref/foot/foot-bones.gif`. Last accessed on February 20, 2010. 4, 6

[13] Wikipedia. Planes of Human Anatomy. `http://upload.wikimedia.org/wikipedia/commons/e/e1/Human_anatomy_planes.svg`. Last accessed on May 27, 2010. 5

[14] C.C. Norkin and P.K. Levangie. *Joint structure and function: a comprehensive analysis*. FA Davis Philadelphia, 1992. 5, 6

[15] T.G. McPoil and H.G. Knecht. Biomechanics of the foot in walking: a function approach. *The Journal of orthopaedic and sports physical therapy*, 7(2):69, 1985. 6, 7

[16] S.K. Spooner. The subtalar joint axis Locator. *Journal of the American Podiatric Medical Association*, 96(3):213, 2006. 7

[17] P. Ball and G.R. Johnson. Technique for the measurement of hindfoot inversion and eversion and its use to study a normal population. *Clinical Biomechanics*, 11(3):165–169, 1996. 7, 23

[18] T.J. Ouzounian and M.J. Shereff. In vitro determination of midfoot motion. *Foot and Ankle*, 10(3):140, 1989. 7

[19] Wikipedia. Lateral view of musculature in right ankle and foot. `http://en.wikipedia.org/wiki/File:Gray1241.png`. Last accessed on May 27, 2010. 9

[20] Wikipedia. Medial view of musculature in right ankle and foot. `http://en.wikipedia.org/wiki/File:Gray442.png`. Last accessed on May 27, 2010. 10

[21] Wikipedia. Posterior view of musculature in right ankle and foot. `http://en.wikipedia.org/wiki/File:Gray438.png`. Last accessed on May 27, 2010. 11

[22] M.L. Palmer. Sagittal plane characterization of normal human ankle function across a range of walking gait speeds. Master's thesis, Massachusetts Institute of Technology, 2002. 14, 16, 62, 67

[23] D.A. Winter. *Biomechanics and motor control of human movement*. Wiley, 2009. 14, 67, 68, 122

[24] D.A. Winter. Human balance and posture control during standing and walking. *Gait and Posture*, 3(4):193–214, 1995. 19, 20, 22, 25, 85

[25] A.L. Hof, M.G.J. Gazendam, and W.E. Sinke. The condition for dynamic stability. *Journal of Biomechanics*, 38(1):1–8, 2005. 19

[26] D.A. Winter, A.E. Patla, J.S. Frank, and S.E. Walt. Biomechanical walking pattern changes in the fit and healthy elderly. *Physical Therapy*, 70(6):340, 1990. 23

[27] L. Sturnieks, R. St George, and S.R. Lord. Balance disorders in the elderly. *Clinical Neurophysiology*, 38(6):467–478, 2008. 23

[28] M.G. Tucker, J.J. Kavanagh, R.S. Barrett, and S. Morrison. Age-related differences in postural reaction time and coordination during voluntary sway movements. *Human Movement Science*, 27(5):728–737, 2008. 23

[29] E.T. Hsiao-Wecksler. Biomechanical and age-related differences in balance recovery using the tether-release method. *Journal of Electromyography and Kinesiology*, 18(2):179–187, 2008. 23

[30] D.C. Kerrigan, M.K. Todd, U. Della Croce, L.A. Lipsitz, and J.J. Collins. Biomechanical gait alterations independent of speed in the healthy elderly: evidence for specific limiting impairments. *Archives of Physical Medicine and Rehabilitation*, 79(3):317–22, 1998. 23

[31] P. DeVita and T. Hortobagyi. Age causes a redistribution of joint torques and powers during gait. *Journal of Applied Physiology*, 88(5):1804, 2000. 23

[32] E. Morag and P.R. Cavanagh. Structural and functional predictors of regional peak pressures under the foot during walking. *Journal of Biomechanics*, 32(4):359–370, 1999. 24

[33] M.J. Hessert, M. Vyas, J. Leach, K. Hu, L.A. Lipsitz, and V. Novak. Foot pressure distribution during walking in young and old adults. *BMC Geriatrics*, 5(1):8, 2005. 24

[34] H.B. Menz and M.E. Morris. Clinical determinants of plantar forces and pressures during walking in older people. *Gait and Posture*, 24(2):229–236, 2006. 24, 25, 26

[35] A. Gefen. Simulations of foot stability during gait characteristic of ankle dorsiflexor weakness in the elderly. *IEEE Transactions on Neural Systems and Rehabilitation Engineering*, 9(4):333–337, 2001. 24, 26

[36] J.C. Dean, N.B. Alexander, and A.D. Kuo. The effect of lateral stabilization on walking in young and old adults. *IEEE Transactions on Biomedical Engineering*, 54(11):1919–1926, 2007. 25

[37] M.E. Hahn and L.S. Chou. Can motion of individual body segments identify dynamic instability in the elderly? *Clinical Biomechanics*, 18(8):737–744, 2003. 25

[38] T. Masud and R.O. Morris. Epidemiology of falls. *Age and Ageing*, 30(Supplement 4):3, 2001. 25

[39] S. Hart-Hughes, P. Quigley, T. Bulat, P. Palacios, and S. Scott. An interdisciplinary approach to reducing fall risks and falls. *The Journal of Rehabilitation*, 70(4):46–52, 2004. 25

[40] J.M. Hausdorff, H.K. Edelberg, S.L. Mitchell, A.L. Goldberger, and J.Y. Wei. Increased gait unsteadiness in community-dwelling elderly fallers. *Archives of Physical Medicine and Rehabilitation*, 78(3):278–283, 1997. 25

[41] J.A. Stevens. Fatalities and injuries from falls among older adults–United States, 1993-2003 and 2001-2005. *Journal of Amercian Medical Association*, 297(1):32, 2007. 25

[42] L.S. Chou, K.R. Kaufman, M.E. Hahn, and R.H. Brey. Medio-lateral motion of the center of mass during obstacle crossing distinguishes elderly individuals with imbalance. *Gait and Posture*, 18(3):125–133, 2003. 25

[43] G. Kemoun, P. Thoumie, D. Boisson, and J.D. Guieu. Ankle dorsiflexion delay can predict falls in the elderly. *Journal of Rehabilitation Medicine*, 34(6):278–283, 2002. 25

[44] B.E. Maki. Gait changes in elderly fallers: predictors of risk or indicators of fear? *Journal of the American Geriatrics Society*, 45(3):313–320, 1996. 25

[45] O. Tirosh and W.A. Sparrow. Gait termination in young and older adults: effects of stopping stimulus probability and stimulus delay. *Gait and Posture*, 19(3):243–251, 2004. 26

[46] G. Yogev, M. Plotnik, C. Peretz, N. Giladi, and J.M. Hausdorff. Gait asymmetry in patients with Parkinsons disease and elderly fallers: when does the bilateral coordination of gait require attention? *Experimental Brain Research*, 177(3):336–346, 2007. 26

[47] D.C. Kerrigan, L.W. Lee, T.J. Nieto, J.D. Markman, J.J. Collins, and P.O. Riley. Kinetic alterations independent of walking speed in elderly fallers. *Archives of Physical Medicine and Rehabilitation*, 81(6):730–735, 2000. 26

[48] C.R. Kovacs. Age-related changes in gait and obstacle avoidance capabilities in older adults: a review. *Journal of Applied Gerontology*, 24(1):21, 2005. 26

[49] M. Pijnappels, N.D. Reeves, C.N. Maganaris, and J.H. van Dieën. Tripping without falling; lower limb strength, a limitation for balance recovery and a target for training in the elderly. *Journal of Electromyography and Kinesiology*, 18(2):188–196, 2008. 27

[50] B.E. Maki and W.E. McIlroy. Control of rapid limb movements for balance recovery: age-related changes and implications for fall prevention. *Age and Ageing*, 35(Supplement 2), 2006. 27

[51] L.R. Sheffler, M.T. Hennessey, G.G. Naples, and J. Chae. Peroneal nerve stimulation versus an ankle foot orthosis for correction of footdrop in stroke: impact on functional ambulation. *Neurorehabilitation and Neural Repair*, 20(3):355, 2006. 27, 68

[52] J.G. Furey. Complications following hip fractures. *Journal of Chronic Diseases*, 20(2):103–113, 1967. 27

[53] K. Wilkins. Medications and fall-related fractures in the elderly. *Statistics Canada, Catalogue 82-003, Health Reports*, 11(1):45–53, 1999. 27

[54] S. Fatone, S.A. Gard, and B.S. Malas. Effect of ankle-foot orthosis alignment and foot-plate length on the gait of adults with poststroke hemiplegia. *Archives of Physical Medicine and Rehabilitation*, 90(5):810–818, 2009. 28, 68, 71, 73, 75, 79

[55] J. Blaya. Force-controllable ankle foot orthosis (AFO) to assist drop foot gait. Master's thesis, Massachusetts Institute of Technology, 2003. 29

[56] RA Meals. Peroneal-nerve palsy complicating ankle sprain. Report of two cases and review of the literature. *The Journal of Bone and Joint Surgery*, 59(7):966, 1977. 29

[57] JD Sidey. Weak ankles. A study of common peroneal entrapment neuropathy. *British Medical Journal*, 3(5671):623, 1969. 29

[58] Ortho Rehab Designs. Image of hip hiking in drop foot patient. `http://www.ordesignslv.com/images/foot_drop.gif`. Last accessed on May 27, 2010. 29

[59] D.H. Richie Jr. Functional instability of the ankle and the role of neuromuscular control: a comprehensive review. *The Journal of Foot and Ankle Surgery*, 40(4):240–251, 2001. 29

[60] J. Munn, D.J. Beard, K.M. Refshauge, and R.Y.W. Lee. Eccentric muscle strength in functional ankle instability. *Medicine and Science in Sports and Exercise*, 35(2):245, 2003. 29, 30, 86

[61] K. Monaghan, E. Delahunt, and B. Caulfield. Ankle function during gait in patients with chronic ankle instability compared to controls. *Clinical Biomechanics*, 21(2):168–174, 2006. 29, 30

[62] J. Ty Hopkins, T. McLoda, and S. McCaw. Muscle activation following sudden ankle inversion during standing and walking. *European Journal of Applied Physiology*, 99(4):371–378, 2007. 30, 31, 85, 86

[63] H. Iwamoto, Y. Urabe, H. Kanazawa, and T. Shirakawa. Kinematic analysis of an ankle inversion sprain: a new evaluation technique. *Japanese Journal of Physical Fitness and Sports Medicine*, 55:141–144, 2006. 30, 31, 86

[64] J. Leanderson, M. Bergqvist, C. Rolf, P. Westblad, S. Wigelius-Roovers, and T. Wredmark. Early influence of an ankle sprain on objective measures of ankle joint function A prospective randomised study of ankle brace treatment. *Knee Surgery, Sports Traumatology, Arthroscopy*, 7(1):51–58, 1999. 30, 86

[65] T. Willems, E. Witvrouw, J. Verstuyft, P. Vaes, and D. De Clercq. Proprioception and muscle strength in subjects with a history of ankle sprains and chronic instability. *Journal of Athletic Training*, 37(4):487, 2002. 30, 31, 85

[66] J. Karlsson and G.O. Andreasson. The effect of external ankle support in chronic lateral ankle joint instability: an electromyographic study. *The American Journal of Sports Medicine*, 20(3):257–261, 1992. 30

[67] L.K. Drewes, P.O. McKeon, G. Paolini, P. Riley, D.C. Kerrigan, C.D. Ingersoll, and J. Hertel. Altered ankle kinematics and shank-rear-foot coupling in those with chronic ankle instability. *Journal of Sport Rehabilitation*, 18(3):375–388, 2009. 30

[68] E. Delahunt, K. Monaghan, and B. Caulfield. Altered neuromuscular control and ankle joint kinematics during walking in subjects with functional instability of the

ankle joint. *The American Journal of Sports Medicine*, 34(12):1970–1976, 2006. 30, 31

[69] P. Nieuwenhuijzen, C. Grüneberg, and J. Duysens. Mechanically induced ankle inversion during human walking and jumping. *Journal of Neuroscience Methods*, 117(2):133–140, 2002. 31, 85

[70] The Official Aircast Blog. Image of Aircast stirrup ankle brace. `http://www.shopaircast.com/blog/wp-content/uploads/2009/06/aircast-air-stirrup-ankle-brace-3-273x300.jpg`. Last accessed on May 27, 2010. 34

[71] SV Sports. Image of McDavid lace-up ankle brace. `http://www.svsports.com/store/images/cart/McDavid-Lace-Up-Ankle-ItemImg_5203021.jpg`. Last accessed on May 27, 2010. 34

[72] Orthotape.com. Image of Ossur Game Day prophylactic ankle brace. `http://www.orthotape.com/images/products/Default/royce/Game_day_ankle_brace.JPG`. Last accessed on May 27, 2010. 34

[73] D. Rosenbaum, N. Kamps, K. Bosch, L. Thorwesten, K. Völker, and E. Eils. The influence of external ankle braces on subjective and objective parameters of performance in a sports-related agility course. *Knee Surgery, Sports Traumatology, Arthroscopy*, 13(5):419–425, 2005. 34

[74] OrthopaedicsAndTrauma.com. Image of CAM Walker AFO. `http://www.orthopaedicsandtrauma.com/acatalog/Maxtrax_Fixed_Ankle.gif`. Last accessed on July 16, 2010. 35

[75] HealthAndCare.co.uk. Image of Leg Brace AFO. `http://www.healthandcare.co.uk/user/products/large/Leg%20Brace.jpg`. Last accessed on July 16, 2010. 35

[76] Kevin AFO. Images of AFOs for neurologic involvement. `http://kevinafo.com/images/traditional_afo_pic.png`. Last accessed on May 27, 2010. 35

[77] Opentip.com. Image of Ossur Foot-Up dorsiflexion assist AFO. `http://www.opentip.com/images/imagecache/OSS/OSS-07810-1_280_280.jpg`. Last accessed on May 27, 2010. 35

[78] S.A. Radtka, S.R. Skinner, and M. Elise Johanson. A comparison of gait with solid and hinged ankle-foot orthoses in children with spastic diplegic cerebral palsy. *Gait and Posture*, 21(3):303–310, 2005. 36, 68

[79] K. Desloovere, G. Molenaers, L. Van Gestel, C. Huenaerts, A. Van Campenhout, B. Callewaert, P. Van de Walle, and J. Seyler. How can push-off be preserved during use of an ankle foot orthosis in children with hemiplegia? A prospective controlled study. *Gait and Posture*, 24(2):142–151, 2006. 36

[80] M. Alimusaj, I. Knie, S. Wolf, A. Fuchs, F. Braatz, and L. Döderlein. Functional impact of carbon fiber springs in ankle-foot orthoses. *Der Orthopäde*, 36(8):752, 2007. 36

[81] Å. Bartonek, M. Eriksson, and E.M. Gutierrez-Farewik. A new carbon fibre spring orthosis for children with plantarflexor weakness. *Gait and Posture*, 25(4):652–656, 2007. 36

[82] W.E. Carlson, C.L. Vaughan, D.L. Damiano, and M.F. Abel. Orthotic Management of Gait in Spastic Diplegia1. *American Journal of Physical Medicine and Rehabilitation*, 76(3):219–225, 1997. 37

[83] J.F. Lehmann, S.M. Condon, B.J. De Lateur, and R. Price. Gait abnormalities in peroneal nerve paralysis and their corrections by orthoses: a biomechanical study. *Archives of Physical Medicine and Rehabilitation*, 67(6):380–386, 1986. 37, 38

[84] R. Chin, E.T. Hsiao-Wecksler, E. Loth, G. Kogler, S.D. Manwaring, S.N. Tyson, K.A. Shorter, and J.N. Gilmer. A pneumatic power harvesting ankle-foot orthosis to prevent foot-drop. *Journal of Neuroengineering and Rehabilitation*, 6(1):19, 2009. 37, 38, 40, 41, 90

[85] S. Yamamoto, A. Hagiwara, T. Mizobe, O. Yokoyama, and T. Yasui. Development of an ankle-foot orthosis with an oil damper. *Prosthetics and Orthotics International*, 29(3):209–219, 2005. 37, 39, 40, 90

[86] D. Cattaneo, F. Marazzini, A. Crippa, and R. Cardini. Do static or dynamic AFOs improve balance? *Clinical Rehabilitation*, 16(8):894–899, 2002. 37

[87] A. Manzoor, H. Elkhbai, and Z. Ekwaneen. Adaptive Control of Foot Orthosis. Master's thesis, School of Information Science, Computer and Electrical Engineering, Halmstad University, 2007. 37, 40, 41

[88] Y. Bar-Cohen and C.L. Breazeal. *Biologically inspired intelligent robots*. The Society of Photo-Optical Instrumentation Engineers, 2003. 39, 50

[89] S.M. Chang and D. Rincon. Biofeedback controlled ankle foot orthosis for stroke rehabilitation to improve gait symmetry. *2006 Florida Conference on Recent Advances in Robotics*, 12:17–22, 2006. 41

[90] K.E. Gordon and D.P. Ferris. Learning to walk with a robotic ankle exoskeleton. *Journal of Biomechanics*, 40(12):2636–2644, 2007. 42

[91] S. Hwang, J. Kim, J. Yi, K. Tae, K. Ryu, and Y. Kim. Development of an active ankle foot orthosis for the prevention of foot drop and toe drag. In *Biomedical and Pharmaceutical Engineering, 2006. ICBPE 2006. International Conference on*, pages 418–423, 2006. 44, 45, 88, 135

[92] D.P. Ferris, K.E. Gordon, G.S. Sawicki, and A. Peethambaran. An improved powered ankle-foot orthosis using proportional myoelectric control. *Gait and Posture*, 23(4):425–428, 2006. 44, 45

[93] G.S. Sawicki, A. Domingo, and D.P. Ferris. The effects of powered ankle-foot orthoses on joint kinematics and muscle activation during walking in individuals with incomplete spinal cord injury. *Journal of Neuroengineering and Rehabilitation*, 3(1):1–17, 2006. 44

[94] A. Agrawal, V. Sangwan, S.K. Banala, S.K. Agrawal, S.A. Binder-Macleod, et al. Design of a novel two degree-of-freedom ankle-foot orthosis. *Journal of Mechanical Design*, 129:1137–1143, 2007. 46, 47

[95] K. Bharadwaj, T.G. Sugar, J.B. Koeneman, and E.J. Koeneman. Design of a robotic gait trainer using spring over muscle actuators for ankle stroke rehabilitation. *Journal of Biomechanical Engineering*, 127:1009–1013, 2005. 46, 47

[96] J.L. Pons. *Emerging actuator technologies: A micromechatronic approach.* John Wiley and Sons Inc, 2005. 48, 49, 50

[97] K.W. Hollander and T.G. Sugar. Design of lightweight lead screw actuators for wearable robotic applications. *Journal of Mechanical Design*, 128:644–648, 2006. 49, 108

[98] C. Mavroidis, J. Nikitczuk, B. Weinberg, G. Danaher, K. Jensen, P. Pelletier, J. Prugnarola, R. Stuart, R. Arango, M. Leahey, et al. Smart portable rehabilitation devices. *Journal of Neuroengineering and Rehabilitation*, 2(1):18, 2005. 50

[99] N.P. Cheremisinoff. *Encyclopedia of fluid mechanics: Rheology and non-Newtonian flows.* Gulf Publishing Company, 1988. 50

[100] C.L. Ogden, C.D. Fryar, M.D. Carroll, and K.M. Flegal. Mean body weight, height, and body mass index, United States 1960–2002. *Advance Data*, 347:1–17, 2004. 55

[101] J. Ryu, J. Jung, and S. Choi. Perceived magnitudes of vibrations transmitted through mobile device. In *Proceedings of the 2008 Symposium on Haptic Interfaces for Virtual Environment and Teleoperator Systems*, pages 139–140. IEEE Computer Society, 2008. 56

[102] R.C. Browning, J.R. Modica, R. Kram, and A. Goswami. The effects of adding mass to the legs on the energetics and biomechanics of walking. *Medicine and Science in Sports and Exercise*, 39(3):515–525, 2007. 56

[103] A.H. Hansen, D.S. Childress, S.C. Miff, S.A. Gard, and K.P. Mesplay. The human ankle during walking: Implications for design of biomimetic ankle prostheses. *Journal of Biomechanics*, 37(10):1467–1474, 2004. 62, 67

[104] S.K. Au, P. Dilworth, and H. Herr. An ankle-foot emulation system for the study of human walking biomechanics. In *Proceedings of International Conference on Robotics and Automation*, pages 2939–2945, 2006. 67

[105] NASA. Volume I, Section 3: Anthropometry and biomechanics. `http://msis.jsc.nasa.gov/sections/section03.htm`. Last accessed on May 27, 2010. 68, 122

[106] Q. Shao and T.S. Buchanan. A biomechanical model to estimate corrective changes in muscle activation patterns for stroke patients. *Journal of Biomechanics*, 41(14):3097–3100, 2008. 68, 71, 73, 75, 78

[107] N.D. Neckel, N. Blonien, D. Nichols, and J. Hidler. Abnormal joint torque patterns exhibited by chronic stroke subjects while walking with a prescribed physiological gait pattern. *Journal of Neuroengineering and Rehabilitation*, 5(1):19, 2008. 68

[108] D.P. Ferris, Z.A. Bohra, J.R. Lukos, and C.R. Kinnaird. Neuromechanical adaptation to hopping with an elastic ankle-foot orthosis. *Journal of Applied Physiology*, 100(1):163–170, 2006. 68

[109] R. Don, M. Serrao, P. Vinci, A. Ranavolo, A. Cacchio, F. Ioppolo, M. Paoloni, R. Procaccianti, F. Frascarelli, F. De Santis, et al. Foot drop and plantar flexion failure determine different gait strategies in Charcot-Marie-Tooth patients. *Clinical Biomechanics*, 22(8):905–916, 2007. 71, 74, 75, 80

[110] H.M. Herr, S.K. Au, P. Dilworth, and D.J. Paluska. Artificial ankle-foot system with spring, variable-damping, and series-elastic actuator components, July 2006. US Patent App. 11/495,140. 90

[111] Festo. Fluidic Muscle DMSP with press-fitted connections and Fluidic Muscle MAS with screwed connections. `http://www.festo.com/net/en-us_us/downloads/downloadcache.ashx?lnk=26780/info_501_en.pdf`. Last accessed on May 27, 2010. 92, 93

[112] T. Sugar and K. Hollander. Adjustable Stiffness Leafspring Actuators, May 2009. US Patent No. 7,527,253 B2. 94

[113] Smalley Steel Ring Company. Communications, January 2010. 107

[114] W.G. Davids, H. Zhang, A.W. Turner, and M. Peterson. Beam finite-element analysis of pressurized fabric tubes. *Journal of Structural Engineering*, 133:990–998, 2007. 109, 110

[115] P.V. Cavallaro, M.E. Johnson, and A.M. Sadegh. Mechanics of plain-woven fabrics for inflated structures. *Composite Structures*, 61(4):375–393, 2003. 110

[116] HDT Engineered Technologies. Communications, January–March 2010. 110, 112, 114, 115

[117] M.A.R. Koehl, K.J. Quillin, and C.A. Pell. Mechanical design of fiber-wound hydraulic skeletons: The stiffening and straightening of embryonic notochords. *Integrative and Comparative Biology*, 40(1):28, 2000. 110

[118] J.C. Thomas and C. Wielgosz. Deflections of highly inflated fabric tubes. *Thin-Walled Structures*, 42(7):1049–1066, 2004. 110

[119] A. Le Van and C. Wielgosz. Bending and buckling of inflatable beams: Some new theoretical results. *Thin-Walled Structures*, 43(8):1166–1187, 2005. 110

[120] W.G. Davids and H. Zhang. Beam finite element for nonlinear analysis of pressurized fabric beam-columns. *Engineering Structures*, 30(7):1969–1980, 2008. 110

[121] A&P Technology. Image of airbeam supporting vehicle. `http://saltshake.com/?get=1.10.206.in=500x300_q=90`. Last accessed on May 27, 2010. 110

[122] C-Tech. Image of C-Tech airbattens. `http://www.myboatsgear.com/images/products/prod_660_enlarged.jpg`. Last accessed on May 27, 2010. 111

[123] Alibaba.com. Image of airsprings. `http://img.alibaba.com/photo/212626508/Air_Spring_Air_Bellow.jpg`. Last accessed on May 27, 2010. 116

[124] IRP Industrial Rubber Ltd. Communications, April 2010. 124, 125

[125] Engineershandbook.com. Reference Tables - Coefficient of Friction. http://www.engineershandbook.com/Tables/frictioncoefficients.htm. Last accessed on July 20, 2010. 124

[126] J. Ennis Fabrics. Cordura 1000 7 Black. http://www.jennisfabrics.com/JEnnisFabrics/productProfile.jef?prdCode=00001478\&invType=REG. Last accessed on May 27, 2010. 127

[127] Otto-Bock. Image of Otto-Bock Malleo Sensa. http://www.ottobock.com/cps/rde/xbcr/ob_us_en/img_prod_malleo_sensa_rdax_85.jpg. Last accessed on May 27, 2010. 128

[128] National Instruments. Image of cDAQ-9174. http://sine.ni.com/images/products/us/cdaq-9174_m.jpg. Last accessed on May 27, 2010. 134

[129] National Instruments. Image of NI9215. http://sine.ni.com/images/products/us/040729_crio9215_m.jpg. Last accessed on May 27, 2010. 134

[130] National Instruments. Image of NI9263. http://sine.ni.com/images/products/us/040729_crio9263_m.jpg. Last accessed on May 27, 2010. 134

[131] ControlAir Inc. Image of T900X pressure transducer. http://www.controlair.com/transducers/trans_images/900.jpg. Last accessed on May 27, 2010. 134

[132] ControlAir Inc. Specifications of T900X pressure transducer. http://www.controlair.com/downloads/900_spec.pdf. Last accessed on May 27, 2010. 135

[133] ControlAir Inc. Instructions for T900X pressure transducer. http://www.controlair.com/downloads/900_instr.pdf. Last accessed on May 27, 2010. 135

[134] Biometrics Ltd. Image of two-dimensional flexible goniometers. http://www.biometricsltd.com/images/gonios%20w700.jpg. Last accessed on May 27, 2010. 135

[135] Tekscan Inc-BTS Bioengineering. Image of F-Scan in-shoe sensor pad. http://www.btsbioengineering.com/images/phocagallery/Productsandservices/FScan/Right/thumbs/phoca_thumb_l_fscan_sensor.png. Last accessed on May 27, 2010. 136

APPENDICES

Appendix A

Raw Data for Functional Requirements

	Young Healthy Adult at Natural Cadence (Winter, 1991) [1]				Elderly Individuals at Natural Cadence (Winter, 1991) [1]	
% Gait Cycle	Angle (deg)	Angular Velocity (rad/s)	Moment (Nm/kg)	Power (W/kg)	Angle (deg)	Moment (Nm/kg)
0	0.2	-0.8	0.009	-0.02	-0.87	-0.011
2	-2.06	-1	0.034	-0.061	-2.58	-0.002
4	-3.88	-0.8	0.064	-0.09	-4.57	0.064
6	-4.6	0.3	0.051	-0.083	-6.03	0.108
8	-3.98	1.4	-0.028	-0.102	-6.32	0.097
10	-2.4	1.5	-0.143	-0.224	-5.48	0.045
12	-0.45	1.4	-0.26	-0.358	-3.93	-0.027
14	1.45	1.2	-0.368	-0.442	-2.1	-0.102
16	3.04	0.8	-0.469	-0.436	-0.33	-0.176
18	4.27	0.5	-0.545	-0.367	1.25	-0.247
20	5.13	0.3	-0.601	-0.275	2.6	-0.314
22	5.71	0.2	-0.65	-0.204	3.74	-0.374
24	6.1	0.2	-0.692	-0.173	4.7	-0.428
26	6.43	0.2	-0.736	-0.184	5.54	-0.478
28	6.76	0.2	-0.78	-0.23	6.31	-0.527
30	7.12	0.2	-0.825	-0.289	7.05	-0.58
32	7.54	0.2	-0.881	-0.338	7.78	-0.642
34	7.99	0.2	-0.951	-0.37	8.51	-0.716
36	8.44	0.2	-1.037	-0.385	9.25	-0.805
38	8.86	0.2	-1.144	-0.382	9.98	-0.911
40	9.23	0	-1.26	-0.333	10.68	-1.031
42	9.51	-0.5	-1.388	-0.2	11.34	-1.159
44	9.62	-1	-1.513	0.088	11.9	-1.281
46	9.43	-1.5	-1.608	0.619	12.27	-1.38
48	8.7	-2	-1.628	1.441	12.35	-1.437
50	7.2	-2.5	-1.565	2.448	11.96	-1.435
52	4.69	-3	-1.388	3.266	10.89	-1.355
54	1.15	-3.5	-1.073	3.331	8.9	-1.177
56	-3.26	-3.6	-0.69	2.552	5.81	-0.892
58	-8.17	-3.4	-0.335	1.35	1.67	-0.544
60	-13.05	-1.7	-0.102	0.408	-3.08	-0.24
62	-17.13	0	0.001	0.01	-7.63	-0.059
64	-19.52	1.7	0.028	-0.032	-11.01	0.012
66	-19.77	3.4	0.023	0.008	-12.53	0.026
68	-18.12	3.5	0.019	0.033	-12.15	0.024
70	-15.29	3.4	0.015	0.036	-10.39	0.02
72	-12.04	2.6	0.012	0.03	-7.93	0.017
74	-8.85	1.8	0.01	0.023	-5.29	0.013
76	-5.96	1	0.01	0.019	-2.78	0.011
78	-3.51	0.2	0.01	0.017	-0.63	0.009
80	-1.64	0	0.011	0.013	1.03	0.009
82	-0.5	0.08	0.012	0.008	2.14	0.009
84	-0.07	0.16	0.013	0.004	2.67	0.009
86	-0.16	0.24	0.013	0.002	2.68	0.01
88	-0.42	0.32	0.011	0	2.3	0.009
90	-0.52	0.4	0.006	0.001	1.75	0.007
92	-0.26	0.32	-0.001	-0.001	1.29	0.003
94	0.36	0.25	0.007	-0.004	1.07	-0.003
96	1	0.15	-0.011	-0.003	1.07	-0.007
98	1.2	-0.15	-0.01	0.001	1.05	-0.009
100	0.58	-0.75	-0.004	0.001	0.64	-0.006

	Drop Foot Patient ("Stroke Victim 1") (Shao et al., 2008) [106]		Drop Foot Patient ("No AFO") (Fatone et al., 2009) [54]		Drop Foot Patient ("Whole Group") (Don et al., 2007) [109]	
% Gait Cycle	Angle (deg)	Moment (Nm/kg)	Angle (deg)	Moment (Nm/kg)	Angle (deg)	Moment (Nm/kg)
0	-7	0	-10	0	-9	0
2	-5	-0.10667	-11	-0.03	-8.2	-0.1
4	-2.5	-0.2	-11	-0.1	-7.4	-0.15
6	0	-0.26667	-10.75	-0.15	-6.6	-0.19
8	2.5	-0.29067	-10	-0.17	-5.8	-0.22
10	5	-0.31467	-9	-0.2	-5	-0.25
12	5.45	-0.33867	-7.5	-0.2008	-4.2	-0.28
14	5.9	-0.36267	-7	-0.2016	-3.4	-0.31
16	6.35	-0.38667	-6	-0.2024	-2.6	-0.34
18	6.8	-0.41067	-5	-0.2032	-1.8	-0.36
20	7.25	-0.43467	-4	-0.21	-1	-0.38
22	7.7	-0.45867	-3.1	-0.25	-0.2	-0.39
24	8.15	-0.48267	-2.2	-0.29	0.6	-0.4
26	8.6	-0.50667	-1.3	-0.33	1.4	-0.41
28	9.05	-0.53067	-0.4	-0.37	2.2	-0.42
30	9.5	-0.53333	0.5	-0.41	3	-0.43
32	9.95	-0.58	1.4	-0.45	3.5	-0.44
34	10.4	-0.62667	2.3	-0.49	4	-0.45
36	10.85	-0.67333	3.2	-0.53	4.4	-0.46
38	11.3	-0.72	4.1	-0.57	4.8	-0.48
40	11.75	-0.76667	5	-0.6	5	-0.55
42	12.2	-0.81333	5.9	-0.635	4.8	-0.6
44	12.65	-0.86	6.8	-0.65	4.4	-0.68
46	13	-0.86667	7	-0.62	4	-0.8
48	12	-0.74667	6.5	-0.57	3.4	-0.95
50	10	-0.62667	5.25	-0.5	2.8	-1
52	8	-0.50667	3.75	-0.4075	2.2	-0.8
54	6	-0.38667	2	-0.315	1.6	-0.4
56	3	-0.26667	0	-0.2225	1	-0.15
58	-1	-0.14667	-1.4	-0.13	0.5	-0.05
60	-3	0	-2.8	-0.1	0	0
62	-5	0	-4.2	-0.07	-0.9	0
64	-6	0	-5.6	-0.03	-1.8	0
66	-5.8	0	-7	0	-2.7	0
68	-5.4	0	-7	0	-3.6	0
70	-5.1	0	-6.9	0	-4.5	0
72	-4.9	0	-6.8	0	-5.4	0
74	-4.5	0	-6.7	0	-6	0
76	-4	0	-6.7	0	-5.8	0
78	-4.5	0	-6.7	0	-5.5	0
80	-5.5	0	-6.7	0	-5.2	0
82	-6.5	0	-6.7	0	-4.9	0
84	-7.5	0	-6.7	0	-4.6	0
86	-8.5	0	-6.7	0	-4.4	0
88	-9.5	0	-6.7	0	-4.2	0
90	-10.5	0	-7	0	-4	0
92	-11.5	0	-7.3	0	-4.5	0
94	-12	0	-7.6	0	-6.2	0
96	-11.5	0	-8.4	0	-8	0
98	-9	0	-9.2	0	-9.5	0
100	-7	0	-10	0	-10	0